Functional analysis of *MEMO / MHO1*, an evolutionary conserved gene, in yeast and mammalian cells.

Inauguraldissertation

zur

Erlangung der Würde eines Doktors der Philosophie

vorgelegt der

Philosophisch-Naturwissenschaftlichen Fakultät

der Universität Basel

von

Ivan Schlatter

aus Zofingen, Schweiz

Basel, 2013

Genehmigt von der Philosophisch-Naturwissenschaftlichen Fakultät

auf Antrag von

Prof. Dr. Nancy E. Hynes

Prof. Dr. Micheal N. Hall

Basel, den 18.09.2012   Prof. Dr. Jörg Schibler

                                                                            Dekan

Abstract

The protein Memo (Mediator of ErbB2 driven cell motility) was identified in a screen for ErbB2 receptor tyrosine kinase (RTK) interacting proteins that have roles in cancer cell motility. A single Memo protein of 297 amino acids is encoded in the human genome. Memo is evolutionarily conserved and homologs are found in all branches of life. The human and the yeast protein share an identity of more than 40% and a similarity of more than 50%. Memo is not homologous to any known signaling proteins and based on its conservation we expect it to have functions in addition to promoting motility in response to RTK activation. In the work described here, we used the model organism *S. cerevisiae* to characterize Mho1 (Yjr008wp) and to investigate its function in yeast. *MHO1* expression is strongly induced in conditions of stress. In stationary phase, one stress condition, a high percentage of Memo is present in the nucleus. In mammalian cells, Memo is also found throughout the cell. Memo has no obvious NLS (nuclear localization sequence), however, an NES (nuclear export sequence) is present in all Memo homologs. In mammalian cells, blocking nuclear export with Leptomycin B led to nuclear Memo accumulation, suggesting that it is actively exported from the nucleus. Since invasive growth in *S. cerevisiea* can be induced by stress, e.g., nitrogen deprivation, or alcohol induced, we tested the role of Mho1 in this response. Deletion of *MHO1* had no effect on the formation of pseudohyphoa or invasion. Growth of *mho1δ* cells was not affected by stress inducers including (HU, CoCl2, Heat-shock, Latrunculin, Nocodazol). Interestingly, however, overexpression of Mho1 blocked the ability of the yeast cells to invade. In a synthetic lethal (SL) screen we found *MHO1* as a novel SL partner of *PLC1*. Plc1 is the only phospholipase C in yeast and hydrolyzes phosphatidylinositol 4,5-biphosphate (PIP2) to generate the signaling molecules inositol 1,4,5-triphosphate (IP3)

and 1,2-diacylglycerol (DAG). In the absence of *MHO1* and *PLC1*, double deleted spores still germinate but proliferation is impaired after 2 to 10 cell cycles by an unknown mechanism. Introduction of human *MEMO* into the *memo∆plc1∆* strain could rescue the SL phenotype showing that the specific function of Mho1/Memo needed to overcome the synthetic lethal phenotype is conserved.

"When Thomas Edison worked late into the night on the electric light, he had to do it by gas lamp or candle. I'm sure it made the work seem that much more urgent."

George Carlin

Acknowledgements

I would like to thank my supervisors Nancy Hynes and Rao Movva for giving me the chance to work on this exciting project. Rao introduced me into science in a industrial and commercial environment and I had the exciting opportunity to work in the "lab of the future". Since the project was always a collaborative one, I had the great chance to work both in a professional and academic working environment. I also want to acknowledge the remaining members of my thesis committee, Mike Hall and Marc Bühler, for the discussions and suggestions for my project. A special thanks goes to Marc who showed me how to lyse large amounts of yeast cells and helped me to purify TAP tagged proteins. I hope you and your Lab continue to do great science and kee the good and friendly atmosphere.

I want to thank all the present and former members of the Hynes Lab! I try to remember all the Names... Albana Gattelli, Alessia Bottos, Amine Issa, Anna Frei, Anne Boulay, Barbara Hnzi, Berengere Fayard, Constanze Heinrich, Francisca Maurer, Gwen MacDonald, Ivan Nalvarte, Ivana Samarzija, Jakub Zmajkovic, Jason Gill, Julien Dey, Maria Meira, Patrick Kaeser, Shunya Kondo, Susanne Lienhard, Tatiana Smirnova, Thomas Schlange, Tina Stoelzle, Vanessa Ueberschlag, Yutaka Matsuda. I hope I mentioned all of you.

Also a big thank to the Novartis lab. Especially I would like to mention Dominic Hoepfner who always had a spare minute to listen to my problems and giveing my good advise. But also a big thank to Stephen Helliwell, Ireos Filipuzzi, Heather Sadlish and the rest of the Yeasty Boys and Girls.

A special thanks goes to the FMI and all the great facilities. Without them the great research done at the moment in the institute would not be possible. My thanks goes to Patrick Schwab, Laurent Gelman, and Steven Bourke, for

iv

Contents

List of Figures

List of Tables

Glossary

AA   amino acid

ATP   adenosintriphosphate

ADF   actin depolymerizing factor

BSA   bovine serum albumin

Ca^{2+}   Calcium

cAMP   cyclic adenosine monophosphate

DAG   diacylglycerol

DAPI   4',6-diamidino-2-phenylindole

DMSO   dimethyl sulfoxide

dSLAM heterozygote diploid-based synthetic lethality analysis with microarrays

EDTA   Ethylene-diamine-tetraacetic acid

FA   focal adhesion

FCS   fetal calf serum

FITC   fluorescein isothiocyanate

G418   also known as Geneticin, a registered trademark of Gibco BRL Life Technologies, Inc.

GEF   guanine-nucleotide exchange factor

GFP   green fluorescent protein

GTP   guanidine triphosphate

HIP   Haploinsufficiency Profiling

HOP   Homozygous deletion Profiling

HRG   heregulin β-1

INM   inner nuclear membrane

InsPs   inositol phosphates

IP$_3$ inosito 1,4,5-ltriphosphate

IP$_4$ inositol 1,3,4,5-tetrakisphate

IP$_5$ Inositol1,2,3,4,5-pentakisphosphate

IP$_6$ Inositol1,2,3,4,5,6 hexakisphosphate

KD   knockdown

LiAc   lithium acetate

mAb   monoclonal antibody

MAPK   Mitogen-activated protein kinase

Memo   mediator of ErbB2-driven cell motility

MHO1   Memo Homolog 1

Mn$^2+$ Manganese

mRNA   messenger RNA

MT   micro tubules

NE   nuclear envelope

NES   Nuclear Export Sequence

NLS   Nuclear Import Sequence

ONM   outer nuclear membrane

NPC   nuclear pore complex

ORF   open reading frame

P   phosphorylated

PA   phosphatidic acid

PAGE   polyacrylamide gel electrophoresis

PEG   Polyethylene glycol

PH   Pleckstrin homology

PI   phosphatidylinositide

PI3K   phosphatidylinositol-3-kinase

PIP   phosphatidylinositolphosphate

PIP$_2$ phosphatidylinositol 4,5-bisphosphate

PIP$_3$ phosphatidylinositol 3,4,5-trisphosphate

PKA   protein kinase A

PKC   protein kinase C

PLC   phospholipase C

PM   point mutation

RNA   ribonucleic acid

RTK   receptor tyrosine kinase

SDS   sodium dodecylsulfate

SGD   Saccharomyces Genome Database

SH2   Src homology 2

SH3   Src homology 3

SL   synthetic lethal

SS   single strand

TAP   Tandem Affinity Purification

TF   transcription factor

WCE   whole cell extract

YFG   your favorite gene

YKO   Yeast Knockout

1

Introduction

1.1 MEMO

1.1.1 The function of Memo in ErbB2 driven cell migration

The protein Memo (Mediator of ErbB2 driven cell motility) was identified in a screen for ErbB2 receptor tyrosine kinase (RTK) interacting proteins that have roles in cancer cell motility. A single Memo protein of 297 amino acids is encoded in the human genome. Memo is evolutionarily conserved and homologs are found in all branches of life. Downregulation of Memo in breast tumor cells resulted in a defect in cell migration upon treatment with HRG, which has been shown to activate ErbB2-ErbB3 heterodimers and thereby stimulate migration. This indicates a critical role for Memo in ErbB2 induced cell migration (67) (96).

Remodeling of the actin cytoskeleton, formation of lamellipodia and microtubule outgrowth are critical steps during cell migration (61). Memo knockdown cells form actin fibers and grow lamellipodia, but fail to extend microtubules towards the cell cortex upon stimulation with HRG (67). In another study it was shown that the reduced microtubule network upon knockdown of Memo was caused by alterations in the transition frequencies between microtubular growth and shortening phases. Additionally, Memo knockdown cells showed less small (short-lived) focal adhesions (FAs) but more large FAs which are known to last longer (118). These results contribute to the understanding of the motility defect in Memo knockdown cells as the short-lived adhesion sites are known to be involved in membrane protrusion whereas large FAs are required for the anchoring of a cell (52).

To investigate how Memo influences the organization of the lamellipodial actin network, studies with mDia1, which is known to control actin polymerization, and the RhoA guanosine triphosphatase were performed. Memo was found to be required for the localization of the active GTP-bound RhoA and its effector mDia1 to the plasma membrane. It was shown that Memo-RhoA-mDia1 coordinates the formation of focal adhesions, microtubular outgrowth and the organization of the lamellipodial actin network (118).

Memo and PLCγ interact with specific ErbB2 phosphorylation sites (Figure 1.1), and both were shown to be essential for HRG induced chemotaxis. Upon Memo or PLCγ knockdown, cells can still migrate, although to a lesser extent, but lose the ability for directional cell migration. A reduced HRG-induced phosphorylation level of PLCγ was observed in Memo knockdown cells suggesting that Memo regulates PLCγ activation by a still unknown mechanism. In a screen for interaction partners of Memo, cofilin, a member of the actin depolymerizing factor (ADF)/cofilin family was identified (70). Proteins of these family control actin-filament assembly and disassembly, which is required for cell migration (26). It was shown in an invitro assay that Memo enhances cofilin depolymerizing activity, which suggests a role of Memo in the control of actin dynamics (70). Together these results strongly support an important role of Memo in ErbB2 induced cell migration. Memo is likely to be involved in several important steps in cellular migration, as its involvement in the organization of the actin network, in the formation of focal adhesions and microtubular outgrowth has been demonstrated.

1.1.2 Memo protein structure is homologous to nonheme iron dioxygenases

The crystal structure of the full-length human Memo protein was determined by Qui et al. using a single wavelength anomalous diffraction (89). The resulting atomic model was then refined to a 2.1 Å resolution. Only the last 5 N-terminal amino acids could not be modeled. The modeled Memo structure adopts a single domain structure with a mixed seven-strand β-sheet surrounded by nine α-helices (Figure 1.2). The β-strands and the α-helices have been designated with numbers, letters respectively, according to their appearance in the primary sequence (Figure 1.2). With the program DALI a search for structural Memo homologs revealed that Memo is homologous to LigB, the
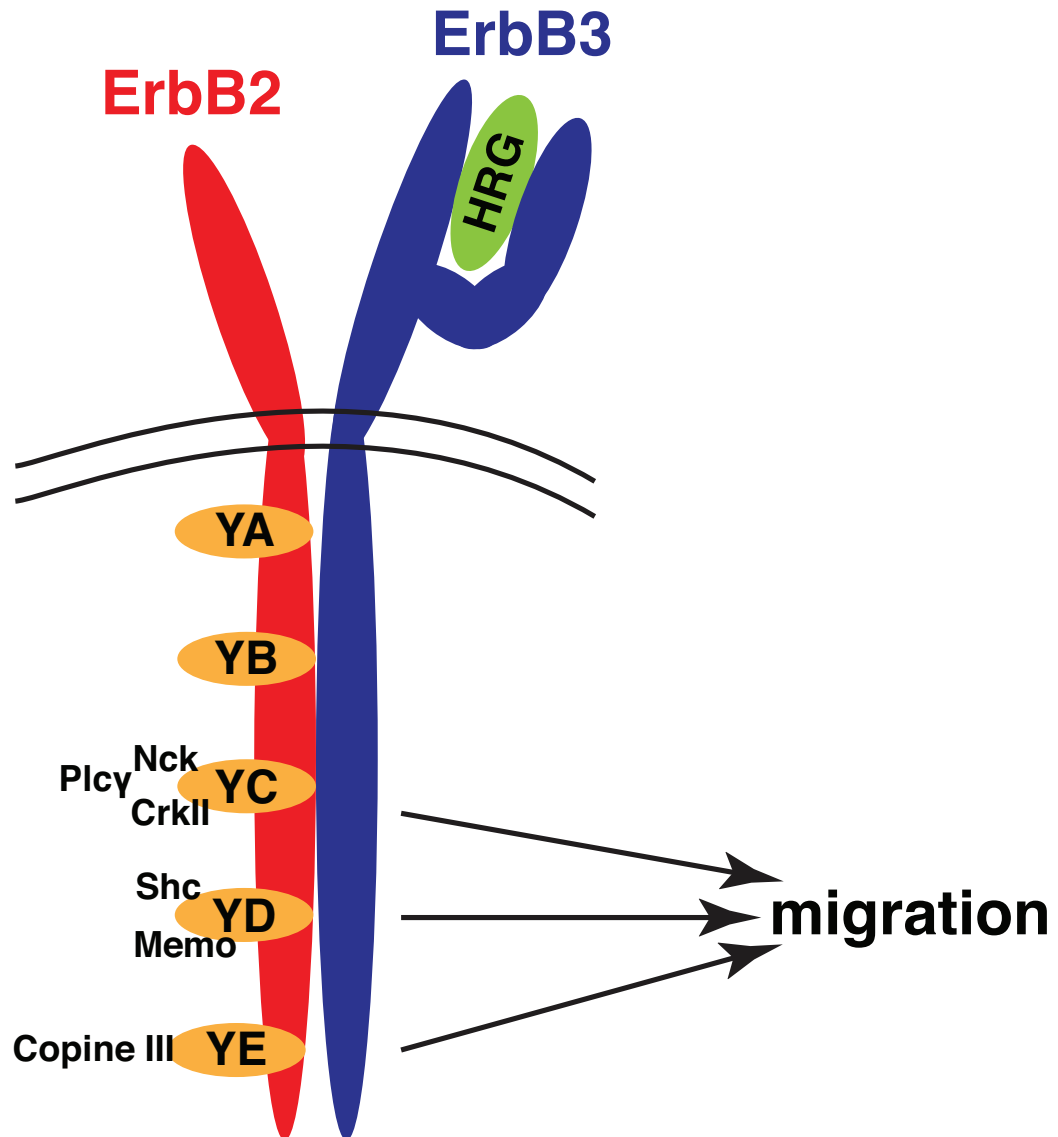
Figure 1.1: ErbB2/ErbB3 heterodimer and autophosphorylation - ErbB2 and ErbB3 form a heterodimer upon HRG (heregulin) binding to the extracellular domain of ErbB3. The heterodimerization leads to the autophosphorylation of the intracellular phospho-Tyrosine sites of ErbB2, PTyr-1023, PTyr-1139, PTyr- 1196, PTyr-1222, and PTyr-1248. The phospho-Tyrosine sites of ErbB2 are shown as orange ovals and the sites are named YA - YE (22). The YC (81, 83), YD (67),and YE sites (46) are known to have a role in cellular migration. Memo was found to bind the P-YD peptide site (67) directly, in cells it is likely to be via Shc (Src homology 2 domain containing).

catalytic β-subunit of the protocatechuate 4,5-dioxygenase LigAB from *Sphingomonas paucimobilis* (47)(102).

LigAB is a class III nonheme iron(II)-dependent extradiol-type catechol dioxygenase that catalyzes oxidative cleavage of substituted catechols in bacterial aromatic degradation pathway (76). The primary protein sequence homology between Memo and class III nonheme iron(II) dependent dioxygenases is low, the identity is less than 15%. The catalytic activity of LigB is mediated by an iron ion, which is coordinated by the amino acids His-12, His-61, Glu-242, and a water molecule (102) (Figure 1.2). A third histidine, His-195, is believed to function as a general base during catalysis. All three histidine are conserved in Memo and have the number His-49, His-81, and His-192, respectively. But the Glu-242 of the LigB is missing in Memo and was replaced by a cysteine (Cys-244) (Figure 1.2). This substitution does not necessary exclude the possibility of a metal binding. The cysteine side chain is capable of coordinating many metal ions including iron. Memo has also an aspartic acid at position 189 (Asp-189) the side chain of which could coordinate a metal ion bound at this site and balance the positive charge. As all known LigB non heme dioxygenases members in bacteria have a glutamate in the active site it is unlikely that Memo has the same function. However, the possibility that Memo has an enzymatic function has not been excluded.

Recently a 2.3 $\mathring{A}$ crystal structure of the uncharacterized *E. coli* protein ygiD (JW3007) has been released. This *E. coli* protein has been shown to be an other structural homolog of Memo. ygiD shares only 11% protein sequence homology to Memo, but clearly shares the same structural topology with Memo (Figure 1.2). The yigD protein coordinates three zinc ions, one of which is positioned in a site homologous to the putative metal-binding site in Memo. This zinc ion is ligated by a water molecule and three histidine (His-22, His-57,and His-234). These 3 histidine correspond to the residues His-49, His-81, and Cys-244 in Memo.

1.2   Why study MEMO in *Saccharomyces cerevisiae*?

Saccharomyces cerevisiae is maybe the most useful yeast species. It has been used since ancient times for baking and brewing, most of the time even without people knowing and realizing it. *S. cerevisiae*, it is believed, was originally isolated from the skin of grapes (yeast is one component of the thin white film one can see on the skin

adapted from Qui et. al 2008
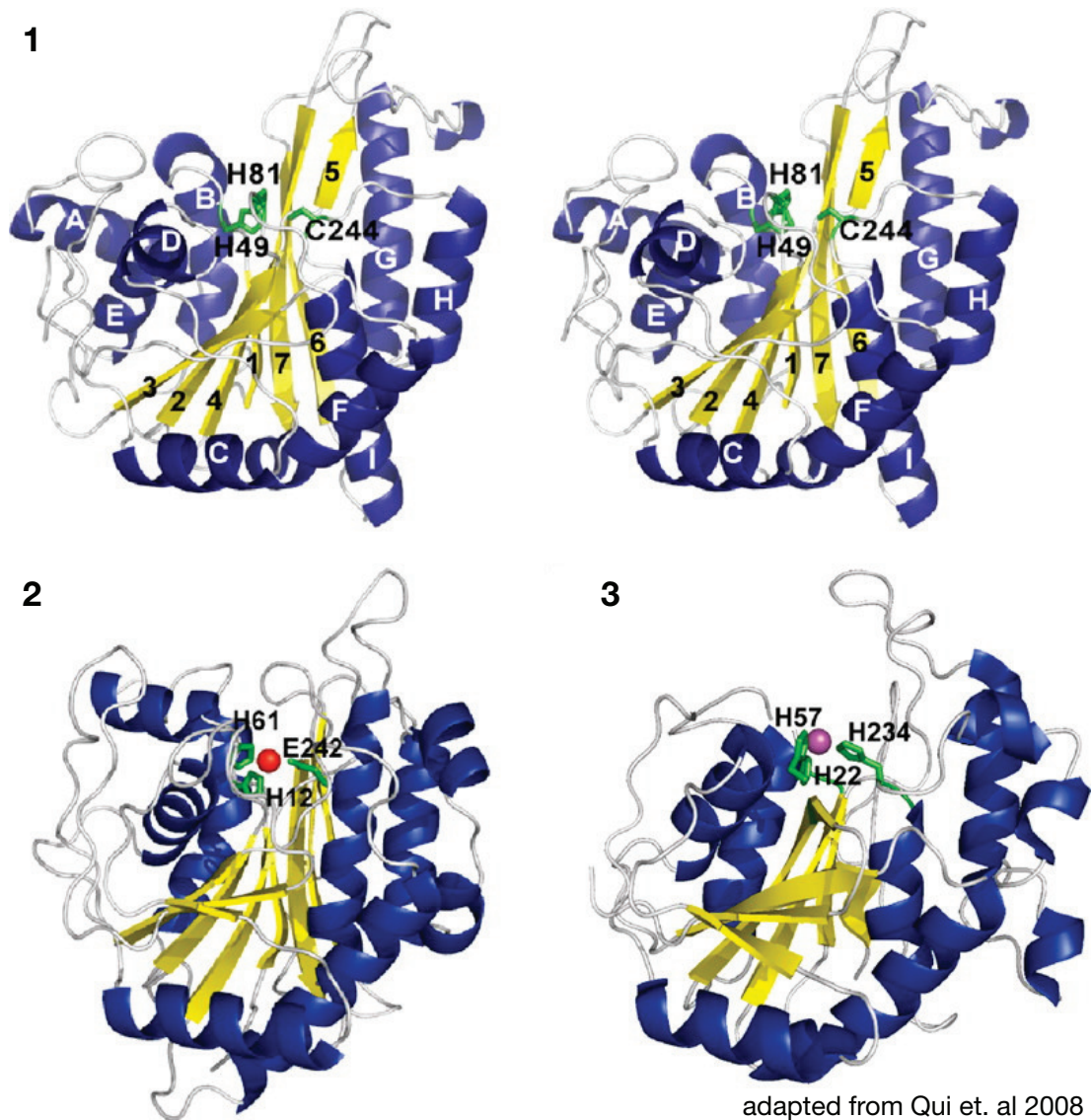
Figure 1.2: Memo and the structural homology to a Nonheme Iron Dioxygenases - 1) ribbon diagram of Memo in stereo. Side chains of His-49, His-81, and Cys-244 are shown as green sticks. 2) ribbon diagram of LigB (Protein Data Bank code 1BOU). The iron ion is indicated by a red sphere, and the residues coordinating the iron, His-12, His-61, and Glu-242, are shown in green. 3) ribbon diagram of ygiD (Protein Data Bank code 2pw6). The zinc ion is indicated by a magenta sphere, and the residues coordinating the zinc, His-22, His-57, and His-234 are shown in green (Figure adapted from (89)).

of dark colored fruits like plums or grapes). *S. cerevisiae* is not only indispensable in the kitchen, but also in research it has become a model organism in cell biology. It is one of the most studied eukaryotic cells and has a status comparable to *Escherichia coli* as the model bacterium. *S. cerevisiae* cells are 5 - 10 micrometers in diameter and often ovoid shaped. The single celled yeasts reproduce by budding of a daughter cell from the mother cell. During "normal" proliferation the mother cells grow a bud which then develops to their daughter cells. Most types of fermentation are driven by the microorganism *S. cerevisiae*.

Below some aspects are listed guessing why *S. cerevisiae* has developed as a model organism:

- As a single celled organism *S. cerevisiae* is small with a short generation time (doubling time 90 minutes at 30°C (103)) and can be easily cultured. The production and maintenance of multiple specimen lines can be kept at low cost.

- *S. cerevisiae* can efficiently be transformed through homologous recombination allowing for either the addition of new genes or deletion of genes. Furthermore, the ability of growing *S. cerevisiae* as haploid cells simplifies the production of gene knockouts strains or whole gene deletion collections.

- As a eukaryote, *S. cerevisiae* shares most of the major cell structure complexes with other eukaryotic cells like plants and animals. However, *S. cerevisiae* does not have the high percentage of non-coding DNA found in most "higher" eukaryotes.

- Many important and conserved proteins were first discovered and studied in yeast before the mammalian homolog was found and studied. Some of these proteins include cell cycle proteins, signaling proteins, and protein-processing enzymes.

Also in terms of tools, large-scale screens, genetics, and many more reasons *S. cerevisiae* has developed as a major model organism::

- Genome sequencing

  The first eukaryotic genome that was completely sequenced was the one from *S. cerevisiae* (39). On April 24, 1996, the genome sequence was made public

and since then regularly updated at the *Saccharomyces* Genome Database (SGD (28)). The SGD is highly annotated and cross-referenced and one of the tools frequently used by yeast scientists. The *S. cerevisiae* genome is composed of about 12'000 kilo base pairs (kbp) and approx. 6'300 genes, compactly organized on 16 chromosomes. Only about 5,800 of these are believed to be true functional genes. About 23% of the yeast genes (approx. 1'500 genes) do have a human homologous gene with an percent identity $\geq 30\%$ (13).

- Other tools in yeast research

One of the main features in *S. cerevisiae* research is the availability of the entire genome sequence and different sets of commercially available deletion strains (invitrogen). But also the development of protein interaction screens made *S. cerevisiae* a powerful model in many branches of science.

- Yeast cell-based assays for receptor tyrosine kinases (RTKs)

The major working model for Receptor Tyrosine Kinases (RTKs) is the homo- or hetero-dimerization after ligand binding. This dimerization leads to the activation resulting in phosphorylation at specific Tyrosine residues. RTKs are regulator of various intracellular signaling-transduction pathways and enhanced RTK activity, due to mutations, overexpression or other, is associated with various human diseases.

The advantage of studying RTKs in yeast is the fact that yeast cells do not have endogenous RTKs. This means there is no interference from redundant processes like other RTKs activating downstream signaling. The assay is specific and clean.

By doing experiments in yeast the RTKs are still in an eukaryotic environment. This is advantageous as this addresses cell-compatibility and membrane permeation. In screens for small chemical inhibitors the eukaryotic environment facilitates the elimination of metabolic unstable and toxic components.

In *S.cerevisiae* it is possible to do reliable HTS (High-throughput) assays which are relatively rapidly established and are very cost-effective.

In yeast the specific control is already built-in due to the absence of endogenous Tyrosine-kinases.

- Bar-coded yeast are discussed in more detail in the section 1.2.4 Bar-coded yeast and the *Saccharomyces* genome-deletion project.

- Astrobiology

  A sample of *S. cerevisiae* will be included in the Living Interplanetary Flight Experiment. The plan is to send a small sample on a three-year interplanetary journey in the Russian Fobos-Grunt spacecraft (19). Main objective of the mission is to test if the selected organism can survive some years in deep space. The researches want to test the hypothesis if life can survive space travel, if for example protected inside a rock and so bring live to other planets.

- Brewing

  Beer-Brewers classify *Saccharomyces cerevisiae* "top cropping" (or "top-fermenting") and "bottom-cropping" (or "bottom-fermenting") (**?**). Top cropping (or "top-fermenting") yeast, as its name says, are found in the foam arising during the fermentation process. The hydrophobic surface of the yeast clumps, so called flocs (flocculated yeast: cells tend to stick together once all sugar has been fermented into etanol) adhere to produced CO_2 and due to this effect are found on "top". "Bottom-cropping" (or "bottom-fermenting") yeasts are used to brew lager or ale beer. In contrast to top cropping yeasts Bottom-cropping yeasts need lower temperatures for fermentation. A bottom-cropping yeast is *Saccharomyces pastorianus* which was also known as *S. carlsbergensis*.

  The different yeast strains used for beer brewing are chosen accordingly to the kind of beer one wants to get. As a yeast population in not genetically identical, but shows random variation, the nowadays typically, and unique for each beer, yeast strains could be "selected" and grown. For example cells that stay in suspension and flocculate later tend to end up at the top of the yeast bed and can easily be collected and be reused for the next brewing. Repetition of the selection for a specific cretiria will change the profile of the culture and alter fermentation characteristics.

Nutritional requirements for growth of *S. cerevisiae*:

For aerobic growth all *S. cerevisiae* strains need the sugars glucose, maltose, and mycose, but can not use lactose and cellobiose. Depending on the genetic background an on whether the yeast grow aerobically or anaerobically they use different sugars. For example the best fermenting sugars are galactose or fructose. Common for all strains is that they can use ammonia and urea as the unique nitrogen source. As yeast can not reduce nitrate to ammonium ions this nitrogen source is not usable for yeast. On the other hans they can use most nitrogen bases, amino acids, and small peptides, as a nitrogen source. As textitS. cerevisiae does not excrete proteases extracellular protein cannot be used as a source for their metabolism.

1.2.1 Mating type and the life cycle of *Saccharomyces cerevisiae*

Saccharomyces cerevisiae is a single celled eukaryote with two variants of existence, as diploid and haploid cells. Only haploid yeast cells can mate. The cells can be either a or α (alpha) mating type and thus display simple sexual differentiation. The mating type of the cells is determined by a single locus, *MAT*, which controls the sexual behavior of both haploid and diploid cells. Haploid yeast can switch the mating type as often as every cell cycle through a form of genetic recombination. *S. cerevisiae* can stably exist as either a diploid or haploid. Haploid and diploid yeast cells reproduce by mitosis, with daughter cells budding off from mother cells. Haploid cells are capable of mating with other haploid cells of the opposite mating type (an a cell can only mate with an α cell, and vice versa) to produce a stable diploid cell. If diploid cells are facing stressful conditions such as nutrient depletion, they can stop proliferating and instead undergo meiosis to produce four haploid spores: two a spores and two α spores.

1.2.1.1 What are the Differences between a and α cells?

The two opposite mating type cells produce two distinct mating type pheromones to signal their presence and attract cells from the opposite mating type. This means that a cells produce a-factor, to signal their presence to an α cell. On the other hand a cells respond to the mating pheromone of an α cell, called α-factor, by growing a projection (known as a shmoo, due to its appearance resembling the famous cartoon characters (see Figure 1.3) towards the source of α-factor).

In an analogous manner, α cells respond to a-factor by outgrowing a shmoo toward the source and producing the α-factor. The mating response is only induced if a haploid
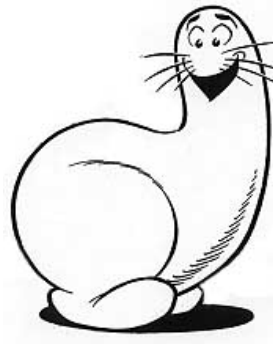
Figure 1.3: SHMOO - A SHMOO as it first appeared in "Li'l Abner" in August 1948, by Al Capp.

cell senses the mating pheromone of the opposite mating type, but not by the same mating type. The accurate regulation of mating type specific genes in the cells of the two mating types leads to the phenotypic differences. An a cell activates genes which produce a-factor and the a cell specific cell surface receptor (Ste2). Ste2, also called α-factor receptor, binds to α factor which then triggers signaling within the cell. Genes associated with being an α cell are repressed in a cells. Similarly, α cells activate specific genes to produce α-factor and Ste3 (a cell surface receptor) which binds and responds to a-factor. On topα cells repress gene transcription of genes associated with being an a cell. The presence of one of the two alleles of the locus called *MAT*: *MATa* or *Matα* causes the different sets of transcriptional repression and activation which characterize a and α cells. The *MATa* allele of *MAT* encodes a gene called a1, which then regulates the a-specific gene transcription (e.g. expressing *STE2* and regressing *STE3*).The MATα allele of *MAT* locus encodes the α1 and α2 genes, which regulate the transcription of the α-specific transcriptional program (e.g. expressing *STE3* and repressing *STE2*).

1.2.1.2   What are the differences between haploid and diploid cells?

Haploid yeast cells can can have one of the above mentioned mating type, either a or α. If two cells of opposite mating type sense each other by recognizing the pheromones they can extend a shmoo and fuse their cell wall, cytoplasm, and nuclei and by this becoming a diploid cell (Figure 1.4).

The haploid yeast cells proliferate by undergoing mitotic cell divisions but cannot
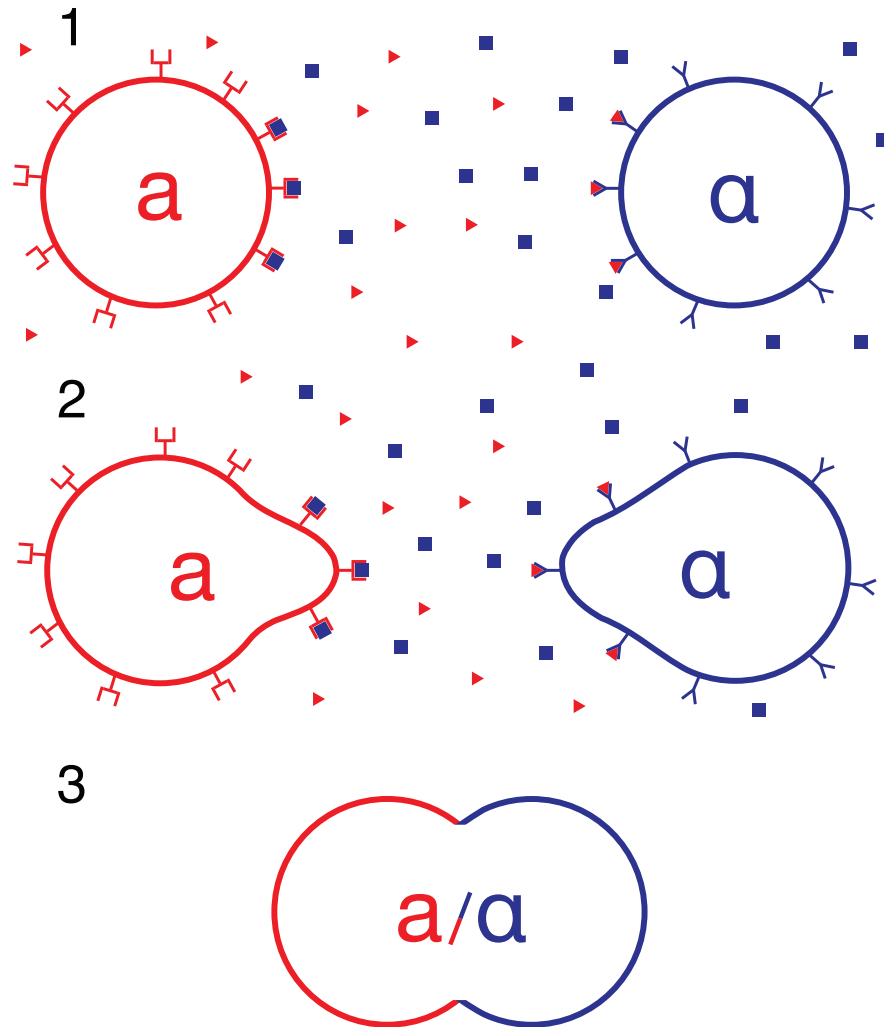
Figure 1.4: Mating of yeast cells - 1. A red MATa cell secretes the a mating pheromone and expresses the α-factor receptor on its surface, whereas a blue MATα cells secretes the α-factor pheromone and expresses the a-factor receptor 2. Upon recognition of the opposite mating pheromone the cells stop in cell cycle in G1 and extend a shmoo toward the source of the mating factor 3. When the two opposite mating type cells meet they first fuse their cell wall and membrane and mix their cytoplasm followed by fusion of the two nuclei to become a diploid cell.

undergo meiosis. In contrast in diploid cells the production or response to either mating pheromone is repressed and due to this they can not mate. However, under specific environmental growth conditions diploid yeast cells can undergo meiosis to produce four haploid cells (spores). As described for the difference between the two mating types, the phenotypic differences between haploid and diploid yeast cells is regulated at the level of gene transcription. Haploid cell not only have a specific transcriptional pattern for a and α mating type, they both share a specific haploid transcriptional pattern. Haploid yeast cells transcribe haploid-specific genes like *HO*, but actively repress diploid-specific genes like *IME1*. On the other hand, diploid cells enforce transcription of diploid-specific genes and repress the transcription of diploid-specific genes. This described difference in expression patterns between haploid and diploid cells is due to the *MAT* locus. Haploid cells only have one copy of each of the 16 chromosomes in *S. cerevisiae* and so by definition can only have one allele of *MAT* (either *MATa* or MATα). The one *MAT* locus they posses determines their mating type. Two haploid yeast cells of opposite mating type become one diploid yeast cell after mating. The mating results in a cell having 32 chromosomes (in 16 pairs), one chromosome encoding the *MATa* allele and another chromosome encoding the *MATα* allele. The combination of the two opposing *MAT* alleles triggers a diploid-specific gene transcription program. In haploid cells only one *MAT* allele can be present. The of genetic information of only one *MAT* allele starts the haploid-specific gene transcription program. The fact that the information encoded by the *MAT* locus is enough the explain the mating-type behavior can be showed nicely by some genetic manipulations of haploid and diploid cells. For example if a haploid cells gets an extra-copy of the opposing *MAT* locus it starts to behave like a diploid cell. In contrast by deleting a *MAT* allele in a diploid cell will force the cell to behave like a haploid cell

1.2.1.3   Isotropic vs. polarized growth

In all kingdoms of life there are cells that can polarize in response to external (e.g. chemical gradients, cell-cell contacts, or environment) and/or internal stimuli. In general eukaryotic cells react to these stimuli by assembling a polarized actin cytoskeleton at the cellular cortex. Together with microtubules it coordinates the guidance of membranes. Recruitment and rearrangement of actin and mirotubules finally leads to polarized events internally and at the cell surface (27). *S. cerevisiae* uses polarized growth

to direct the budding of the daughter cell from the mother during cell replication and shmoo formation as a response to mating pheromones. the following steps are essential to guarantee cell growth in *S. cerevisiae*:

1. Weakening of the cell wall by digestive enzymes to allow cell expansion

2. Insertion of new plasma membrane at the cell surface

3. Synthesis of a new cell wall by biosynthetic enzymes

For polarized growth the secretory pathway has to deliver the needed enzymes and membranes to discrete growth sites at the cellular surface. Adams and Pringle, 1984 (2) showed that actin localizes to sites of cell expansion during the cell cycle. Work following this break through showed that secretory vesicles are transported only along actin cables to support growth, instead of actin cables and microtubules like most "higher" cells (for review, see (15)(30)). Actin also orients the mitotic spindle at early stages of cell division by microtubule-actin interactions (104). The inheritance of mitochondria, peroxysomes, and the vacuole into the bud depends on the polarization of the actin cytoskeleton. Almost all aspects of polarized growth in yeast start from the polarity of the actin cytoskeleton. Thus, it is important that elaborate controls carefully monitor and regulate cytoskeletal structure during all steps of the yeast cell cycle. In yeast, F-actin is manly organized into cortical actin patches and actin cables. Cortical patches are discrete F-actin rich bodies, whereas actin cables are long F-actin bundles (2)(4). Cables and patches are polarized in a cell-cycle-dependent manner and are located at the cell cortex. If the cell enters a new round of cell cycle in G1 (Start), the first step is to select the site of budding (Figure 1.5) (87). Actin patches, which bundle the actin cables for membrane and enzyme transport, form an actin ring. As soon as a bud emerges, cortical actin patches cluster at its tip thereby extending actin cables from the mother cell into the bud and the bud grows apically (from the tip). While the bud is still growing, patches and cables within the bud redistribute randomly while the actin cables in the mother cell still extend to the bud neck thus providing the daughter cell with the needed organelles, membranes and proteins. The bud expands isotropically into an ellipsoid shape. An alternative filamentous morphology that is induced in some *S. cerevisiae* strains by a variety of environmental growth conditions leads to the prolongation of apical growth to generate highly elongated cells, called pseudohyphal

or filamentous growth ((Figure 1.5); (56)(63)(66). At the end of vegetative bud growth, a cytokinetic F-actin ring assembles at the bud neck, contracts and disassembles the daughter from the mother cell (29). After cytokinesis, patches and cables in the mother and daughter repolarize to the site of cell scission to direct synthesis of cell walls between the two new cells.

During the mating response and the following schmoo formation actin also has to polarize (Figure 1.5). Pheromone stimulated cells become arrested in G1 and start to express the needed proteins for polarized growth and orient growth toward the source of the mating pheromone. The yeast cells polarize their actin cytoskeleton by sensing the pheromone concentration gradient (56). During bud formation, almost all growth is directed into the bud. In a proliferating population uniformly sized mother cells having variously sized buds can be found. If the polarized growth is defective the cells have either elongated buds as a consequence of excessive apical growth, or have spherical buds as a consequence of excessive isotropic growth. When growth is only isotropic, this means completely undirected, bud formation is completely abolished and mother cells grow into huge, round, and unbudded cells.

The key player that regulates actin polarization is the essential Rho GTPase Cdc42. Cdc42 controls the polarization of the actin cytoskeleton during the different phases of cell cycle. Essential for this regulatory function is the recruitment of Cdc42p to growth sites on the plasma membrane, where the GTPase activates effectors that signal to the actin cytoskeleton (119). The loss of Cdc42 leads to large, round, unbudded cells due to the disorganization of the actin patches and cables (Adams et al., 1990). In mutants in which Cdc43vlose this ability to localize to the plasma membrane polarization is also lost (1). Like other Rho GTPases, Cdc42p signals to effectors only in an active GTP-bound state. GTP binding requires the guanine-nucleotide-exchange factor (GEF) Cdc24 (44). Normal Cdc42p function also requires inactivation by GTP hydrolysis (Figure 1.6 b)).

1.2.1.4   Filamentous growth of *Saccharomyces cerevisiae*

Fungal dimorphism is a complex phenomenon induced by a large variety of environmental factors. Cells switch from "normal cell division cycle" to a reversible alternating pattern of growth between elliptical and filamentous forms of cells. When diploid *S. cerevisiae* sense a lack of nitrogen in their environment cells stop budding and form
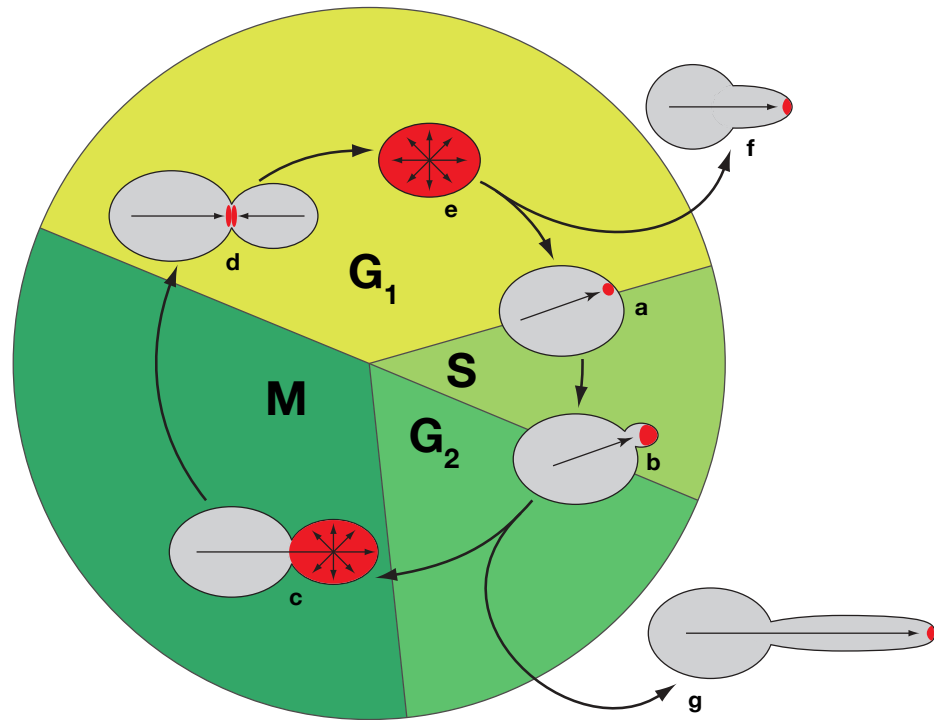
Figure 1.5: Cell polarity in budding yeast - Polarized growth sites (red), where the Rho GTPase Cdc42 is active, change during the cell cycle and so also reorienting the actin cytoskeleton via Cdc42 related proteins. In turn, the actin cytoskeleton guides secretory vesicles to the cell surface, where they accumulate (red) and fuse. (a) The cell cycle begins in G1 with establishment of a nascent bud site. (b) Clustering of Cdc42p directs early bud growth toward the tip. (c) Redistribution of Cdc42p over the bud surface during G2-M redirects bud growth isotropically, and results in an ellipsoidal shaped bud. (d) With the completion of bud growth, cables and patches disorganize, and a cytokinetic ring forms, then contracts and disassembles after mitosis. Cdc42p reorients actin and growth between the two new cells to generate new cell walls. The mother cell resumes budding immediately. (e) The new daughter undergoes a period of undirected growth. (f) Mating pheromones arrest haploid yeast in G1 and polarize Cdc42p toward potential mating partners to generate a mating projection (shmoo) (g) Under certain growth conditions, some strains of *S. cerevisiae* differentiate into a filamentous state that leave out the transition in G2-M from tip-directed to isotropic growth. The resulting cells are highly elongated.

pseudohyphae . By switching from budding to filamentous growth the cells get an advantage in nutrient retrieval. This nitrogen sensing process is at least controlled by at least two signaling transduction pathways:

1. The MAP kinase (MAPK) pathway (Figure1.6)

2. The PKA (cAMP-dependent protein kinase A) pathway (Figure 1.6)

Both pathways activate the expression of pseudohypha-specific genes and lead to a G2 delay in the cell cycle for a prolonged period of polarized growth.

Haploid yeast cells show a similar pseudohyphal growth phenotype after running short of nutrients. This happens if yeast cells were grown for several days on rich medium plates. In contrast to the diploid cells, haploid cells do not elongate in shape but they form chains and invade into the agar on the edge of the colony. This growth form is referred as haploid invasive growth. Another stimulus which can induce filamentous growth in haploid and diploid cells is alcohol (64). The yeast cells become aberrant and elongated in shape.

1.2.2   The filamentous fungus *Ashbya gossypii* (from the master thesis "Function of the four homologs of yeast Dynamins in the filamentous Ascomycete *Ashby gossypii*", I. Schlatter, 2005)

The filamentous fungus *Ashbya gossypii*, an Ascomycete, belongs to the order of Endomycetales in the family of Saccharomycetaceae (86). Ashby and Nowell first described this fungus in 1926 as a cotton pathogen that can also infect citrus fruits and tomatoes (6). Stigmatomycosis, the disease caused by *Ashbya*, affects the development of hair cells in cotton bolls and leads to dehydration and collapse of infected citrus fruits (6)(98). Insects such as Antestia and Dysdercus spread the disease from plant to plant. The needle-shaped spores of *A. gossypii* stick to the body of insects while they are visiting Ashbyas host plants [4]. On a medium, favorable for germination, the development of *A. gossypii* starts with a phase of isotropic growth (Figure 1.7).

The middle part of needle-shaped spores forms a germ bubble, in which actin patches localize randomly at the cortex. Afterwards, actin patches start to concentrate at one region at the cortex perpendicular to the axis of the needle, thus marking the site of germ tube emergence. This polarized actin cytoskeleton directs growth from this region
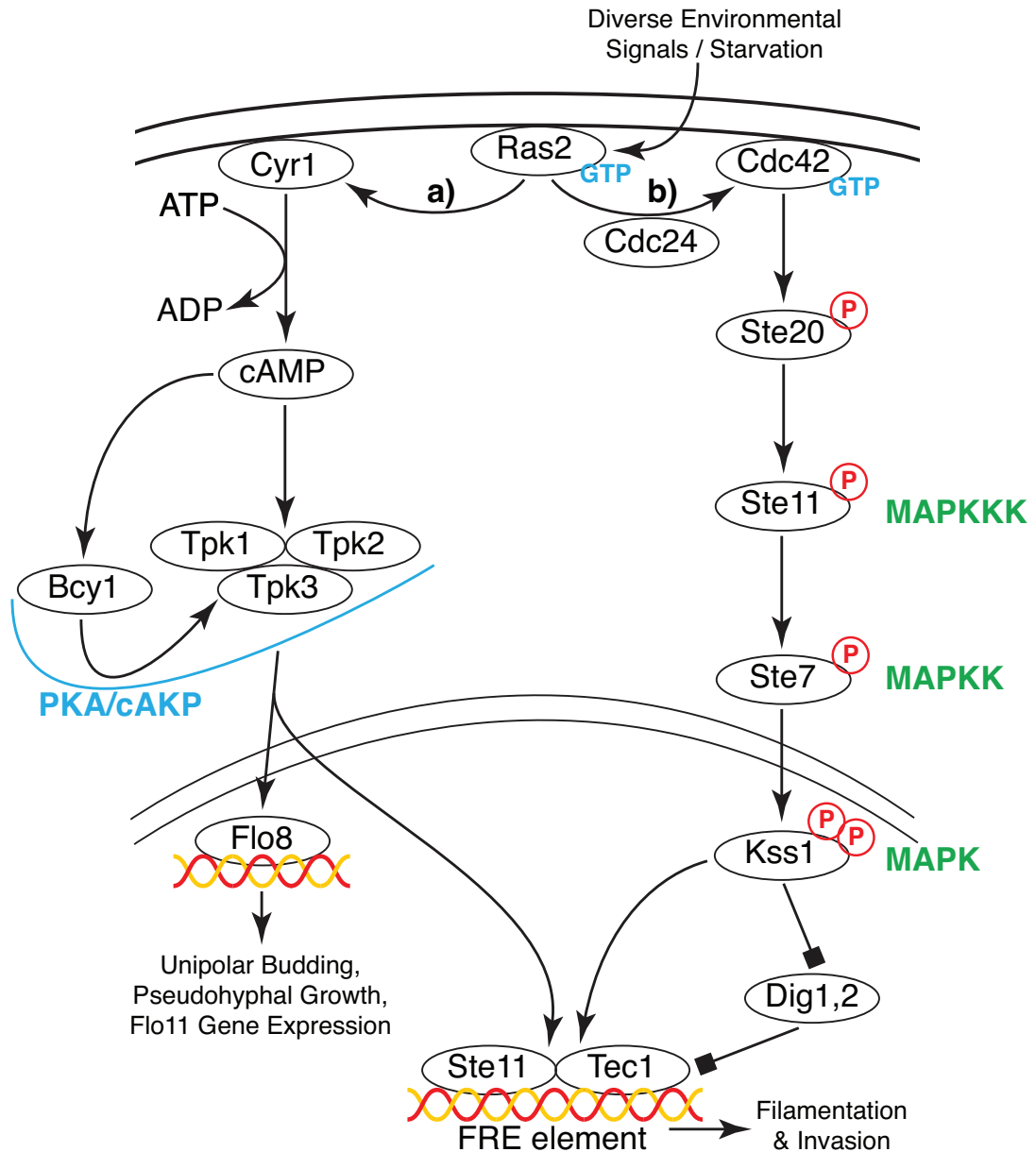
Figure 1.6: cAMP-PKA pathway and MAPK pathway - a) cAMP-PKA pathway regulates filamentous growth in *S. cerevisiea*. Activation of Ras2 stimulates the adenylate cyclase, Cyr1, and the resulting increase in cAMP level causes an activation of the Tpks (Tpk1,2,3 are the 3 catalytic subunits of the yeast PKA homolog (highlighted in blue), whereas Bcy1 is the regulatory subunit). These specifically activate or inhibit a number of proteins which act on different target genes. b) In *S. cerevisiae* filamentous growth is regulated by the MAPK pathway. Ras2 gets activated by external signals which, in turn, causes the phosphorylation of the MAPKKK Ste11, The MAPKK Ste7, and the MAPK Kss1. The genes which are targeted by this signal cascade have a FRE element in their promoter.
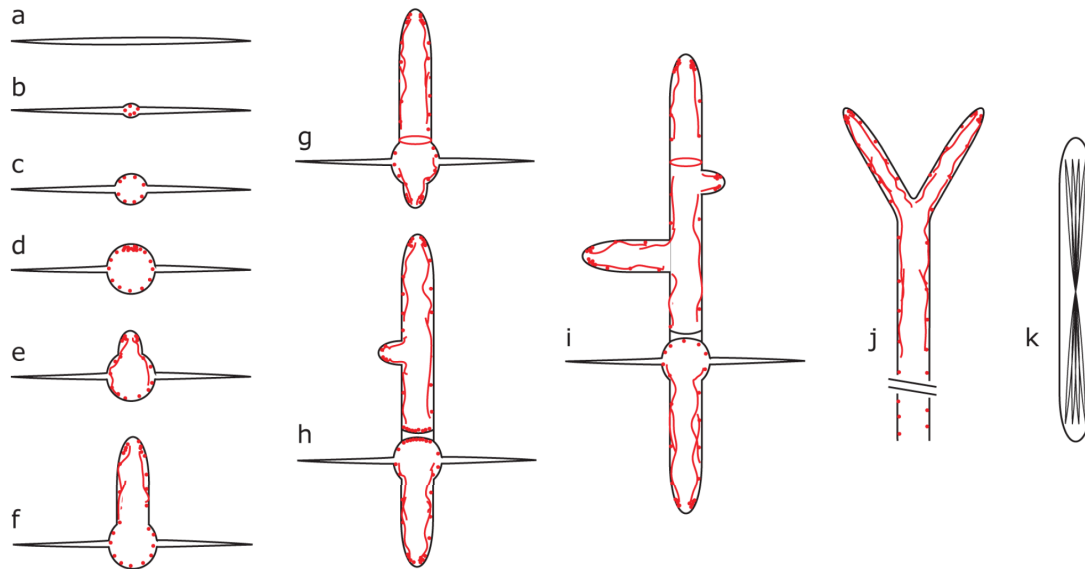
Figure 1.7: Development of *A. gossypii*. - The pictures represent cross section through *A. gossypii* at different developmental stages. The red dots represent actin patches, the red lines actin cables and the red ellipses actin rings. (a) Ungerminated spore. (b), (c) Formation of a germ bubble by isotropic growth. The actin patches are distributed evenly among cell cortex. (d) Concentration of actin patches to the site of branch emergence. (e) Unipolar germling actin patches are concentrated at the site of growth, and actin cables are reaching from the tip into the germ bubble. (f) Continued apical growth phase in the unipolar germling. Actin patches are concentrated at the tip. The very apical part is free of actin patches. Actin cables run along the hyphal cortex. (g) Emergence of a second germ tube. An actin ring localizes to the neck between the first germ tube and the germ bubble as a precursor for septation. (h) Emergence of the first lateral branch, and induction of a septum at the neck where the actin ring was localized. Actin patches localize transiently at the site of septum formation. (i) Continued apical growth at all tips. The generated septum is now free of actin. (j) Apical branching in mature hyphae. (k) Sporangia containing spores.

causing the first germ tube to extend and form a unipolar germling. Actin localizes as cortical patches to the tip of the germ tube and less frequently to the hyphal cortex. Actin cables run from the tip into the hypha. The germ tube maintains polarization and extends consistently in one direction. On the opposite side of the germ bubble, a second germ tube is formed to give rise to a bipolar germling. Additional sites of polarity are established at the hyphal cortex and initiate lateral branches. Actin rings are formed at sites that will later form septa, a chitin-rich ring-like structure. The first septum is preferably formed at the neck between the germ bubble and the first germ tube. The speed of hyphal tip growth increases during maturation and apical tip branching occurs in mature mycelium(7)(109)(110). As no cytokinesis occurs in *A. gossypii*, hyphae consist of multi-nucleated compartments that are only intersected by septa. After 5 - 8 days, depending on environmental conditions, the mycelium forms vegetative spores. These spores attach to each other through a filament (Figure 1.8).
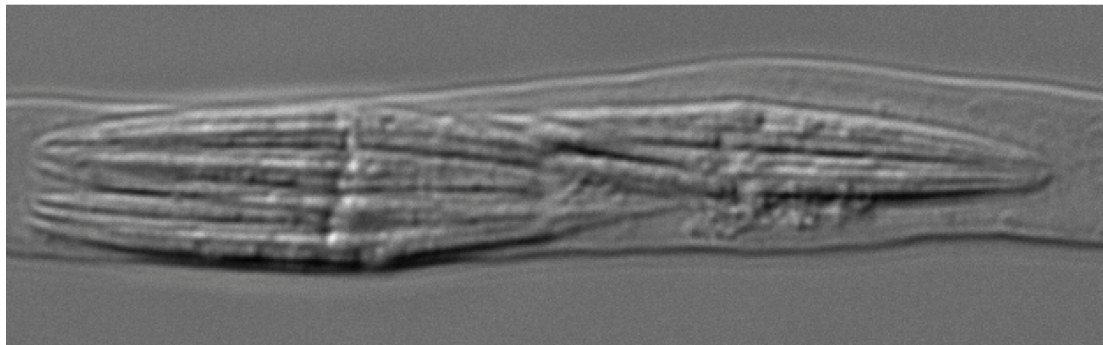
Figure 1.8: Sporangium with spores attached to each other. - As *A. gossypii* does not undergo cytokinesis this fungus has a multinucleate cytoplasm. Segments of hyphae containing 8 nuclei are enclosed by single actin rings which then duplicate and contract. The formed septum then separates 8 nuclei compartments from each other in the older parts of the filament. If the fungus grows for several days on the same plate nutrients gets limited and *A. gossypii* can form spores. A septum containing the 8 nuclei can produce a Sporangium with 8 spores. As *A. gossypii* is always haploid it does not need to undergo Mitosis during sporulation, like the diploid *S. cerevisiae* cells, but can directly produce a sporangium with spores. The spores are needle shaped and can stick to the body of insects while they are visiting *A. gossypii* host plants. In the figure the sporangium has lost two cells, so only six spores are visible.

For the haploid *A. gossypii* no sexual cycle is known. The genome of *Ashbya gossypii* contains most homologs of the genes that are part of the *Saccharomyces cere-*

visiae pheromone-signal transduction cascade. However, the sequenced strain bears three identical copies encoding *MATa*. Some finding now showed, that there could be a sexual cycle even in *A. gossypii* in nature (111). *Ashbya gossypii* naturally produces and excretes riboflavin, vitamin B2, in large quantities (113), which makes it interesting for biotechnological purposes. Like two other overproducers of this vitamin, *Candida famata* and *Bacillus subtilis*, *Ashbya* is currently used in industrial riboflavin production. Thus, chemical production of this vitamin is now replaced by microbial processes, which reduce costs as well as waste and energy consumption while using renewable resources (97). In order to optimize biosynthetic processes, molecular tools in respective organisms have to be developed. *A. gossypii* does integrative recombination exclusively via homologous recombination (99). This allows PCR-based one-step gene-targeting (106). A PCR generated knockout cassette consists of a dominant selectable marker, which is flanked by short guide sequences with 40 – 46 bp of homology to two sequences of the targeted gene (109). In this study, we used sequences with 50 – 60 bp homology to reduce the number of false positives and to increase efficiency. *GEN3* is a nonhomologous selection marker, constructed for the use in *A. gossypii*. It consists of the E. coli *kanR* gene under the control of promoter and terminator sequences of the highly expressed *S. cerevisiae TEF2* ORF, thus preventing recombination with *A. gossypii* promoter and terminator sequences. *GEN3* mediates resistance against G418/geneticin (109). The advantage of this fast growing fungus compared to *S. cerevisiae* is, that it needs sustained polarization at the growing hyphal tip. For this the interplay between the cytoskeletal structures like actin and micro tubules but also the correct localization of polarization determining protein is essential (54).

1.2.3   Synthetic lethality in *Saccharomyces cerevisiae*

Synthetic lethality is commonly known as the genetic interaction of two by its own not lethal mutations but when combined in one cell are lethal (25). SL has been one of the most powerful tools to elucidate the functions of many yeast genes (10). By doing global synthetic lethality analysis yeast scientists hope to identify the cellular pathways that can compensate for each other biologically (43). Of the approximately 6000 yeast genes 4800 single deletions strains are viable when plated on full medium plates at standard conditions. This means the proteins encoded by one of this 4800 genes is not needed under this condition. Also possible is that the protein function of

the deleted gene or the pathway in which it signals can be complemented by another protein/pathway bypassing the lack of one protein. Only if both genes are deleted, which means both pathways are interrupted, the double deleted cells die (Figure 1.9).
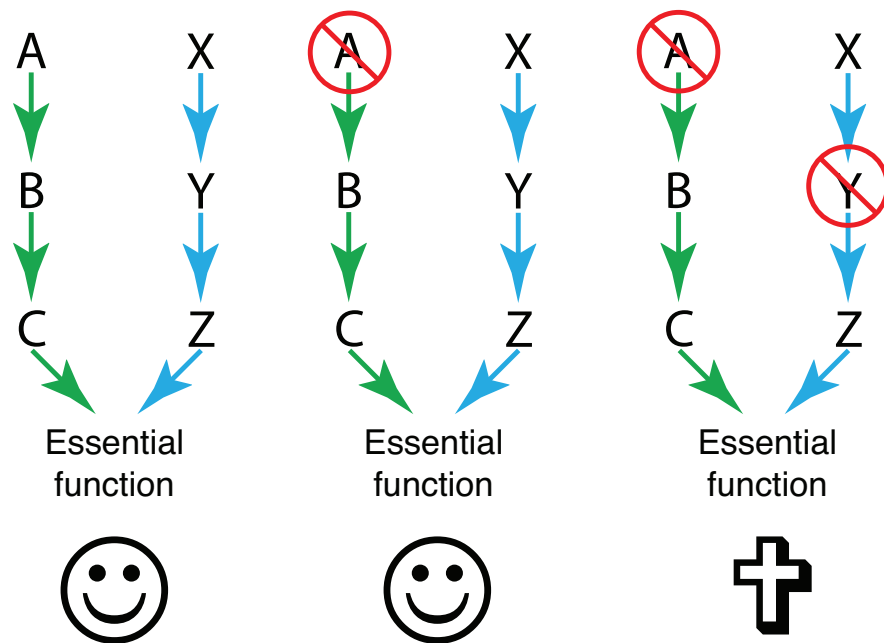
Figure 1.9: Synthetic lethality - Approximately 4800 yeast genes are not essential because other gene products / pathways buffer against their loss. But if two single deletions, which alone are viable, are combined and the yeast do not grow it is called synthetic lethality.

Most signaling pathways are not completely separate from each other, but are interconnected at many steps and can signal or inhibit to each other. It is not enough to interrupt two pathways by deleting two random genes of the parallel pathways, but it is necessary to hit two proteins needed in pathway steps were there is no compensation by the other. To fully understand two pathways and identify all the inter-pathway

cross-talk it is necessary to make all the possible double deletions with all the genes involved. After analysis of the viable, slower growing and dead double deletions it could be possible to understand how the two "separate" pathways are regulated by each other ((Figure 1.10)).
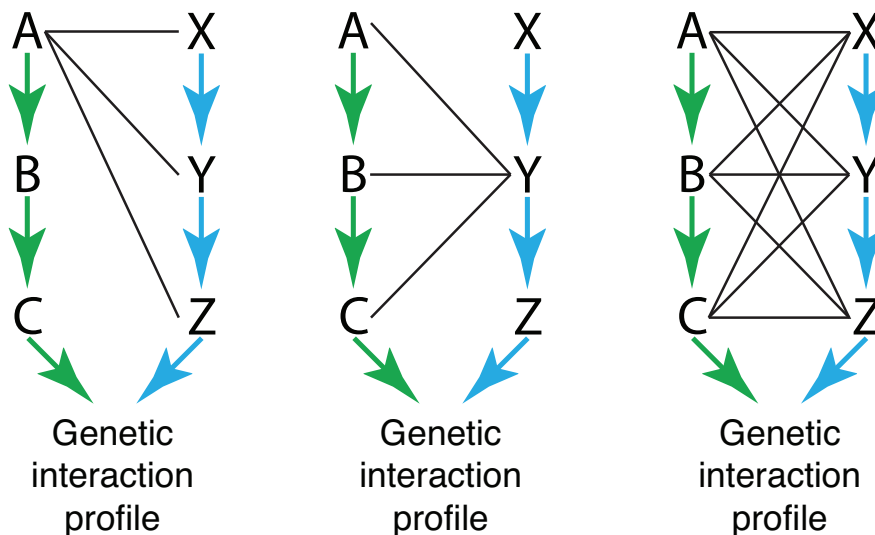
Figure 1.10: Genetic interaction Profile - In theory one could use the idea of synthetic lethality to build up networks of pathways based purely upon genetic analysis.

If the concept of synthetic lethality is thought further the logical consequence would be to find all the synthetic lethal partner of one gene of interest, the "query strain". As query strain a haploid strain with the deletion of "your favorite gene" (YFG) is used. The *yfg*Δ strain is then consequently mated to a collection of the 4800 viable haploid single deletion strains of the opposite mating type which are pinned on agar plates. Each of the 4800 single deletion strain has it defined spot on the agar plates. The resulting diploid strains are heterozygous for *YFG* and one of the non essential genes. The newly created diploid strains are then sporulated and the now haploid yeast

cells are selected for the double deletion. No one can look for spots on the agar plates were slow growing ore non growing colonies can be detected which indicates a "negative genetic interaction" (Figure 1.11).

This method is robust but a lot of special plates for the pinning robot devise are needed with different selection and sporulation media. The analysis can be done by eye or colony-size can be detected by camera and analyzed by a software (21). The ultimate goal would be to get a data grid with the crossing of all 4800 haploid single deletion strains against each other.

1.2.4   Bar-coded yeast and the *Saccharomyces* genome-deletion project

The *Saccharomyces* genome-deletion project is a worldwide collaborative effort to create a systematic deletion collection for almost all annotated yeast ORFs. The single gene deletions were made by replacement with the *kanMX4* cassette that confers resistance to the drug G418 (114). These 'yeast knockout' (YKO) mutants were created by chromosomal integration of PCR-generated disruption cassettes via homologous recombination (Figure 1.12). The YKOs exist in four formats (114):

1. *MATa* haploid

2. *MATα* haploid

3. *MATa and MATα* homozygous diploid (used for HOP - Homozygous deletion Profiling)

4. *MATa and MATα* heterozygous diploid (used for HIP - HaploInsufficiency Profiling)

The first three sets (*MATa* haploid, *MATα* haploid, *MATa* and *MATα* homozygous diploid) contain only nonessential gene YKOs whereas the heterozygous diploid deletion collection contains approximately 96% of the yeast genome which is over 6000 individual yeast strains. These YKO mutant collections perfect for large-scale screens to analyze genome functionality. They have been used to study gene-function in a variety of biological processes, cellular response to various stresses and drugs resistance. In Ron Davis' laboratory these deletion collections were developed further by the systematic incorporation of unambiguous DNA sequence identifiers called "TAGs" in each mutant
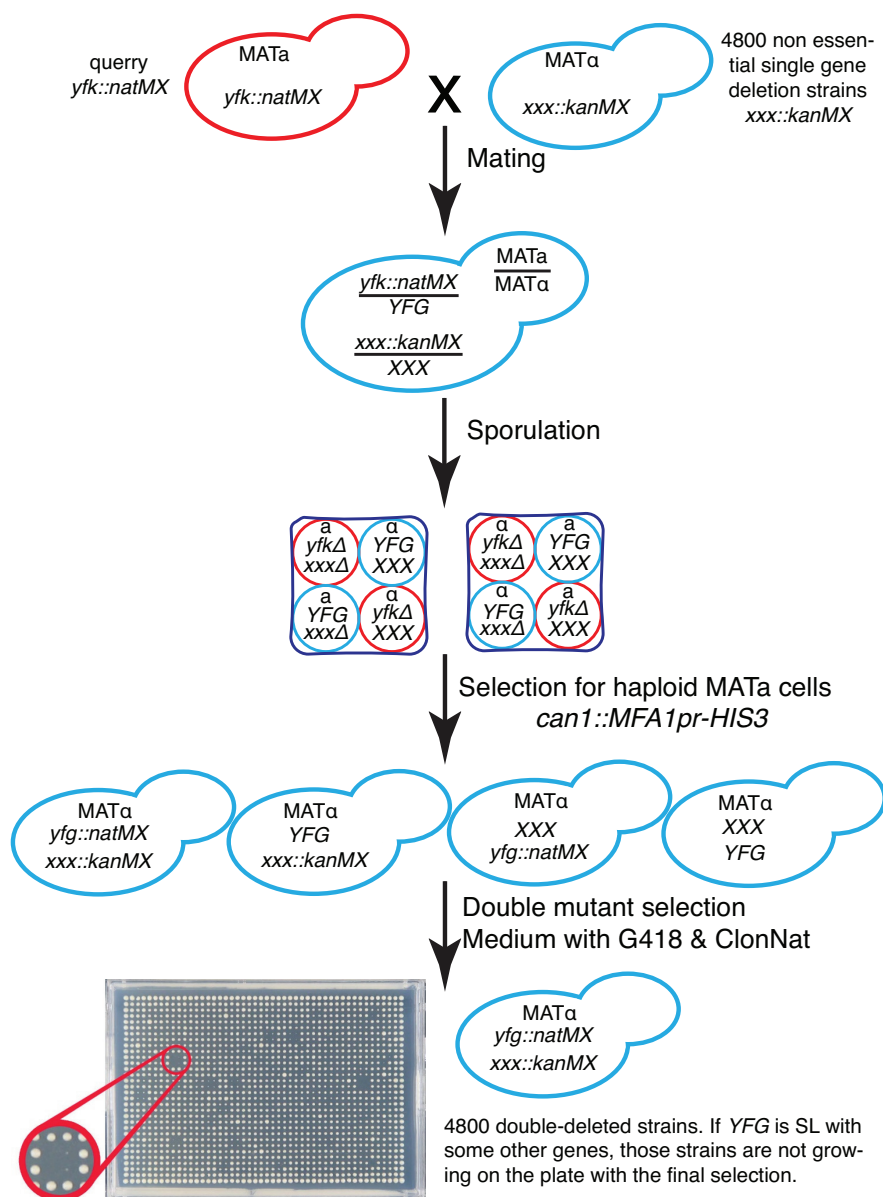
Figure 1.11: Synthetic genetic array (SGA) - A *MATα* strain (red) carrying a query mutation (*yfgΔ*) linked to a dominant selectable marker, such as the nourseothricin-resistance marker *natMX* that confers resistance to the antibiotic nourseothricin (clon-NAT), and the *MFA1pr-HIS3*, is mated to a collection of *MATa* (blue) viable yeast deletion mutants, each carrying a gene deletion mutation (*xxxΔ*) linked to a kanamycin-resistance marker *kanMX* that confers resistance to the antibiotic geneticin (G418). Growth of resultant diploid zygotes is selected for on medium containing nourseothricin and geneticin. The heterozygous diploids are transferred to medium with reduced levels of carbon and nitrogen to induce sporulation and the formation of haploid meiotic spores. These spores are transferred to synthetic medium lacking histidine, which allows for selective germination of *MATa* spores because only these cells express the *MFA1pr-HIS3* reporter. The *MATa* cells are then transferred to medium that contains G418 and clonNAT, which then selects for growth of double mutant (*yfg::natMX xxx::kanMX*).
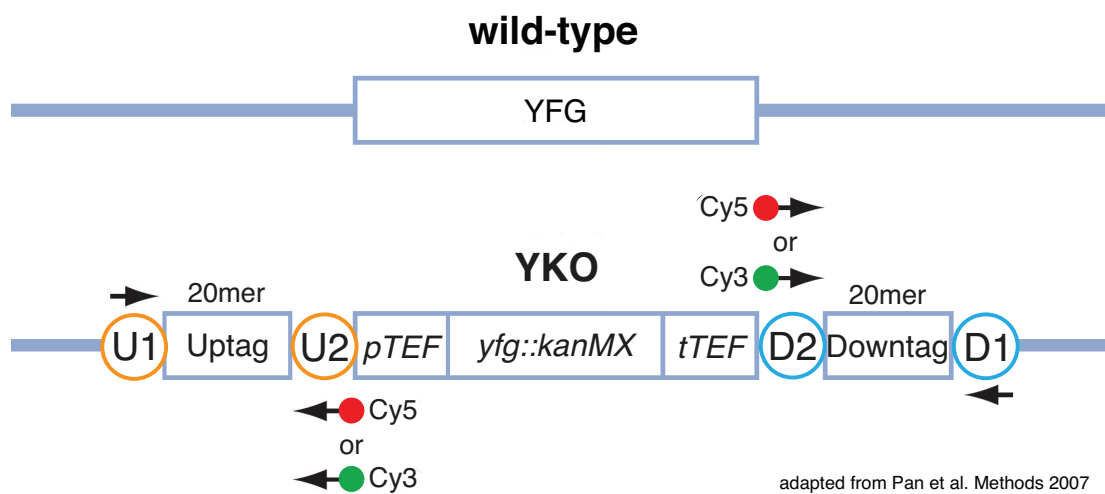
Figure 1.12: Genotype of a barcoded heterozygous deletion strain - A diagram for the yeast knockout construct. Each YKO consists of a *kanMX* module that confers resistance to the antibiotic G418 flanked by unique 20-mer molecular barcodes or Tags called the Uptag and Downtag. All Uptags and all Downtags are themselves flanked by two common set of priming sites (U1 and U2 for the "Uptags" within the orange circles) and (D1 and D2 for "Downtags" within the cyan circles). By using these common priming sites all Uptags or all Downtags in a population can be used for PCR amplification and microarray analysis. YFG stands for Your Favorite Gene. In the case of the HIP for most annotated yeast genes (Figure adapted from (79)).

(114)(94). All by this method created YKO mutation contains two 20-nucleotide TAGs (also called "molecular barcodes"), which are unique for each deleted gene (Figure 1.12). The gene-specific Uptag and Downtag are flanked by universal priming sites. In a collection of over 6000 individual deletion strains, each having its own individual Up- and Downtag, there are over 12000 TAGs. They were designed to be as different from each other as possible, but retained relatively similar hybridization properties (114)(94). All of these properties were essential for functional profiling and the genetic manipulation of the deletion strains as a pool (114)(94)(11)(38)(100). Functional profiling allows quantitative analysis of the fitness of the deletion strain under a defined condition. All the strains in the pool can now be analyzed in parallel. By PCR amplifying the TAGs of the YKO pool before and after applying the selection, genes required to survive the choosen selection can be identified (Figure 1.13). After hybridization of the TAGs on a chip the resulting patterns can be used to determine the presence, absence, under- or over-representation of a particular deletion strain in the population (Figure 1.13). Mutants that are underrepresented after treatment are identified because they have a greater TAG signal intensity in the control than in the experiment (94)(11)(100)(65). Functional profiling of populations using TAG microarrays greatly expedites genetic screens and makes them intrinsically quantitative.

The bar-coded heterozygous diploid deletion collection is also the basis for the synthetic lethal screen "dSLAM" (heterozygote diploid-based synthetic lethality analysis with microarrays) we performed and that will be discussed later in this thesis. The big advantage is that all approx. 6000 strains can be handled in liquid as a pool and the query deletion will be introduced in one big transformation in all the strains. Compared to the "traditional" SL screen with pinning the non-essential haploid deletion strains on agar plates and mating them with the query strain harboring the deletion of "YFG" in the dSLAM experiment also the essential genes are included and it is possible do detect synthetic rescue, meaning a second deletion can overcome the lethal phenotype of a single deletion.

1.3   Phospholipase C

As in this study we show that in yeast *PLC1* is a novel synthetic lethal partner with *MHO1* (the yeast homolog of Memo) and Maria et al. (70) showed that Memo Co-
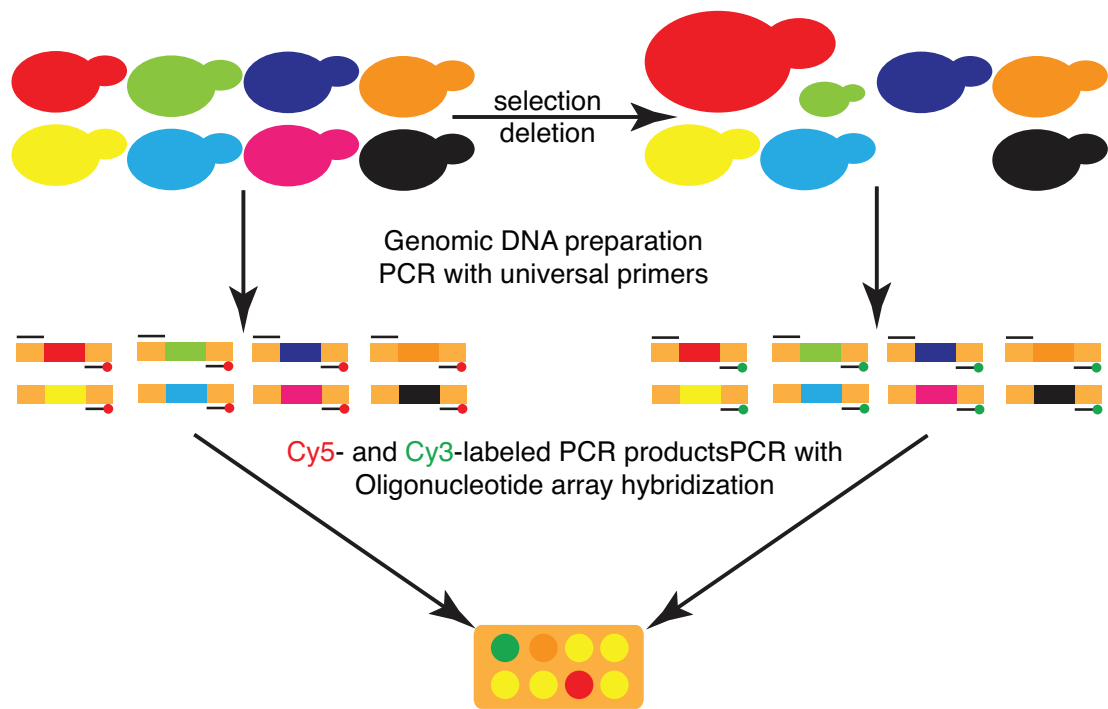
Figure 1.13: Genetic screen by micro array - Molecular bar-coding facilitates genetic screens by microarray analysis. The UPTAG and DNTAG "labels" of each strain enable numerous YKO mutants to be pooled and analyzed in parallel. Pools of mutants can be exposed to various conditions or specific selections. Genomic DNA can then be isolated from YKO pools before and after condition change / selection, and can be used as a PCR template to amplify the DNTAGs or UPTAGs of the present strains. By using Cy5- (in red) and Cy3- (in green) labeled universal primers, respectively the number of each YKO strains in both conditions can be compared. The fluorescently-labeled probes are then hybridized to an oligonucleotide array. A defective mutant (shown in pink) that did not survive the induced test condition would only show up in the Cy5 channel. Also a strain that grows better in the test condition (shown in red) would have a brighter Cy3 signal compared to Cy 3 or a strain growing slower in the test condition would have a brighter Cy5 signal compared to Cy3. So from all the ratios of the Cy5 to Cy3 signals the growth rates of each individual YKO can be determined.

immunoprecipitates with PLC-gamma1 and Memo regulates heregulin induced PLC-gamma1 phosphorylation in the next section we will introduce yeast and mammalian PLC.

In general phospholypases are enzymes which hydrolyzes phospholipids into fatty acids and other lipophilic substances. Depending on their cleavage site they fall into different categories (see also Figure 1.14):

- Phospholipase A1 and A1 cleave the fatty acid chains off from the glycerol backbone of the phospholipid the at the C1-, C2-Position, respectively.

- Phospholipase B cleaves both ester bond at C1 and C2, it has the activity of Phospholipase A1 and A2 together.

- Phospholipase C cleaves just before the phosphate group of phospholipids.

- Phospholipase D cleaves just after the phosphate group of phospholipids.

Phospholipase C (PLC) is a conserved gene family found in eukaryotic cells, but also in bacteria, trypanosomes, and archea. The enzymatic activity for PLC in all kingdoms of life is always the cleavage of Phosphatidylinositol 4,5-bisphosphate (PIP_2) into the second messengers diacylglycerol (DAG) and inositol 1,4,5-trisphosphate (IP3). PIP_2 is cleaved by PLCs just before the phosphate of the phospholipid, where the inositoltrisphosphate is bound to the C3-atom of the glycerol backbone (Figure 1.15). The DAG produced by this reaction the remains bound to the membrane, and IP_3 is released as a soluble structure into the cytosol. Even though PLCs enzymatic activity is conserved throughout evolution, DAG and IP_3 may act differently on cell signaling depending on the species. In this chapter *S. cerevisiae's* unique PLC and the well studied human PLC isoforms will be discussed.

1.3.1 PLC1 in yeast

In *S. cerevisiae* the only PLC is encoded by the gene *PLC1* (31, 115). The Plc1 protein consists of an N-terminally PH (Pleckstrin homology)domain, a EF-hand like domain, a catalytic domain, and a C-terminal C2 domain (75). Yeast Plc1p is structurally most similar to the mammalian PLCδ isoform (see Figure 1.18) and hydrolyzes phosphatidyli-nositol 4,5-biphosphate (PIP_2) to generate the signaling molecules diacylglycerol (DAG)
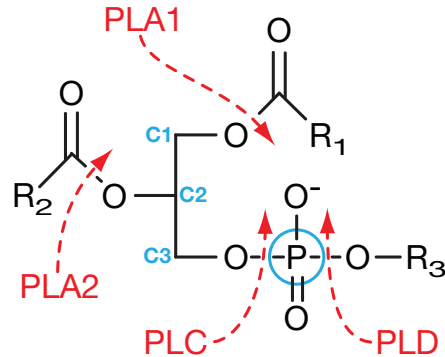
Figure 1.14: Cleavage sites of phospholipases - Cleavage sites of phospholipases. Phospholipase A1 and A2 cut the esterbond at position C1 and C2 of the phospholipid. The C1, C2, and C3 positions of the glycerol backbone are indicated in light blue. Phospholipase C enzymes cut just before the phosphate (light blue circle) attached to the R3 moiety, which in case of PIP_2 is inositol triphosphate. Phospholipase D cuts just after the indicated phosphate.
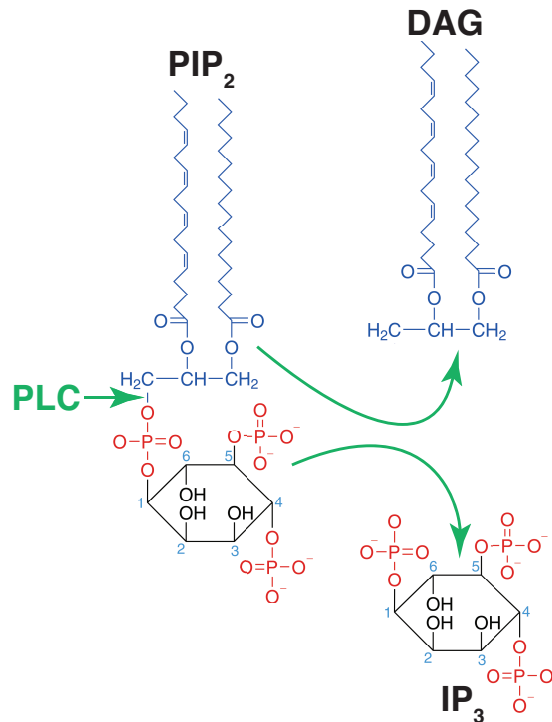
Figure 1.15: PIP2 cleavage by phospholypase C - In the picture the structural formula of PIP_2 is shown and at which position it gets cleaved by PLC. The resulting DAG and IP_3 are also shown as structural formula. IP_3 is soluble and gets released to the cytoplasm whereas DAG remains membrane bound via the two fatty acid side chains.

and inositol 1,4,5-triphosphate (IP3). IP_3 is released from the plasma membrane and is further processed by four inositol polyphosphate kinases (Ipk2/Arg82, Ipk1, Ksc1, and Vip1) which then constitute a nuclear signaling pathway that has multiple effects depending on the produced IPs which influence nutrient sensing, filamentous growth, nuclear export of mRNA, actin organization, protein synthesis, kinetochore function, transcriptional regulation, vacuolar fusion, and PKA-mediated stress response (For a summary see Figure 1.16). However, the exact mechanisms how Plc1 is actively regulated and itself regulates downstream pathways is still mainly unknown. Less is known for the yeast PLC signaling pathway compared to humans. For example in contrast to higher eukaryotes yeast has no IP_3 receptors on the ER, which after binding regulates Ca^2+ release. The only yeast Protein Kinase C (Pkc1) does have a potential DAG binding site, but PKC activation is independent of this site as Jacoby et al. (50) have shown.

The genetic background or the nutrient content of the media can influence the growth defect of the $plc1\Delta$ strains. In some strain backgrounds, the null mutant is inviable, while in other strains cell growth rate is slightly reduced and lethality is only seen when grown at higher temperatures. Other $plc1\Delta$ phenotypes include extreme sensitivity to hyperosmotic stress; increased resistance to calcium inhibition; defects in sporulation; failure to form pseudohyphae under filamentous growth-inducing conditions; increased aberrant chromosome segregation; and, when shifted to higher temperatures arrests as large, multi-budded cells. Affected by PLC1 deletion are amongst others: transcriptional control (400-500 transcripts are altered by PLC1 deletion), export of mRNA from the nucleus, homologous DNA recombination, cell death, and telomere length. In the last years the influence of Plc1 in cAMP/PKA signaling has becoming more evident. It has been shown that $plc1\Delta$ cells accumulate glycogen to a significantly higher level than wild-type cells indicating a low PKA activity. Consistent with that finding is that in $plc1\Delta$ cells cAMP synthesis following the addition of glucose is diminished. This result suggests that the lower level of PKA signaling in $plc1\Delta$ cells can be explained by decreased synthesis of cAMP (Figure 1.17. The PKA pathway is also involved in induction of filamentous growth after Nitrogen depletion.

Little is known about the regulation of PLC1 RNA expression, but consensus binding sites for the transcription factors Hsf1 and Rap1 have been identified upstream of the PLC1 gene.
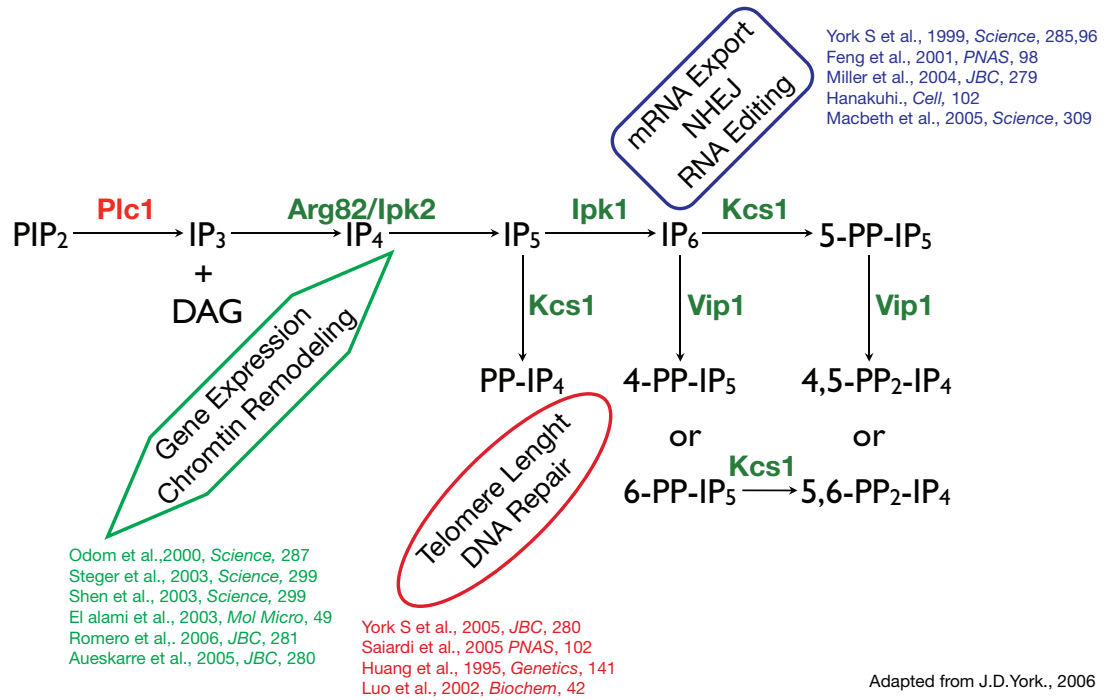
Figure 1.16: The nuclear IP signaling pathway in *Saccharomyces cerevisiae* (Figure adapted from (116)) -
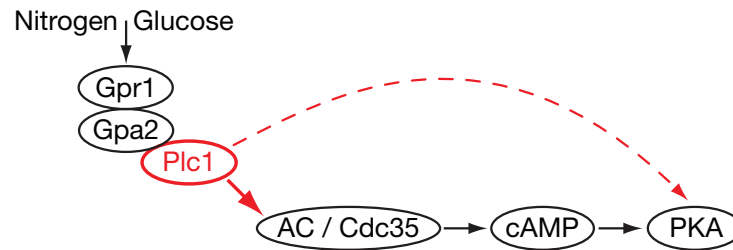
Figure 1.17: Plc1 regulates the PKA pathway by altering Cdc35 activity -

1.3.2   Phospholipase C in mammals - from β to ζ

Other than yeast, human cells have several isoforms of PLCs. Human PLCs act as key proteins in the cellular signaling of many hormones, neurotransmitters, growth factors, and other extracellular stimuli. PLCs are soluble and cytosolic but some isoforms can also associate with membranes or interact with G-proteins via their PH domain. PLC-gamma, in contrast to the other isoforms, can interact with receptor tyrosine kinases via a SH2 or SH3 domain.

Thirteen kinds of mammalian phospholipase C are known. They are classified into six isotypes (β, γ, δ, ϵ, η, ζ) according to their structure. All PLC isoforms have in common those structures: a EF-hand domain (has a helix-loop-helix topology in which the Ca^{2+} ions are coordinated, this might cause conformational changes that enable Ca^{2+}-regulated functions and activity (55)), a catalytic domain (cleavage of PIP_2 into DAG and IP_3), and a C2 domain (which generally is involved in calcium-dependent phospholipid binding (23)). The PH domain is present in most PLCs (Pleckstrin homology domain). This domain can bind Phosphatidylinositol lipids within biological membranes like PIP_3 or PIP_2 (107), and proteins such as the $\beta\gamma$-subunits of heterotrimeric G proteins (108), and protein kinase C (5).

The mammalian PLC variants are:

- beta: PLCB1, PLCB2, PLCB3, PLCB4

- gamma: PLCG1, PLCG2

- delta: PLCD1, PLCD3, PLCD4

- epsilon: PLCE1

- eta: PLCH1, PLCH2

- zeta: PLCZ1

- The structures of the different isoforms are shown in Figure 1.18.

In mammalian cells PLC cuts Phosphatidylinositol 4,5-bisphosphate (PIP2) into diacyl glycerol (DAG) and inositol 1,4,5-trisphosphate (IP3). DAG remains bound to the membrane, where as IP3 is released and diffuses through the cytosol and binds IP3
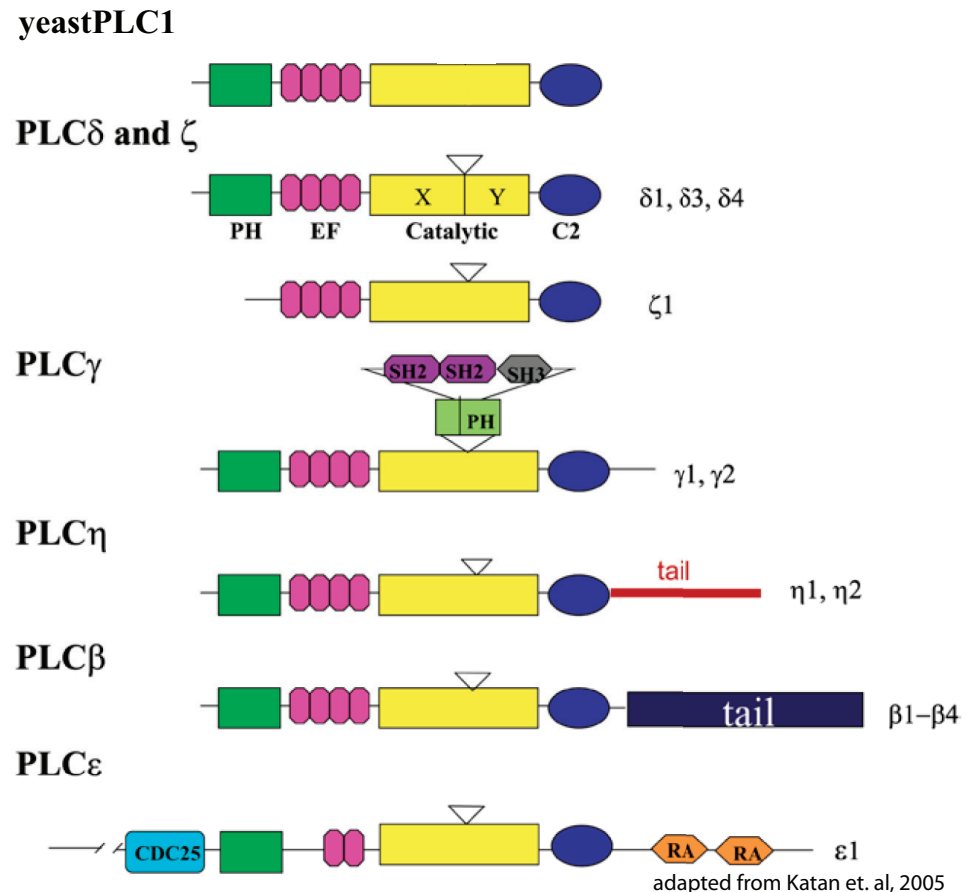
Figure 1.18: The structures of the different mammalian PLC isoforms and the yeast only PLC (Plc1) - The four domains of PLCδ, the PH domain, EF-hands (EF), catalytic domain (containing highly conserved X and Y regions) and the C2 domain (C2) are also present in most isoforms of other PLC families. The unique region of PLCγ , inserted through a flexible loop of the catalytic domain, includes the second PH domain, two SH2 (Src homology 2) regions and one SH3 (Src homology 3) region. PLCη contains the domain with a guanyl-nucleotide exchange factor activity (CDC25) and two predicted RA (Ras association) domains that are implicated in the binding of small GTPases from the Ras family. In PLCβ, the unique region (tail) is present at the C-terminus. The sequences unique to PLCζ (tail) are, as in PLCβ, located at the C-terminus. Although the domain organization of PLCζ resembles that of PLCβ. Yeast has only one PLC (Plc1) which is most homologous to mammalian PLCδ and expresses the same domains (Figure adapted from (51)).

receptors. IP3 receptors are particular calcium channels in the endoplasmic reticulum (ER). IP3 binding to the IP3 receptors leads to an increase in the cytosolic concentration of calcium, causing a cascade of intracellular changes and activity, e.g. activating C2- and EF- domain containing proteins like PLCs. A change of intracellular Ca^{2+} concentration can regulate many intracellular processes like: enzymatic activity, gene transcription, synaptic potential in neurons, contraction of muscle fibers, and many more (3). In addition, the calcium increase and DAG together work to activate protein kinase C (PKC). Activated PKC then goes on to phosphorylate other molecules, leading to altered cellular activity. In Figure 1.19 it is shown how the different PLC isoforms are activated and how downstream signaling is affected. In the following section the human PLC isoforms β and γ are discussed in more detail. PLC-β is cytoplasmic and nuclear and it has been shown that Memo influences PLC-γ activation (70).

1.3.2.1 Phospholipase Cβ

Mammalian PLCβ isozymes are differentially distributed in tissues, with the PLCβ1 being most widely expressed, especially in specific regions of the brain. PLCβ1 exists as alternatively spliced variants β1a and β1b, which differ in their carboxy-terminal residues (8). In the cytoplasm, PLCβ isozymes function as effector enzymes. They can activate receptors belonging to the rhodopsin superfamily of transmembrane proteins that contain seven transmembrane spanning segments. They are activated by a variety of stimuli and require special combinations of Gα and Gβ/γ subunits to couple to the effector.

In the nucleus of several cell lines, PLCβ1 is the predominant isoform (24)(68). For this nucleolar localization the C-terminal has an essential role (53). The first demonstration came from observations on Swiss 3T3 mouse fibroblasts brought to a quiescent state and then stimulated with the mitogen insulin-like growth factor-1 (IGF-1).

1.3.2.2 Phospholipase Cγ

PLC-γ is unique as it is the only PLC isoform expressing a SH2 and SH3 domains. SH2 (Src Homology 2) and SH3 (Src Homology 3) are small peptide sequences. These sequences mediate protein tyrosine kinases induced protein-protein interactions in signal transduction pathways. SH2 domains bind to short phosphotyrosine-containing
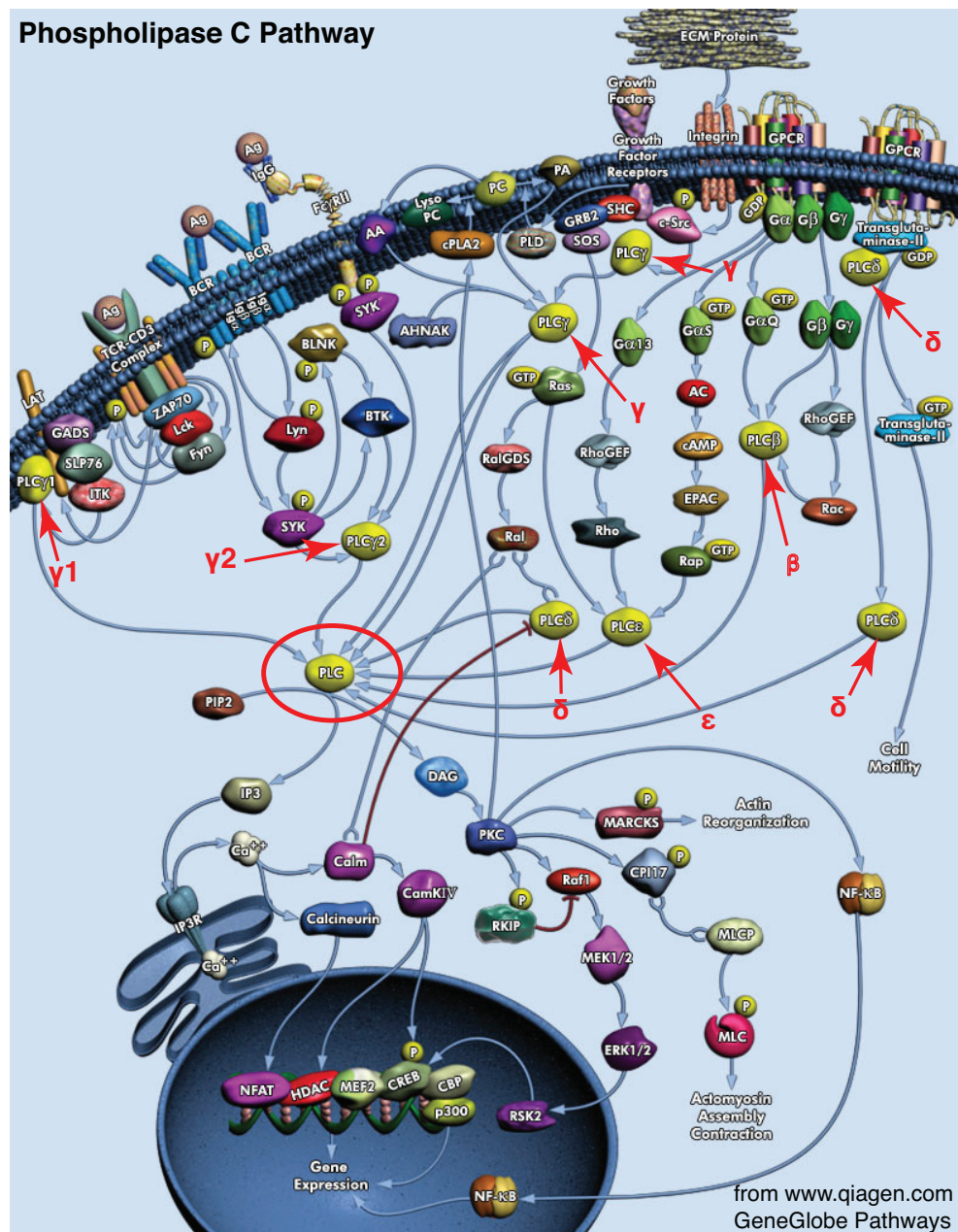
Figure 1.19: Phospholipase C isoforms and Pathways - The PLC family in human is comprised of 13 subtypes. On the basis of their structure,they have been divided into six classes,PLC-β (β1,2,3 and 4),PLC-γ (γ 1 and 2),PLC-δ (δ 1,3 and 4),PLC-ϵ,PLC-ζ and PLC-η (η and 2) types. The above described groups vary in many aspects like weight or how they get activated upon ligand binding of various receptors. Plc association with membrane receptors which form a positive regulation are best known for the Beta- and Gamma-type isozymes. In this figure the PLC subtypes are marked with a red arrow and the greek letter. The hydrolyzation of (PIP2) to generate the signaling molecules inositol IP3 and DAG by PLCs is highlighted by a red ring and is shown in the middle of the cell (not at the plasmamembrane).

sequences in growth factor receptors and other phosphoproteins. SH3 domains bind target proteins by recognizing a proline and hydrophobic amino acids containing sequence.

SH2 and SH3 domain containing proteins, such as Grb2 and phospholipase C gamma, utilize these modules in order to link receptor and cytoplasmic protein tyrosine kinases to the Ras signaling pathway and to phosphatidylinositol hydrolysis, respectively.

PLC-γ is generally stimulated by growth factors. Due to this it is a prime candidate for the induction of cell growth and proliferation, although the absolute requirement of this enzyme for mitogenic signaling is species and cell-type dependent.

Experiments with differential expression of rat brain PLC isoforms in development and ageing demonstrated showed that PLCγ activity was highest in fetal tissue and suggested that this isoform was therefore particularly involved in cell division and growth. In addition to that, PLCγ expression is significantly upregulated in colorectal and human breast carcinomas compared with normal tissue and is also highly expressed in a number of colon carcinoma cell lines (77).

Experiments in which wild-type PLCγ1 was overexpressed showed induction of DNA synthesis and alteration of both the growth rate and the morphology of quiescent fibroblasts. Interesting was the finding that lipase-deficient mutants of PLCγ1 can also induce DNA synthesis in quiescent fibroblasts, although not to maximal levels. Coinjection of IP3 and DAG with the lipase-defective PLCγ1 mutant restored maximal DNA synthesis; thus catalytic activity potentiated the mitogenic response under these circumstances. This suggests that regions other than the catalytic domain may be responsible, at least in part, for mitogenic signaling. Further studies in this area have demonstrated that microinjection of the complete SH domain (two SH2 and one SH3 domain) of PLCγ1 induces a 25-fold increase in DNA synthesis in quiescent fibroblasts, whereas microinjection of the PH domain had no effect. Fragments of the complete SH domain, including the two SH2 domains and the SH3 domain preceded by tyrosine phosphorylated residues at positions 771 and 783, each induced a partial response. These responses were additive on coinjection (95). Intriguingly, there is also increasing evidence from a number of tissues, including VSM, that tyrosine phosphorylation, although undoubtedly necessary, may not always be sufficient to induce full activation of

PLCγ. Indeed, tyrosine phosphorylation of PLCγ may instead be critical for translocation of the enzyme from the cytosol to the actin cytoskeleton (117). Platelet-derived growth factor stimulation of fibroblasts results in the localization of tyrosine 783 phosphorylated PLCγ1 at membrane ruffles and stress fibers, where it colocalized with actin filaments. Both this localization and the subsequent depolymerization of actin filaments can be prevented by injection of both an antibody to tyrosine 783 phosphorylated PLCγ1 and by a PLCγ1-2SH2 domain protein. Intriguingly, microinjection of a 13-amino acid phosphorylated peptide, containing tyrosine 783 alone, can also induce disassembly of actin filaments and membrane ruffling in fibroblasts, suggesting that catalytic activity is not necessary for actin rearrangement (Figure 1.20). In accordance with these studies, the introduction of a mutant PLCγ1 in which phenylalanine had been substituted for tyrosine at position 783 resulted in cells taking on a different morphology from those expressing wild-type PLCγ1, exhibiting both much thicker actin filaments and reduced DNA synthesis (82).

Clearly then, PLCγ isoforms are implicated in mitogenic signaling, with a major role of these isoforms being the reorganization of the actin cytoskeleton, which can occur independently of the catalytic activity of this enzyme.

1.4 Nuclear import and export

The most prominent feature of eukaryotic cells compared to procaryotic cells is the presence of a nucleus, which is defined by the nuclear envelope (NE). The NE physically separates nuclear DNA from the cytoplasm. This membrane specially devides the sites of gene transcription and ribosome biogenesis from the site of protein synthesis. This compartmentalization allows the cell to strictly coordinate numerous key cellular processes, it requires a efficient shuttling system of proteins and RNAs between nucleus and cytoplasm. To understand the mechanisms that drive nucleo-cytoplasmic transport pathways, and how they influence cell growth, numerous studies have focused on unraveling the web of physical interactions that facilitate transport (reviewed in (32)).

1.4.1 Nuclear import

In the nucleus most of the genetic information is stored. Because transcription is localized to the cytoplasm and translation takes place in the nucleus the two actions are kept
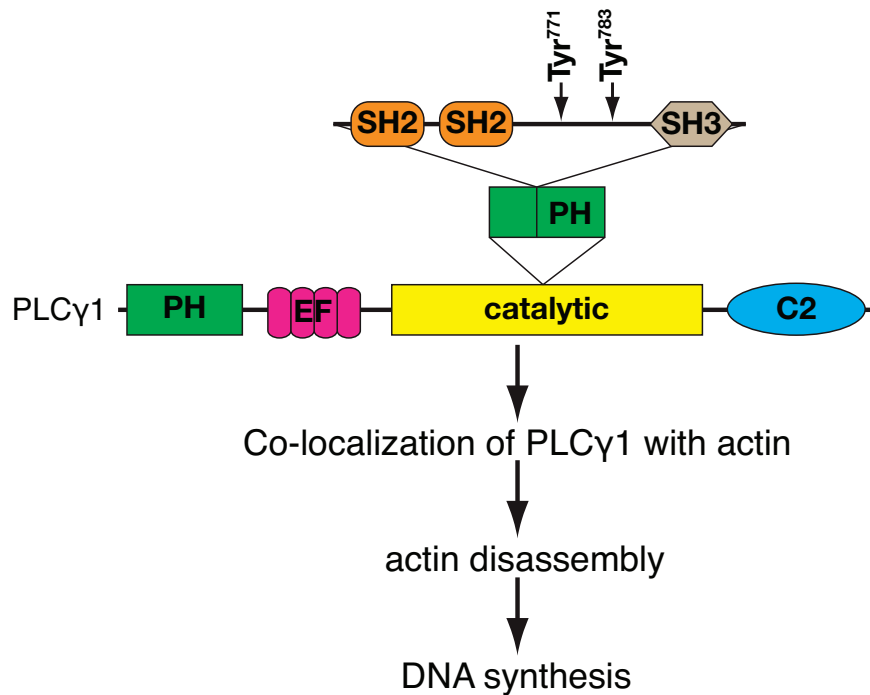
Figure 1.20: signaling through PLCγ1 without production of IP3 and 1,2-diacylglycerol (DAG) - The figure shows a schematic depicts effects of complete SH domain of PLCγ1. Between the 2 SH2 domains and the SH3 domain the two Tyr residues Tyr771 and Tyr783 are shown. Upon their phosphorylation PLCγ1 can co-localize with actin and induce/support actin disassembly which itself can control transcription, e.g via MRTF (myocardin-related transcription factors) and SRF (serum response factof) (reviewed in (78, 85)).

apart from each other by a double lipid bilayer also known as the nuclear envelope (NE). The nuclear envelope is composed of an inner and an outer nuclear membrane (INM and ONM). To allow material transport between the two compartments the INM and ONM are cross-linked at well defined points by large macromolecules. These macromolecules form a pore through the two membranes which are known as the nuclear pore complex (NPC). This setup allows only transport through the NPC to shuttle material between nucleus and cytoplasm. The NPC is not a simple channel, but can selectively import or export macromolecules across the two membranes and act as a semi-permeable filter (reviewed in(101)). Accordingly, proteins smaller than approx. 40 kDa can freely diffuse through the NPC, while larger proteins are actively transported through the NPC. That directed transport is organized by dedicated nuclear transport receptors of the β-karyopherin family, which includes at least 20 different known importins and exportins in humans (74).

1.4.1.1   Classical NLS (Nuclear localization sequence)

Importins can recognize protein that must be actively imported to the nucleus from the cytoplasm because they carry a nuclear localization signal (NLS). A NLS is a sequence of amino acids that acts as a tag (73). The NLS can vary in the Aa composition but are most commonly hydrophilic, although hydrophobic sequences have also been found to act as NLS (14).

Importins bind their cargo protein (targeted into the nucleus) in the cytoplasm. The importin-cargo complex is able to interact with the NPC and pass through its channel. Arrived inside the nucleus the interaction of the complex with Ran-GTP causes a change in the conformation in the importins. This conformational change causes the dissociation of the cargo proteins. The newly formed complex of importin and Ran-GTP then recycles back to the cytoplasm (reviewed in (41)) (Figure 1.21).

1.4.2   Nuclear export

In general terms the reversion of nuclear import is the nuclear export. In the nucleus exportins bind the cargo (proteins to be exported) having the appropriate signal sequence and Ran-GTP. The now formed complex gets transported through the nuclear pore into the cytoplasm. In the cytoplasm the complex dissociates. Ran-GTP binds
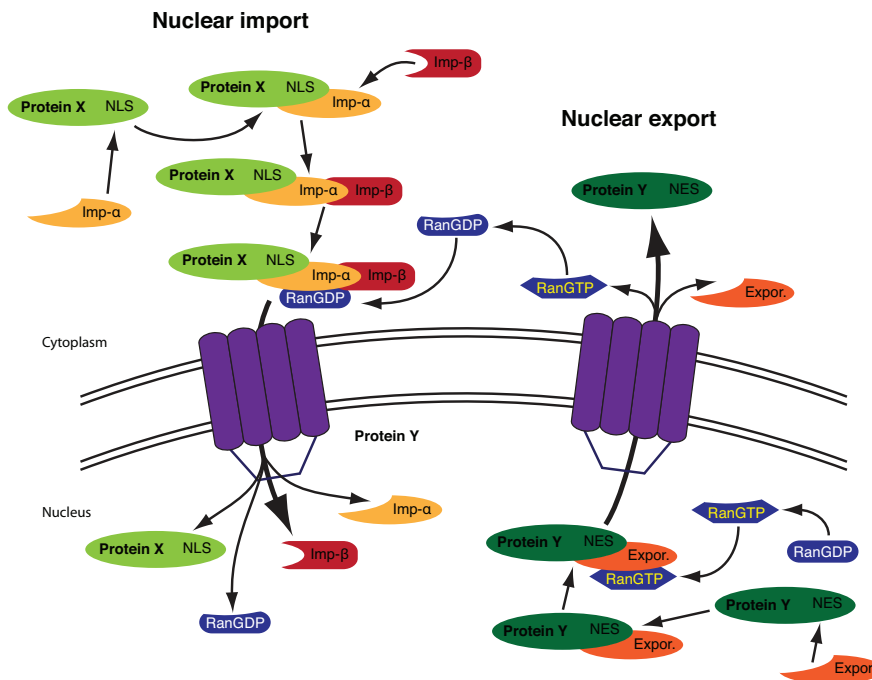
Figure 1.21: Nuclear Import and Export - The recognition of the classical nuclear lo-
calization signal (NLS) of the protein to be imported (Protein X) by importin-α (Imp-α) ini-
tiates the process of nuclear import. Importin-aα subsequently dimerizes with importin-β
and localizes to the nuclear envelope where it binds Ran-guanosine diphosphate (RanGDP)
and docks at the nuclear pore. After passing the nuclear pore the importin complex dis-
sociates and releases its cargo into the nucleus.The imprtins α and β get recyled back to
the cytoplasm. In nuclear export, the exportins (Expor.) recognizes proteins containing
leucine-rich nuclear export signals (NESs) (in this figure Protein Y). For nuclear export
the GTP-bound form of Ran (RanGTP) is required. Export complex formation is favored
by high concentrations of RanGTP in the nucleus, which facilitates translocation through
the central channel of the nuclear pore complex. Upon passing the nuclear pore and arrival
in the cytoplasm, the export complex is disassembled and cargo released.

GAP and the GTP get hydrolyzed, the resulting Ran-GDP recycles back into the nucleus where it exchanges its bound ligand for GTP and the cycle can restart. This means that importins depend on RanGTP to dissociate from their cargo, where as exportins require RanGTP in order to bind to their cargo (84) (Figure 1.21).

To efficiently export newly formed mRNA from the nucleus there is a specialized mRNA exporter protein. After post-transcriptional modifications are completed the mature mRNA gets actively exported by this complex. This translocation process depends on the Ran protein, although the exact mechanism how mRNA export is regulated is not yet fully understood. Some particularly commonly transcribed genes are physically located near nuclear pores to facilitate the translocation process (reviewed in (20)).

1.4.2.1 NES (Nuclear export sequence)

Other than the NLS the nuclear export signal (NES) is not as clear defined. The NES consists of a short Aa sequence of 4 hydrophobic residues. The exportins recognize this residues and bind them. The exportin-cargo-complex then shuttles the cargo from the nucleus to the cytoplasm through the nuclear pore complex. A NES has the opposite effect of a NLS. In silico analysis of known NESs found the most common spacing of the hydrophobic residues to be $L_{xxx}L_{xx}L_xL$, where "L" is a hydrophobic residue (often leucine) and "x" is any other amino acid. A explanation for the spacing of the hydrophobic residues may give examinations of known structures that contain an NES. Usually the critical residues lie on the same side of a protein to facilitate the interaction with the exportins (60).

2

Aims of the project

2.1 Phenotypic and functional analysis of the MEMO homolog in *Saccharomyces cerevisiae MHO1* by using screening techniques to place it in a pathway / Does yeast MEMO have a role in actin and/or microtubule dynamics?

Memo was found to be a novel ErbB2 P-Y binding protein which has a role in ligand induced actin and microtubule depended migration. As Memo is highly conserved in evolution and is also found in *Saccharomyces cerevisiae*, we wanted to use this well studied model organism to elucidate the function of Memo.

To answer this question we used major large scale screen techniques and genetic manipulations in yeast to find a phenotype for Memo deleted cells. We did two different synthetic lethal screens, we tried TAP-tag purification to find binding partners of Memo, and we also did micro-arrays. But not only large scale screens were used, we also took advantage of the genetic manipulation which are better studied in yeast than in mammalian cells.

2.2 MEMO nuclear localization in mammalian and yeast cells

During this work it became evident that not only the yeast Memo protein localizes to the nucleus, but also the mammalian protein is manly found in the nucleus. Confocal

microscopy analysis in quantification of signal intensity in SKBR3 cells labeled for Memo showed that more than 60% of Memo protein is nuclear independent if the cells are starved, grown in full medium or induced with HRG (heregulin). Upon stimulation of the cells with the appropriate factors Memo is also found at the plasma membrane but no conditions are known where it completely leaves the nucleus. We then focused on the questions how the localization of Memo is controlled and if nuclear localization is essential for the function of the protein.

2.3   Could MEMO be an enzyme?

The 3D structure of Memo has been solved and it shows high similarity to a Lig B subunit of LigAB is a class III nonheme iron(II)-dependent extradiol-type catechol dioxygenase found in *Sphingomonas paucimobilis*. Even though the amino acid sequence homology is low (15%) most of the amino acids that are essential for the dioxygenase function (see Figure 2.1)are also present in all Memo protein found in all kingdoms of live. The obvious question we addressed was then, does Memo have a dioxygenase activity? And if not, could this conserved protein still be an enzyme?
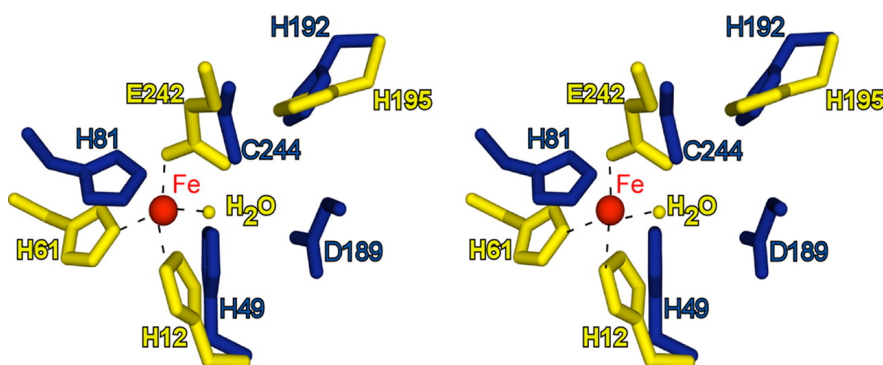
Figure 2.1: Stereo image of a superposition of the LigB active site residues with the homologous residues in Memo. - Memo residues are colored blue, and LigB residues are colored yellow. The E242 from LigB is not present in Memo. Memo has the C244 which coordinates to that specific position. (Figure from (89)).

3

Paper (published in PLoS ONE 2012 March 7)

MHO1, an evolutionarily conserved gene, is synthetic lethal with *PLC1*; Mho1p has a role in invasive growth.

Ivan Schlatter[1], Maria Meira[1]*, Vanessa Ueberschlag[1], Dominic Hoepfner[2], Rao Movva[2], Nancy E. Hynes[1]

[1] Friedrich Miescher Institute for Biomedical Research, 4058-Basel, Switzerland

[2]Novartis Institutes for Biomedical Research, Novartis Campus, 4026-Basel, Switzerland

*Current address: Department of Biomedicine, University Hospital Basel, Basel, Switzerland

Competing interests: there are no competing interests.

3.1 Abstract

The novel protein Memo (Mediator of ErbB2 driven cell motility) was identified in a screen for ErbB2 interacting proteins and found to have an essential function in cell motility. Memo is evolutionarily conserved with homologs found in all branches of life; the human and yeast proteins have a similarity of $> 50\%$. In the present study we used the model organism *S. cerevisiae* to characterize Mho1 (Yjr008wp) and to investigate its function in yeast. In a synthetic lethal screen we found *MHO1* as a novel synthetic lethal partner of *PLC1*, which encodes the single phospholipase C in yeast. In the absence of *MHO1* and *PLC1*, double-deleted spores germinate, but their proliferation is impaired. Introduction of human Memo into the memoΔplc1Δ strain rescued the synthetic lethal phenotype suggesting that yeast and human proteins have similar functions. Mho1 is present in the cytoplasm and the nucleus of yeast cells; the same distribution of Memo was found in mammalian cells. None of the Memo homologues have a characteristic nuclear localization sequence, however, a conserved nuclear export sequence is found in all. In mammalian cells, blocking nuclear export with Leptomycin B led to nuclear Memo accumulation, suggesting that it is actively exported from the nucleus. In yeast *MHO1* expression is induced by stress conditions. Since invasive growth in *S. cerevisiea* is also stress-induced, we tested Mho1s role in this response. *MHO1* deletion had no effect on invasion induced by nutrient deprivation, however, Mho1 overexpression blocked the invasive ability of yeast cells, suggesting that Mho1 might be acting in a dominant negative manner. Taken together, our results show that *MHO1* is a novel synthetic lethal interactor with *PLC1*, and that both gene products are required for proliferation. Moreover, a role for Memo in cell motility/invasion is conserved across species.

3.2 Introduction

Memo (Mediator of ErbB2 driven cell motility) was identified in a screen for ErbB2 receptor tyrosine kinase (RTK) interacting proteins with roles in cell motility. Memo specifically interacted with a phospho-peptide encompassing an autophosphorylation site in the C-terminus of ErbB2. Treatment of tumor cells with the ErbB2 activating ligand heregulin (HRG) induces migration and in siRNA-mediated Memo knock-down (KD) cells, HRG-induced migration is dramatically impaired [1,2]. Memo is encoded

by a gene found in all kingdoms of life, and multiple sequence alignment showed that the protein sequence is highly conserved. Memo has no obvious functional domain and does not belong to a known protein family. Interestingly, Memo is structurally homologous to a LigB, a non-heme iron binding dioxygenase [3], however, Memo lacks an essential glutamate that is present in all LigB family members, making it unlikely to be a functional dioxygenase [3]. The yeast gene *YJR008W* shows more than 50% similarity with the human gene and was named *MHO1* (Memo HOmolog 1). In the present study, we investigated the function of Mho1 (Yjr008wp) in *S. cerevisiae*. We show here that *MHO1* is a novel synthetic lethal (SL) interactor with *PLC1*. Yeast cell germinate in the absence of both genes, however, they cannot proliferate. Moreover, we found that under conditions of nutrient insufficiency Mho1 plays a role in haploid invasive growth. This suggests that a function for Memo in cell motility/invasion appears to be conserved across species

3.3 Results

3.3.1 *MEMO* is a single copy gene conserved throughout evolution

To identify *MEMO* homologs in other sequenced organisms, we performed a blastp search (Basic Local Alignment Search Tool), using the blastp tool provided from NCBI (as described in [4]), and the human Memo protein sequence as query. One copy of a *MEMO* homolog was found in various species representing all kingdoms of life (Figure 3.1 A). By performing multiple sequence alignments we could show that Memo is highly conserved. The human and the yeast protein share an identity of more than 40% and a similarity of more than 50%. Some amino acids are completely conserved from bacteria to human; in particular those close to the predicted vestigial active site of Memo (indicated in red, Figure 3.1 B). This suggests that these amino acids could be essential, for example, for a potential enzymatic activity, or as part of a novel conserved binding domain. The yeast gene, *YJR008W*, was named *MHO1* (Memo HOmolog 1). In this paper the human gene and protein are referred to as *MEMO* and Memo, respectively; the yeast gene and protein are referred to as *MHO1* and Mho1, respectively.

3.3.2   Examination of effects of *MHO1* deletion in *S. cerevisae*

MHO1 was deleted in the wild-type strains BY4741, BY4742, and BY4743 [5] by standard methods. The deletion of *MHO1* in haploid or diploid cells had no effect on viability, nor did it affect growth in liquid culture at 20C, 30C, and 37C. The *mho1Δ* cells were also tested for their sensitivity to various agents including hydroxyurea (HU), NaCl, $CoCl_2$, rapamycin, and benomyll. No difference in growth was observed in *mho1Δ* cells compared to the wild-type cells (Figure S3.8).

Memo is required for migration to tumor cells in response to activation of various RTKs and Memo KD impacts on the actin and microtubule (MT) cytoskeleton [1,2]. Accordingly, we investigated if Mho1 has a role in yeast motility and cytoskeletal morphology. To visualize the MTs, we used a yeast strain expressing a copy of TUB1-GFP using the plasmid pAFS125 [6]. *MHO1* deletion was introduced into this strain by replacement with the *klTRP1* selection marker. Using fluorescent microscopy, we observed no difference in the microtubule cytoskeleton between wild-type and *mho1Δ* strains (Figure 3.2 A). The actin-containing structures (reviewed in [7]) were also examined by microscopy. Neither the cortical actin patches, nor the actin cables differed between the wild-type and *mho1Δ* strains (Figure 3.2 B, 1 and 2, respectively,); actin rings or actin at the site of polarized growth were also unaffected by Mho1 loss. Thus, Mho1 is not required to maintain normal actin or MT cytoskeletal structures.

3.3.3   The deletion of MHO1 in fungal species does not affect polarized growth

To investigate if Mho1 has a role in polarized growth in fungi, we used the well-studied model organism *Asbya gossypii* [8], a filamentous growing ascomycete. Since filaments can grow at 200μm/h, *A. gossypii* requires sustained polarisation at the growing tip; crucial is the interplay between the actin cytoskeleton, microtubules, and proteins involved in polarised growth [9,10]. The *A. gossypii* homolog gene is *AGR321W*, which we will refer to as *MHO1*, for simplicity. The *A. gossypii MHO1* deletion strain was generated by standard means [11]. The *mho1Δ* strain was viable and sporulation efficiency and spore morphology were identical to the wild-type strain. Four actin structures are well defined in *A. gossypii*: 1) cortical actin patches along the entire hypha, 2) actin patches at the tip, 3) actin rings at the site of septation, and 4) actin cables. In

Phalloidin-FITC labelled cells, all four structures were indistinguishable between the wild-type and the *mho1Δ* strain (1-4, respectively, in Figure 3.3A). We also measured radial growth speed after inoculating a few spores on an agar Petri dish containing full medium. Both wild-type and *mho1Δ* strains covered the entire plate within seven days (Figure 3.3B). No differences in growth speed, hyphal morphology or branching patterns were observed.

A. gossypii always uses filamentous growth; there is no switch from isotropic to polarized growth in response to external stimuli or changes in growth conditions. Thus, we also investigated the role of Mho1 in the *S. cerevisiae* mating response. In order to mate, haploid cells recognize pheromone of the opposite mating type cell and extend a shmoo towards the pheromone gradient (reviewed in [12]). Deletion of *MHO1* had no effect on the elongation of a hyphal-like structure in *S. cerevisiae* (Figure 3.3C) and mating efficiency was similar to wild-type.

3.3.4 Mho1 is present in the nucleus and the cytoplasm

To follow Mho1 sub-cellular localization, the endogenous protein was tagged at its C-terminus with GFP, by standard methods [13]. Mho1-GFP expressing cells were grown to stationary phase, since Mho1 expression is up-regulated under these conditions (Figures S3.9 and S3.10), and its localization was examined by fluorescent microscopy. Mho1-GFP was found in the cytoplasm and the nucleus; no GFP signal was detected in the vacuole (Figure 3.4A, labelled c, n and v, resp.). Although Mho1 expression levels are lower in log-phase cells, a similar distribution was observed. To examine the localization of the human Memo in yeast, we cloned the GFP-tagged *hMEMO* gene into an integrative plasmid, which was integrated into the *TRP1* locus. *hMEMO* expression was induced by galactose and GFP was visualized. Human Memo-GFP has a similar distribution as the yeast protein, and is present in cytoplasm and nucleus, but not in the vacuole (Figure 3.4B).

Memo localisation was also examined by immunofluorescence (IF) in mammalian cells using a Memo-specific specific antibody [1]. IF for Memo carried out on mouse embryonic fibroblasts (MEFs) revealed cytoplasmic and nuclear staining, with exclusion from the nucleoli (Figure 3.4C). IF for Memo in SKBR3 breast tumor cells revealed that in growth medium containing 10% fetal calf serum, Memo was distributed in the cytoplasm and the nucleus (Figure 3.4D, left panel). In response to ErbB2 activation,

in HRG-treated cultures, the cytoplasmic Memo is strongly localized at the plasma membrane and appears enhanced in the nucleus (Figure 3.4D, right panel). However, quantification of the images did not reveal any significant differences in nuclear Memo in the two conditions. Thus, the human and the yeast protein are localized to similar sub-cellular compartments.

3.3.5   Memo is actively exported from the nucleus

Although Memo and Mho1 were present in the nucleus of yeast and mammalian cells, neither protein has a nuclear localization signal (NLS). However, a consensus nuclear export sequence (NES), $L_{xxx}L_{xx}L_xL$ (L= Leucine or hydrophobic amino acid and X = any amino acid), was identified in both proteins and was found to be conserved throughout evolution (Figure 3.5A). Using the 3D protein structure of Memo [3] as a model, the NES is located between β-sheet 2 and α-helixC on an approximately 15 residue loop on the surface of the protein (red ribbon in Figure 3.5B).

The 33 KDa Memo could diffuse through the nuclear pore, but might also be actively imported and/or exported from the nucleus. To test this, we used SKBR3 human breast tumor cells and examined the effects of HRG and the nuclear export inhibitor Leptomycin B [14] on Memo distribution. IF revealed that there was no significant difference between nuclear Memo levels in the control compared to the HRG treated cultures (Figure 3.5C, panel A vs. B), confirming the results shown in Figure 3.4D. To block export, SKBR3 cultures were treated overnight with 60 ng/ml Leptomycin B, then were either left untreated or were exposed shortly to HRG. Compared to the control cells in 10% FCS, there was a significant accumulation of nuclear Memo in the Leptomycin B treated SKBR3 tumor cells (Figure 3.5C, panel A vs C). Moreover, after 20 min of HRG treatment, there was a further increase in nuclear Memo in the Leptomycin B treated cultures (Figure 3.5C, panel C vs D). These results suggest that Memo might enter the nucleus passively, either alone or in a complex, but once in the nucleus Memo is actively exported.

3.3.6   *MHO1* is synthetic lethal with *PLC1*

To further analyze Mho1 function, we performed a SL screen in *S. cerevisiae*. A *MHO1* deleted strain was made and mated with each of the 4800 viable haploid deletion strains. The only strain that showed a SL phenotype with *MHO1* deletion was *PLC1* deletion,

the gene encoding the single isoform of phospholipase C found in yeast. To verify these results, we examined the growth of the wild-type strain and strains individually and double- deleted in *MHO1* or *PLC1*. This was accomplished by constructing *Matα mho1::natMX* and *Mata plc1::kanMX* strains, which were mated and sporulated. The dissected spores were then tested for growth on YPD plates plus G418 or ClonNat. Only wild-type cells, and *mho1Δ* or *plc1Δ* deleted cells could grow; none of the double-deleted cells grew (highlighted in Figure 3.6A with a white circle). It should be mentioned that the *plc1Δ* colonies are smaller since the deleted cells grow more slowly. In summary, the SL interaction between *MHO1* and *PLC1* uncovered in the large scale screen, could be verified.

Next, we analyzed if the SL phenotype is due to a germination defect or if it occurs in proliferating cells. For this, we cloned the *PLC1* gene including its endogenous promoter and terminator in a CEN/ARS plasmid with the *URA3* selection marker (Figure 3.6B), and introduced it into the *plc1Δ* cells. After mating with the *mho1Δ* strain and subsequent sporulation, the wild-type, *mho1Δ*, *plc1Δ*, and *mho1Δ plc1Δ* stains, each with the pRS416_PLC1 plasmid, were isolated. After plating on 5-Fluoroorotic acid (5-FOA), which selects for loss of the *URA3* marker, all but the double-deleted strain grew (Figure 3.6C). Once the double-deleted cells loose the Plc1p expression plasmid, the cells stop proliferating. This experiment shows that Mho1 and Plc1 are not required for sporulation, but are needed for proliferation.

3.3.7 Human *MEMO* can replace MHO1 and rescue the SL phenotype with the *plc1Δ* strain

The yeast and the human gene share a similarity of ¿ 50% (Figure 1A). We tested if human MEMO can complement the function of the yeast gene in *plc1Δ* cells by replacing the yeast gene with the human gene. By mating the *mho1::hMEMO_natMX* strain with a *plc1::kanMX* strain and dissecting spores, we could show that haploid strains carrying both selection markers grew. These results demonstrate that human Memo can replace the yeast protein and rescue the SL phenotype with *plc1Δ* (Figure 3.6D).

3.3.8   Mho1 overexpression blocks haploid invasive growth

A large-scale screen examining the effects of gene disruption and overexpression on alcohol-induced filamentous growth uncovered Mho1 as having a potential function in this stress-induced process [15]. Not only alcohol, but other growth conditions including nutrient deprivation induce filamentous growth [16]. Under these conditions a haploid strain extends invasive filaments downward, which is referred to as haploid invasive growth [17]. Thus, we tested if Mho1 expression levels influenced haploid invasive growth in conditions of nutrient insufficiency. For this, Mho1 overexpression and deletion strains were made in the haploid invasive wild-type yeast strain Σ1278B [18]. Two deletion strains (Σ1278B *mho1::kanMX* and Σ1278B *mho1::URA3*) and two overexpression strains (Σ1278B *MHO1::OE* and Σ1278B *His-MHO1::OE*) were constructed (Figure 3.7A). To verify overexpression in response to galactose, extracts from Σ1278B *His-MHO1::OE* were tested in a western analysis using a His specific antiserum to detect Mho1. Only the extracts from cells grown on galactose showed high levels of His-Mho1 (Figure 3.7B).

To monitor invasive growth, the deletion and overexpression strains as well as control strains were streaked on YPD or YPGal plates, incubated for four days, and then washed with tap water to assess invasive potential. The deletion of Mho1 did not influence the invasion of the cells into the agar in any of the growth conditions (Figure 3.7C). In contrast, on the Gal plates, the two strains overexpressing Mho1 (Σ1278B *MHO1::OE* and Σ1278B *His-MHO1::OE*) failed to invade (Figure 3.7C). Taken together, the results suggest that while Mho1 is not essential for invasive growth, abnormal levels of the protein impede the process.

3.4   Discussion

Memo is evolutionarily conserved with homologs found in all branches of life. Memo was initially identified based on its importance in breast cancer cell motility in response to ErbB2 activation [2], where it was shown to have an essential role in promoting the directionality of motile cancer cells [1]. The human and yeast proteins have a similarity of ¿ 50% and in the work presented here we used *S. cerevisiae* to characterize Mho1, the yeast homolog. We uncovered a role for Mho1 in haploid invasive growth, which might be linked to its function in mammalian cells, suggesting that this activity is

conserved across species. Moreover, we uncovered a novel function for Mho1, namely a synthetic lethal interaction with *PLC1*. To date the genes that have been identified as SL with *PLC1, BUB1, BUB3* and *CBF1*, have roles in spindle-assembly checkpoint and damage (Supplemental Table 3.4); Mho1 has not been implicated in these processes. We show here that yeast cells germinate in the absence of *PLC1* and *MHO1*, however, they cannot proliferate.

Based on the importance of Memo in mammalian cell motility, we expected to find a role for Mho1 in yeast MT and/or actin dynamics. However, we were unable to uncover any differences between *mho1Δ* cells and wild-type cells. Neither the MTs nor the actin-containing structures in proliferating *S. cerevisiae* were abnormal in *mho1Δ* cells. Moreover, the filamentous ascomycete *A. gossypii*, which requires coordinated interactions between the actin and the MT cytoskeleton for growth, was not affected by *MHO1* deletion. However, we noticed during our studies that Mho1 levels increased as cells reached stationary phase. A search of publicly available data bases, revealed that *MHO1* RNA expression is induced 5-fold or more in stationary phase and other stress conditions [19] (Supplemental figures 3.9 and 3.10). While *mho1Δ* cells behaved similarly to wild-type cells in many of the stress conditions, we found that nutrient-deprived stress-induced haploid invasive growth was blocked in the presence of high Mho1 levels. Since *mho1Δ* cells were not impaired in haploid invasive growth, these results suggest that overexpressed Mho1p behaves in a dominant negative fashion. In summary, the results suggest that Mho1 might not have an essential role in normal cellular situations, but in a stress condition related to migration/invasion Mho1 levels need to be maintained at physiological levels for a normal response.

A large set of genes (approximately 900) showed a similar response to most of the environmental changes that induce *MHO1* expression [19]. Promoter analysis and subsequent characterization of the responses of strains mutant for some of these genes implicated the transcription factors Yap1, Msn2p and Msn4p in mediating the transcriptional response [19]. We analysed the promoter region of *MHO1* to find binding sites for transcription factors and uncovered potential sites for Msn2/Msn4 and Ino2/Ino4 (Supplemental Figure 3.11A). *MSN4* gene expression is itself Msn2/4p dependent and induced by stress, while *MSN2* expression is constitutive [19]. By consulting the data base from YEASTRACT (Yeast Search for Transcriptional Regulators And Consensus

Tracking) [20] we found additional TF that could potentially directly or indirectly affect *MHO1* transcription (Supplemental Figure 3.11B).

In the SL screen we found *MHO1* as a novel SL partner of *PLC1*. Introduction of human Memo into the *memo∆plc1∆* strain rescued the SL phenotype suggesting that yeast and human proteins have similar functions. The mechanism underlying the SL interaction is not currently known, however, it is interesting to discuss some possibilities. Plc1p hydrolyzes the membrane phospholipid PtdIns(4,5)P2 to produce 1,2 diacylglycerol (DAG) and inositol 1,4,5-trisphosphate (IP3). In mammalian cells, DAG is needed for activation of some PKC isoforms. In yeast, C1, the potential DAG binding domain of Pkcp, is not required to restore viability to *pkc∆* cells, suggesting that Pkcp is not involved in the SL phenotype. Moreover, in yeast multiple pathways provide DAG, making it unlikely that low DAG levels are responsible for the SL interaction with *MHO1*. We had a closer look downstream of IP3, the precursor to IP4, IP5 and IP6. These phospholipids control many processes in yeast cells, such as nuclear mRNA export [21] and chromatin remodeling [22]. (For a full list of activities see Supplement Figure 5). To examine the involvement of this pathway in the SL phenotype, we tested if *MHO1* is SL with *ARG82/IPK2, IPK1, KCS1* or *VIP1*, the four inositol polyphosphate kinases downstream of Plc1. All of the double-deleted strains were viable and grew similarly to *memo∆* cells, suggesting that none of the other InsPs are involved in the SL phenotype with *MHO1*. Thus, we can only speculate that IP3 has an activity outside of its role as a precursor to the other InsPs and that this is required for proliferation in the *memo∆* cells.

The SL phenotype uncovered in yeast is particularly intriguing since one of the mammalian PLC isoforms, PLCγ1, was identified in the same screen that uncovered Memo; PLCγ1 associated with a different ErbB2 autophosphorylation site [1]. Individual knock-down of either Memo or PLCγ1 impaired directed cell motility and simultaneous KD of both proteins totally blocked migration [2]. Since the *memo∆plc1∆* strain failed to proliferate, it was not possible to test for effects on migration. However, both proteins do have roles in invasion/migration. Plc1p is essential for the activity of a nitrogen-controlled signaling pathway that controls pseudohyphal growth, and as we show here, Mho1 overexpression blocks haploid invasive growth.

The fact that Memo is structurally homologous to a bacterial class of dioxygenases, makes it tempting to speculate that Memo might have enzymatic activity. However, as

mentioned in the Introduction, it is unlikely to have the same activity as the bacterial LigB family. Our current working hypothesis is that Memo is an enzyme, which might have acquired additional cellular activities during evolution, one being to serve an adaptor function. Indeed, in SKBR3 breast tumor cells, it was recently shown that Memo controls the association of RhoA and its effector mDia with the plasma membrane in response to ErbB2 activation, thereby impacting on recruitment of actin-binding proteins, MT dynamics [23] and migration [2]. These results suggest that Memo might be acting as an adaptor to localize proteins (and their activity) to specific cellular sites in order to initiate biological responses, in this case motility. The fact that Memo is also present in the nucleus, suggests that it might also have activities in this compartment. Future work will be aimed at uncovering the other roles of Memo and identifying its putative enzymatic activity.

3.5 Materials and methods

3.5.1 Strains and Media

For a complete list and genotypes of yeast strains used in this work, see Tables 3.1 and 3.2. For experiments with *S. cerevisiae* most strains are congenic with BY4741 BY4742, and BY4743 wild-type strains. The haploid and diploid bar-coded systematic deletion collections for nonessential genes are in the strains BY4741 and BY4742 and BY4743, respectively. These were purchased from Invitrogen. For filamentous growth and invasion assays the yeast strain Σ1278B was used (kindly provided by P. Jenoe, Biocenter, Basel). All deletion strains were made by PCR mediated homologous recombination using the *kanMX* [23] or the *natMX* [24] selection. Transformation of the yeast strains was done using the LiAc/SS Carrier DNA/PEG method as described [25]. The A. gossypii strains were constructed by PCR-based gene targeting as described [11] and were cultured as described [26]. Actin staining with Alexa Fluor 488 (Molecular Probes, Eugene, OR) was done as described [27].

3.5.2 DNA Manipulations, Plasmids and Strain Constructions

We applied a PCR-based method to construct gene deletion cassettes that were used in yeast transformations [24]. All deletion strains were made by using the *kanMX* [24],

the *natMX* [25], the *URA3MX* [29] or the *klTRP1* [30] deletion cassettes. Transformation of the yeast strains was done using the LiAc/SS Carrier DNA/PEG method as described [26]. Correct genomic integration of the corresponding construct was verified by analytical PCR [24]. Yeast strains were grown on: YPD-G418 (200 mg/l geneticin) to select for transformants that had integrated *kanMX* deletion cassettes; or on YPD-CloNat (100 mg/l nourseothricin) to select for transformants that had integrated *natMX* deletion cassettes. To replace the yeast gene with the human gene, the *humanMEMO-natMX* cassette was integrated. Growth on SD plates lacking uracil or tryptophan selected for transformants that had integrated *URA3MX* deletion cassettes, selected for the integration of the uptake of the plasmid pRS416, or *klTRP1* integration. Yeast strains were grown on YPD-5-FOA plates (100 mg/l 5-Fluoroorotic Acid) for selecting cells that have lost the *URA3* carrying pRS416 plasmid. The plasmids used in this work are listed in Table 3.3.

3.5.3   Generation of Mouse Embryonic Fibroblasts (MEFs)

Mouse embryonic fibroblasts (MEFs) were generated by standard procedures from Memo fl/fl embryos and were spontaneously immortalized by continued passaging in Dulbeccos modified Eagles medium (DMEM) supplemented with 10% Fetal Calf Serum (GIBCO Invitrogen AG, Basel, Switzerland) and Penicillin and Streptomycin (growth medium).

3.5.4   Microscopy

For yeast microscopy we used an Axioimager Z1 microscope (Carl Zeiss, Feldbach, Switzerland), equipped with a X-Cite 120 EXFO Metal Halide for fluorescence and Halogen for TL, a motorized XYZ stage, and a Plan-APOCHROMAT 100x/1.4 DIC Oil objective. GFP/Alexa488 (Zeiss #10) and DAPI (Zeiss #49) filter sets were used (Carl Zeiss, Feldbach, Switzerland). Fluorescence excitation was controlled by a shutter controller. We used a AxioCam MRm (1388 x 1040 pixels, Pixel size 6.45 ?m) back-illuminated, cooled charge-coupled device camera mounted on the primary port. We used the AxioVision software from Zeiss for data acquisition, processing and analysis.

SKBR3 cells (ATCC, Manassas, Virginia) were grown on glass coverslips (BD Biosciences, San Diego, CA) coated with 25 ug/m rat-tail collagen I (Roche Diagnostics) and MEFs were grown on μ-Slides 8well from ibidi (Martinsried, Germany), in DMEM

containing 10% FCS at 37C and stimulated with 10 nM HRG for 20 minutes. Cells were fixed with 4% paraformaldehyde and 3% sucrose in PBS, permeabilized in 0.2% Triton X-100 in PBS, and blocked with 1% BSA in PBS before incubation with the primary rat anti-?-tubulin antibody and mouse anti-Memo antibody. Alexa-Fluor 546 conjugated anti-rat antibody (Molecular Probes, Eugene, OR) and Alexa-Fluor 488 conjugated anti-mouse antibody (Molecular Probes, Eugene, OR) were used as secondary antibodies. F-actin was stained at room temperature with 2 U/ml FITC-labeled phalloidin (Molecular Probes, Eugene, OR). Cells were washed with PBS-Tween 0.1% and mounted with a mounting solution (ProLong Gold Antifade Reagent, Molecular Probes). Mounted samples were examined using Axioimager Z1 microscope (Carl Zeiss, Feldbach, Switzerland) or using the Laser Scanning Microscope Axio Imager Z2 with the LSM 700 scanning head. Pictures from MEFs were taken with the following equipment: The Axioimager Z1 microscope (Carl Zeiss, Feldbach, Switzerland) was equipped with a X-Cite 120 EXFO Metal Halide for fluorescence and Halogen for TL, a motorized XYZ stage, and a Plan-APOCHROMAT 100x/1.4 DIC Oil objective. GFP/Alexa488 (Zeiss #10) and DAPI (Zeiss #49) filter sets were used (Carl Zeiss, Feldbach, Switzerland). Fluorescence excitation was controlled by a shutter. We used a AxioCam MRm (1388 x 1040 pixels, Pixel size 6.45 μm) back-illuminated cooled charge-coupled device camera mounted on the primary port. We used the AxioVision software from Zeiss for data acquisition, processing and analysis. Pictures from SKBR3 cells were taken with the following equipment: Axio Imager Z2 with the LSM 700 scanning head was equipped with the Laser lines: 405 (5mW), 488 (10mW), 555 (10mW), 639 (5mW); and the Lights: Coolled 405, 490, 565 (RL), Halogen (TL), a motorized XYZ stage, and the objectives: Plan-Apochromat 20x/0,8 M27;?EC Plan-Neofluar 40x/1,30 Oil M27;?Plan-Apochromat 63x/1,40 Oil DIC M27. The Axio Imager Z2 had 2 Epifluorescence PMTs and 1 Transmission PMT. For acquisition we used the ZEN2010 software from Zeiss. Data were further processed and analyzed with Imaris from Bitplane Scientific Software (Zurich, Switzerland).

3.5.5 Signal intensity quantification

Z-stack Images taken with the Axio Imager Z2 with the LSM 700 scanning head were analyzed with ZEN2010 software and 3D image reconstruction was processed with

IMARIS software (Bitplane AG, Zurich, Switzerland). In order to determine the nuclear intensity of the Memo staining, nuclear surfaces were created using the automatic threshold and pixels from this area were extracted from the total surface area to create the cytoplasmic surface. The mean intensities from these two surfaces were then measured. The mean differences in starved cells were compared to those in treated cells using the Students t-test.

3.5.6   Invasion assay

Wild-type, mho1Δ and *MHO1* overexpressing Σ1278b strains were streaked out on YPD (yeast extract/peptone/dextrose) and YPGal (yeast extract/peptone/galactose) plates and were grown for 4-5 days at 30C. The plates were equally washed under a constant water stream to wash of non invasive strains.

3.5.7   SL Screen

In the yeast strain haploid matingtype-selectable Y5563 (*MATα; lys1Δ; his3Δ1; leu2Δ0; ura3Δ0; met15Δ0; can1::Mfapr-His3*) strain we deleted *MHO1* with the *natMX* deletion cassette and thus making it resistant to nourseothricin. The Y5563 *mho1::natMX* strain was then subsequently mated with each of the 4800 viable haploid deletion strains that were purchased from invitrogenTM. The mating was performed on agar plates in a 96-well format using standard methods on a singer pinning robot (RoToR HDA pinning robots from singer; www.singerinstruments.com).

3.6   Acknowledgements

3.7 References

1. Meira M, Masson R, Stagljar I, Lienhard S, Maurer F, et al. (2009) Memo is a cofilin-interacting protein that influences PLCgamma1 and cofilin activities, and is essential for maintaining directionality during ErbB2-induced tumor-cell migration. J Cell Sci 122: 787-797.

2. Marone R, Hess D, Dankort D, Muller WJ, Hynes NE, et al. (2004) Memo mediates ErbB2-driven cell motility. Nat Cell Biol 6: 22.

3. Qiu C, Lienhard S, Hynes NE, Badache A, Leahy DJ (2008) Memo is homologous to nonheme iron dioxygenases and binds an ErbB2-derived phosphopeptide in its vestigial active site. J Biol Chem 283: 40.

4. Papadopoulos JS, Agarwala R (2007) COBALT: constraint-based alignment tool for multiple protein sequences. Bioinformatics 23: 1073-1079.

5. Brachmann CB, Davies A, Cost GJ, Caputo E, Li J, et al. (1998) Designer deletion strains derived from Saccharomyces cerevisiae S288C: a useful set of strains and plasmids for PCR-mediated gene disruption and other applications. Yeast 14: 115-132.

6. Straight AF, Marshall WF, Sedat JW, Murray AW (1997) Mitosis in living budding yeast: anaphase A but no metaphase plate. Science 277: 574-578.

7. Moseley JB, Goode BL (2006) The yeast actin cytoskeleton: from cellular function to biochemical mechanism. Microbiol Mol Biol Rev 70: 605-645.

8. Ashby SF, Nowell W (1926) The Fungi of Stigmatomycosis. Annals of Botany 40: 69-84.

9. Philippsen P, Kaufmann A, Schmitz HP (2005) Homologues of yeast polarity genes control the development of multinucleated hyphae in Ashbya gossypii. Curr Opin Microbiol 8: 370-377.

10. Wendland J, Walther A (2005) Ashbya gossypii: a model for fungal developmental biology. Nat Rev Microbiol 3: 421-429.

11. Wendland J, Ayad-Durieux Y, Knechtle P, Rebischung C, Philippsen P (2000) PCR-based gene targeting in the filamentous fungus Ashbya gossypii. Gene 242: 381-391.

12. Jones SK, Jr., Bennett RJ (2011) Fungal mating pheromones: choreographing the dating game. Fungal Genet Biol 48: 668-676.

13. Wach A, Brachat A, Alberti-Segui C, Rebischung C, Philippsen P (1997) Heterologous HIS3 marker and GFP reporter modules for PCR-targeting in Saccharomyces cerevisiae. Yeast 13: 1065-1075.

14. Wolff B, Sanglier JJ, Wang Y (1997) Leptomycin B is an inhibitor of nuclear export: inhibition of nucleo-cytoplasmic translocation of the human immunodeficiency virus type 1 (HIV-1) Rev protein and Rev-dependent mRNA. Chem Biol 4: 139-147.

15. Jin R, Dobry CJ, McCown PJ, Kumar A (2008) Large-scale analysis of yeast filamentous growth by systematic gene disruption and overexpression. Mol Biol Cell 19: 284-296.

16. Lorenz MC, Cutler NS, Heitman J (2000) Characterization of alcohol-induced filamentous growth in Saccharomyces cerevisiae. Mol Biol Cell 11: 183-199.

17. Gancedo JM (2001) Control of pseudohyphae formation in Saccharomyces cerevisiae. FEMS Microbiol Rev 25: 107-123.

18. Gimeno CJ, Ljungdahl PO, Styles CA, Fink GR (1992) Unipolar cell divisions in the yeast S. cerevisiae lead to filamentous growth: regulation by starvation and RAS. Cell 68: 1077-1090.

19. Gasch AP, Spellman PT, Kao CM, Carmel-Harel O, Eisen MB, et al. (2000) Genomic expression programs in the response of yeast cells to environmental changes. Mol Biol Cell 11: 4241-4257.

20. Abdulrehman D, Monteiro PT, Teixeira MC, Mira NP, Lourenco AB, et al. (2011) YEASTRACT: providing a programmatic access to curated transcriptional regulatory associations in Saccharomyces cerevisiae through a web services interface. Nucleic Acids Res 39: D136-140.

21. York JD, Odom AR, Murphy R, Ives EB, Wente SR (1999) A phospholipase C-dependent inositol polyphosphate kinase pathway required for efficient messenger RNA export. Science 285: 96-100.

22. Desai P, Guha N, Galdieri L, Hadi S, Vancura A (2009) Plc1p is required for proper chromatin structure and activity of the kinetochore in Saccharomyces cerevisiae by facilitating recruitment of the RSC complex. Mol Genet Genomics 281: 23.

23. Zaoui K, Honore S, Isnardon D, Braguer D, Badache A (2008) Memo-RhoA-mDia1 signaling controls microtubules, the actin network, and adhesion site formation in migrating cells. J Cell Biol 183: 401-408.

24. Wach A, Brachat A, Phlmann R, Philippsen P (1994) New heterologous modules for classical or PCR-based gene disruptions in Saccharomyces cerevisiae. Yeast 10: 808.

25. Goldstein AL, McCusker JH (1999) Three new dominant drug resistance cassettes for gene disruption in Saccharomyces cerevisiae. Yeast 15: 53.

26. Gietz RD, Woods RA (2006) Yeast transformation by the LiAc/SS Carrier DNA/PEG method. Methods Mol Biol 313: 20.

27. Steiner S, Wendland J, Wright MC, Philippsen P (1995) Homologous recombination as the main mechanism for DNA integration and cause of rearrangements in the filamentous ascomycete Ashbya gossypii. Genetics 140: 973-987.

28. Ayad-Durieux Y, Knechtle P, Goff S, Dietrich F, Philippsen P (2000) A PAK-like protein kinase is required for maturation of young hyphae and septation in the filamentous ascomycete Ashbya gossypii. J Cell Sci 113 Pt 24: 4563-4575.

29. Goldstein AL, Pan X, McCusker JH (1999) Heterologous URA3MX cassettes for gene replacement in Saccharomyces cerevisiae. Yeast 15: 507-511.

30. Knop M, Siegers K, Pereira G, Zachariae W, Winsor B, et al. (1999) Epitope tagging of yeast genes using a PCR-based strategy: more tags and improved practical routines. Yeast 15: 963-972.

31. Hoepfner D, Brachat A, Philippsen P (2000) Time-lapse video microscopy analysis reveals astral microtubule detachment in the yeast spindle pole mutant cnm67. Mol Biol Cell 11: 1197-1211.

32. Tong AH, Evangelista M, Parsons AB, Xu H, Bader GD, et al. (2001) Systematic genetic analysis with ordered arrays of yeast deletion mutants. Science 294: 2364-2368.

33. Altmann-Johl R, Philippsen P (1996) AgTHR4, a new selection marker for transformation of the filamentous fungus Ashbya gossypii, maps in a four-gene cluster that is conserved between A. gossypii and Saccharomyces cerevisiae. Mol Gen Genet 250: 69-80.

34. Sikorski RS, Hieter P (1989) A system of shuttle vectors and yeast host strains designed for efficient manipulation of DNA in Saccharomyces cerevisiae. Genetics 122: 19-27.

35. Pan X, Yuan DS, Ooi SL, Wang X, Sookhai-Mahadeo S, et al. (2007) dSLAM analysis of genome-wide genetic interactions in Saccharomyces cerevisiae. Methods 41: 206-221.

36. Odom AR, Stahlberg A, Wente SR, York JD (2000) A role for nuclear inositol 1,4,5-trisphosphate kinase in transcriptional control. Science 287: 2026-2029.

37. Steger DJ, Haswell ES, Miller AL, Wente SR, O'Shea EK (2003) Regulation of chromatin remodeling by inositol polyphosphates. Science 299: 114-116.

38. Shen X, Xiao H, Ranallo R, Wu WH, Wu C (2003) Modulation of ATP-dependent chromatin-remodeling complexes by inositol polyphosphates. Science 299: 112-114.

39. El Alami M, Messenguy F, Scherens B, Dubois E (2003) Arg82p is a bifunctional protein whose inositol polyphosphate kinase activity is essential for nitrogen and PHO gene expression but not for Mcm1p chaperoning in yeast. Mol Microbiol 49: 457-468.

40. Romero C, Desai P, DeLillo N, Vancura A (2006) Expression of FLR1 transporter requires phospholipase C and is repressed by Mediator. J Biol Chem 281: 5677-5685.

41. Auesukaree C, Tochio H, Shirakawa M, Kaneko Y, Harashima S (2005) Plc1p, Arg82p, and Kcs1p, enzymes involved in inositol pyrophosphate synthesis, are essential for phosphate regulation and polyphosphate accumulation in Saccharomyces cerevisiae. J Biol Chem 280: 33.

42. York SJ, Armbruster BN, Greenwell P, Petes TD, York JD (2005) Inositol diphosphate signaling regulates telomere length. J Biol Chem 280: 4264-4269.

43. Saiardi A, Resnick AC, Snowman AM, Wendland B, Snyder SH (2005) Inositol pyrophosphates regulate cell death and telomere length through phosphoinositide 3-kinase-related protein kinases. Proc Natl Acad Sci U S A 102: 1911-1914.

44. Huang KN, Symington LS (1995) Suppressors of a Saccharomyces cerevisiae pkc1 mutation identify alleles of the phosphatase gene PTC1 and of a novel gene encoding a putative basic leucine zipper protein. Genetics 141: 1275-1285.

45. Luo HR, Saiardi A, Yu H, Nagata E, Ye K, et al. (2002) Inositol pyrophosphates are required for DNA hyperrecombination in protein kinase c1 mutant yeast. Biochemistry 41: 2509-2515.

46. Feng Y, Wente SR, Majerus PW (2001) Overexpression of the inositol phosphatase SopB in human 293 cells stimulates cellular chloride influx and inhibits nuclear mRNA export. Proc Natl Acad Sci U S A 98: 875-879.

47. Miller AL, Suntharalingam M, Johnson SL, Audhya A, Emr SD, et al. (2004) Cytoplasmic inositol hexakisphosphate production is sufficient for mediating the Gle1-mRNA export pathway. J Biol Chem 279: 51022-51032.

48. Hanakahi LA, Bartlet-Jones M, Chappell C, Pappin D, West SC (2000) Binding of inositol phosphate to DNA-PK and stimulation of double-strand break repair. Cell 102: 721-729.

49. Macbeth MR, Schubert HL, Vandemark AP, Lingam AT, Hill CP, et al. (2005) Inositol hexakisphosphate is bound in the ADAR2 core and required for RNA editing. Science 309: 1534-1539.

3.8   Figure legends

3.8.1   Figure 1: Phylogenetic tree and sequence alignment of Memo homologues in all kingdoms of life.

(A) The evolutionary distances between Memo protein sequences in the listed species are shown, using the human Memo as the query sequence. The % identity and % similarity, respectively, are indicated in brackets. (B) The protein sequence of Memo homologues in the species shown in panel A are presented. The red letters indicate the conserved amino acids in the putative active site [3].

3.8.2   Figure 2: Cytoskeleton analysis of wild-type and *memo*Δ strains of *S. cerevisiae.*

(A) To stain the tubulin cytoskeleton, a GFP-tagged *TUB1* expression vector, under its endogenous promoter was introduced into wild type and *memo*Δ cells. The arrows indicate (1) nuclear microtubules, (2) astral microtubules, and (3) the spindle pole body. (B) Phalloidin-OregonGreen was used to stain wild type and *memo*Δ cells. Two actin structures are stained: (1) cortical actin patches and (2) actin cables. There are no obvious differences in the microtubule structures or the actin cytoskeleton between wild-type and *memo*Δ cells.

3.8.3   Figure 3: Examination of filamentous growth in wild type and *memo*Δ cells.

(A) Actin was visualized in wild type and *memo*Δ *Ashbya gossypii* by staining with Phalloidin-OregonGreen. The stained actin structures are: (1) cortical actin patches, (2) actin patches at the tip, (3) actin rings at sites of septation, and (4) actin cables. There are no observable differences in the actin cytoskeleton between wild type and *memo*Δ strains. (B) A polarized growth assay was performed in *Ashbya gossypii*. Spores from the wild type and the *memo*Δ strain were spotted in the middle of an agar plate with full medium and radial growth was measured during 7 days. The picture was taken at the end of the experiment. (C) Shmoo formantion of wild type and *memo*Δ cells was visualized on YPD agar-coated microscopy slides, following stimulation of MATa cells for 4 hrs with α-factor.

3.8.4 Figure 4: Cellular localization of Memo in yeast and mammalian cells.

(A) Endogenous Mho1 was tagged C-terminally with GFP by homologous recombination in order to visualize Mho1. Yeast cells were grown 48 hrs to stationary phase in YPD and GFP was visualised by fluorescence microscopy. Mho1-GFP is present in the cytoplasm (c), the nucleus (n), and is excluded from the vacuole (v). (B) The human Memo-GFP was expressed in yeast cells and visualized. Memo is present in the cytoplasm, the nucleus and excluded from the vacuole. (C) Endogenous Memo was visualized in mouse embryonic fibroblasts (MEFs) using a specific Memo antiserum [1]. Memo is present in the cytoplasm (2), the nucleus (1) and is excluded from the nucleoli (3). (D) The same antibody was used for Memo staining in SKBR3 breast tumor cells. (left panel) Memo is found in the cytoplasm and the nucleus in cells grown in DMEM containing 10% FCS. (right panel) following treatment of cultures for 20 min with 10 nM HRG, Memo is recruited to the membrane. Quantification of nuclear signal intensity versus signal intensity outside the nucleus showed that the levels of nuclear Memo are approximately the same before and after the treatment.

3.8.5 Figure 5: Identification of a functional nuclear export sequence in Memo homologues.

(A) Using the NetNES 1.1 nuclear export sequence prediction software from CBS (Center for Biological Sequence analysis) a predicted NES, which is conserved various species was identified and highlighted in red. LxxxLxxLxL (L= Leucine or hydrophobic amino acid and X= any amino acid). (B) The NES of Memo is located between β-sheet 2 and α-helixC on a long loop on the surface of the protein (indicated by the red line). (C) IF for endogenous Memo in human SKBR3 breast tumor cells. The cells were treated with: 10% FCS -/+ Leptomycin B (panels A vs C), 10% FCS + HRG -/+ Leptomycin B (panels B vs D). Leptomycin B treatment was overnight.

3.8.6 Figure 6: *MEMO* is synthetic lethal with *PLC1*.

(A) A*memo*Δ a-strain (*memo::kanMX*) was mated to a *plc1*Δ α-strain (*plc1::natMX*). The resulting diploid strain was sporulated, the spores were grown on YPD plates and growing colonies were streaked out on YPD plates with G418 or ClonNat to test

for *memo*Δ and *plc1*Δ, respectively. The location of the *memo*Δ*plc1*Δ spores, where there was no growth, are indicated by white circle. *plc1*Δ colonies grow slower and are smaller. (B) The *PLC1* gene including its endogenous promoter and terminator were cloned into a CEN/ARS plasmid with the *URA3MX* selection marker (pRS416_PLC1). (C) By sporulating a diploid heterozygous *memo*Δ/*MHO1*; *plc1*Δ/*PLC1* deletion strain harbouring the *PLC1* expressing CEN/ARS plasmid, the three haploid deletion strains: *memo*Δ, *plc1*Δ, and *memo*Δ*plc1*Δ were created. Thes three and the wild-type strain were grown on SD-URA plates to select for the pRS416_PLC1 plasmid. When streaked on a 5-FOA plate, which selects for loss of the plasmid, all but the double-deleted cells grow, showing that once Plc1 expression is lost, cells stop growing. (D) A *mho1::hMEMO_natMX* strain was mated with a *plc1::kanMX* strain. The resulting diploid strain was sporulated and the spores were dissected on YPD. The upper portion of the figure shows the growing colonies, the lower portion shows the phenotype. The red triangles indicate the *mho1::hMEMO_natMX plc1::kanMX* strain proving that the human protein can complement for Mho1 in this assay.

3.8.7   Figure 7: Overexpression of Mho1 abolishes invasive growth in the haploid Σ1278B strain.

(A) Mho1 was overexpressed in the invasive yeast strain Σ1278B by integrating the pRS416_pGAL_6HIS-MHO1 and the BYintURA_pGAL_MHO1 plasmids. The *memo*Δ strains were made by replacing the endogenous gene with *kanMX* or *URA3MX*. (B) Overexpression of 6His-Mho1 is shown by western blotting using a His-tag specific antiserum. Mcm2 levels were used as a loading control. The lysates were: 1) Σ1278B wt grown on YPD, 2) Σ1278B wt grown on YPGal, 3) Σ1278B 6His-Mho1 OE grown on YPD, and 4) Σ1278B 6His-Mho1 OE grown on YPGal. (C) To test for invasive growth potential in strains lacking Mho1 or overexpressing the protein, the indicated strains were streaked out on YPD or YPGal (overexpressing conditions) agar plates. As controls, the wt Σ1278B or Σ1278B harbouring the empty pRS416_pGAL and BY-intURA_pGAL plasmid were used. After four days, the plates were washed under the water tap. Only cells overexpressing Mho1 on the YPGal plates were washed off the plates, showing that overexpression blocks haploid invasive growth.

3.9 Supplemental material

3.9.1 Figure S1: Spotting assay of wild-type and *mho1Δ* strains on various compounds

A wild-type and a *mho1Δ* strain were serial diluted and spotted on YPD plates (A) or SD complete plates (B), containing 800μM $CoCl_2$, 100μM benomyl, or 100μM rapamycin (A and B) and 800μM NaCl, or HU 100μM (B). No differences in growth between the *mho1Δ* and the wild-type strains were observed.

3.9.2 Figure S2: *MHO1* expression analysis

A summary of the published *MHO1* microarray data is presented. Conditions that increase or decrease *MHO1* expression are indicated in red or green, respectively. The data was taken from http://transcriptome.ens.fr/ymgv/. MHO1 is upregulated upon Msn2 overexpression leading to the hypothesis that *MHO1* is a a stress response gene.

3.9.3 Figure S3: Comparison of published *MHO1* and *PLC1* microarray data

Microarray data from Gasch et al., 2000 [19] analyzing the gene expression of yeast cells in response to environmental stress was used to compare *MHO1* and *PLC1* regulation.

3.9.4 Figure S4: *MHO1* promoter analysis

(A) An analysis of the *MHO1* promoter region (-1bp to -500bp from the START codon) revealed that there are two potential binding sites for Msn2/Msn4 (shown in green) and a potential UAS_{ino} (inositol-sensitive upstream activating sequence) binding site. The latter is often present in promoters of genes encoding phospholipid, fatty acid, and sterol biosynthetic enzymes. (B) Using the YEASTRACT (Yeast Search for Transcriptional Regulators And Consensus Tracking; database (http://www.yeastract.com/index.php), we identified a list of transcription factors that directly or indirectly regulate *MHO1* transcription

3.9.5 Figure S5: IP_3 signaling pathway

IP_3 and DAG are produced by the cleavage of PIP_2 by Plc1. IP_3 is released from the membrane and is the precursor of all other inositol phosphates (IPs). The four inositol

polyphosphate kinases (Ipk2/Arg82, Ipk1, Ksc1, and VIP1) further process IP_3 and constitute a nuclear signaling pathway. The major functions affected by the different IPs and the primary references are shown in this figure.

$IP_4 \Rightarrow$ Gene expression and Chromatin remodeling: [36,37,38,39,40,41]

$IP_5 \Rightarrow$ Telomere length and DNA repair: [42,43,44,45]

$IP_6 \Rightarrow$ mRNA Export, Non Homologous End Joining, RNA editing: [21,46,47,48,49]

3.9.6 Table S1

Genes involved in the cAMP/PKA/PLC pathway, which were tested with the *mho1Δ* strain; none were SL with *mho1Δ*.

3.10 Tables

Name	Genotype	Reference
BY4741	*MATa; his3Δ1; leu2Δ0; met15Δ0; ura3Δ0*	[5]
BY4742	*MATα; his3Δ1; leu2Δ0; lys2Δ0; ura3Δ0*	[5]
BY4743	*MATa/MAT? his3Δ0/his3Δ0; leu2Δ0/leu2Δ0; met15Δ0/MET15; LYS2/lys2Δ0; ura3Δ0/ura3Δ0*	[5]
DHY194	*MAT?; ura3-52Δ1::GFP-TUB1-URA3(pAFS125); trp1Δ63; leu2Δ1; his3Δ200*	[31]
Y5563	*MATα; lyp1Δ; his3Δ1; leu2Δ0; ura3Δ0; met15Δ0; can1::Mfapr-His3*	[32]
Σ1278	*MATa; ura3Δ0*	[18]
ISY42	*MATα; his3Δ;1 leu2Δ0; lys2Δ0; ura3Δ0; mho1Δ::natMX*	this study
ISY34	*MATa; his3Δ1; leu2Δ0; met15Δ0; ura3Δ0; plc1Δ::kanMX*	this study
ISY5	*MATα; ura3-52Δ1::GFP-TUB1-URA3(pAFS125); trp1Δ63; leu2Δ1; his3Δ200 mho1Δ1::klTRP1*	this study
ISY120	*MATa; ura3Δ0; mho1Δ::natMX*	this study
ISY229	*MATa; ura3Δ0; mho1Δ::URA3*	this study
ISY231	*MATa; ura3Δ0::BYintURA_PGAL_ADHterm_URA3*	this study
ISY129	*MATa; ura3Δ0::BYintURA_PGAL_6His-MHO1_ADHterm_URA3*	this study
ISY38	*MATα; lyp1Δ; his3Δ1; leu2Δ0; ura3Δ0; met15Δ0; can1Δ::Mfapr-His3; mho1Δ::natMX*	this study
ISY120	*MATa; ura3Δ0::mho1Δ::natMX*	this study
ISY229	*MATa; ura3Δ0::mho1Δ::URA3*	this study
ISY211	*MATa; ura3Δ0; pRS416*	this study
ISY203	*MATa; ura3Δ0; pRS416_pGAL_6HIS-MHO1*	this study
ISY203	*MATa; ura3Δ0; pRS416-6HIS-humanMEMO*	this study

Table 3.1: *S. cerevisiae* strains used in this study

Name	Genotype	Reference
WT	*leu2Δ; thr4Δ (Δl Δt)*	[33]
AGR321WΔ	*leu2Δ; thr4Δ; agr321wΔ::GEN3*	this study

Table 3.2: *A. gossypii* strains used in this study

Plasmid	Reference
pFA6_kanMX6	[24]
pFA_GFP(s65t)_kanMX6	[13]
pAG25	[25]
pRS416	[34]
pGEN3	[11]
pSO142	[35]
pRS416_pPLC1_PLC1_PLC1term	this study
pRS416_pGAL_ADHterm	this study
pRS416_pGAL_6HIS-MHO1_ADHterm	this study
BYintURA_pGAL_ADHterm	personal communication
BYintURA_pGAL_eGFP-hMEMO_ADHterm	this study
BYintURA_pGAL_MHO1_ADHterm	this study
pAG25_hMEMO	this study
pAG25_MYC-hMEMO	this study

Table 3.3: Plasmids strains used in this study

3.11 Figures
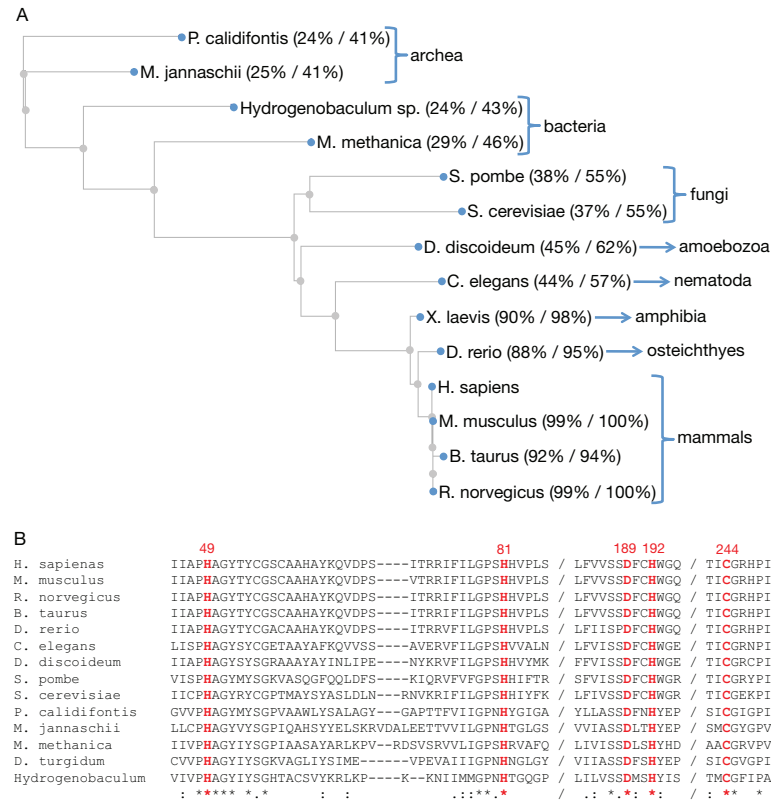
Figure 3.1: Phylogenetic tree and sequence alignment of Memo homologues in all kingdoms of life. -
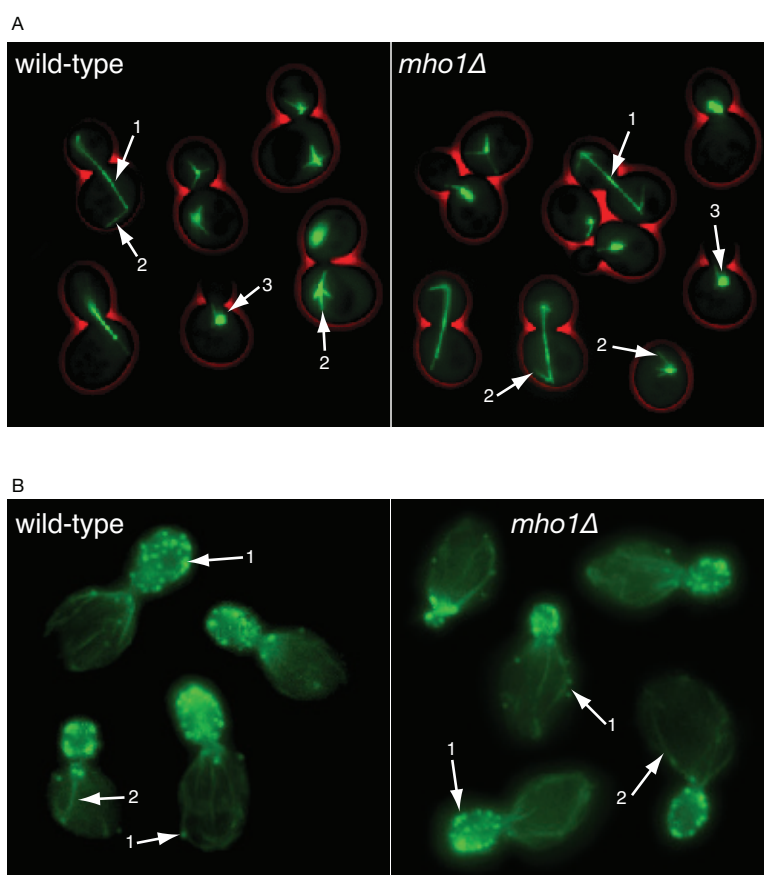
Figure 3.2: Cytoskeleton analysis of wild-type and *memo*Δ strains of *S. cerevisiae*. -
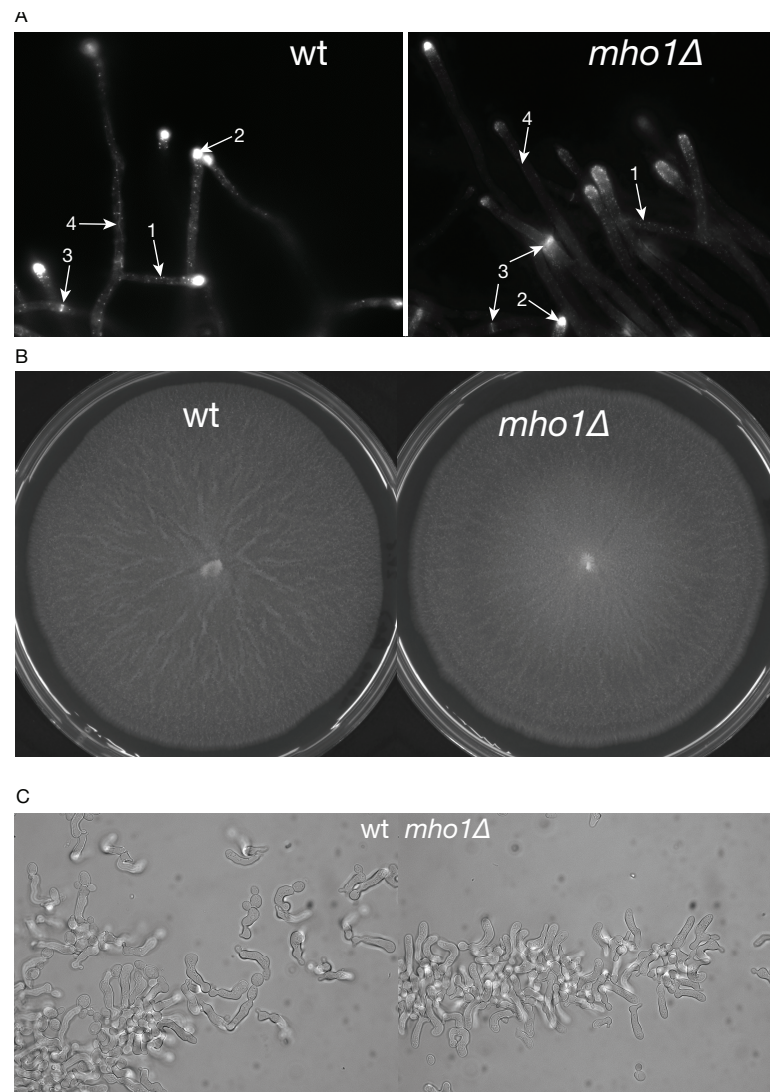
Figure 3.3: **Examination of filamentous growth in wild type and *memo*Δ cells.**
-
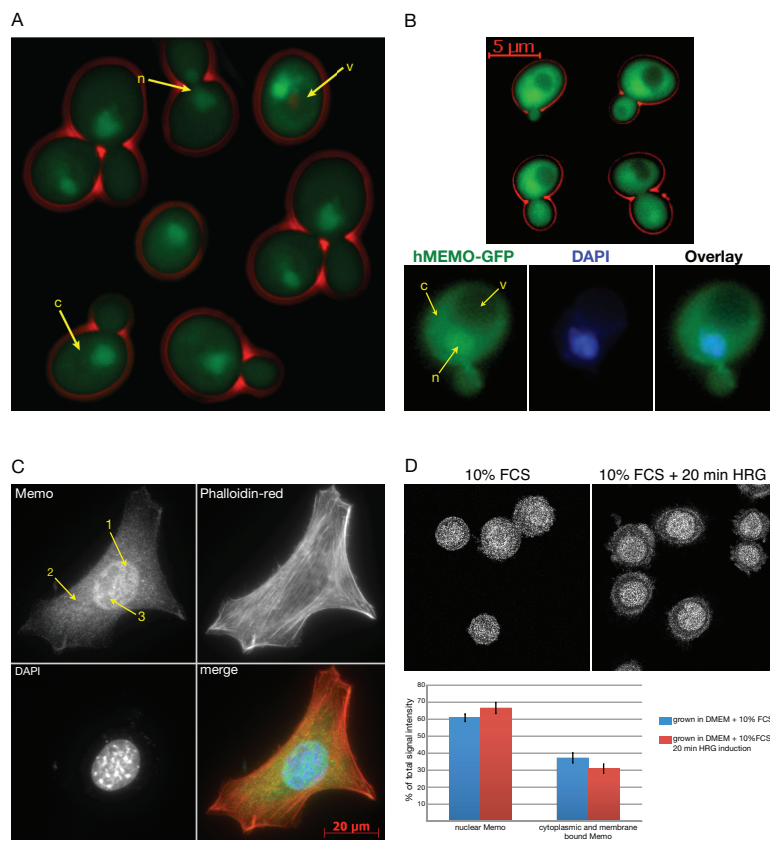
Figure 3.4: Cellular localization of Memo in yeast and mammalian cells. -

A

M. musculus	LSSVDI**Y**RTP**L**YD**L****R**IDQKIYGE
R. norvegicus	LSSVDI**Y**RTP**L**YD**L****R**IDQKIYGE
H. sapiens	LSSVDI**Y**RTP**L**YD**L****R**IDQKIYGE
B. taurus	LSSVDI**Y**RTP**L**YD**L****R**IDQKIYGE
X. laevis	LSTVDI**Y**RTP**L**YD**L**H**V**DQKVYGE
D. rerio	LSPAEV**Y**RTP**L**YD**L****R**IDQKVYAD
C. elegans	ITTCSK**Y**RTP**L**GD**L****I****V**DHKINEE
D. discoideum	LTKLDT**W**ETP**I**GN**L****K****V**DKDTTNK
S. pombe	VSRASI**C**STP**L**GD**L****K****V**DEDLCQK
S. cerevisiae	VSAFSE**L**ETP**L**GN**L****K****V**DTDLCKT
P. calidifontis	IMKSGA**W**ETP**F**GR**V****E****I**DEELASL
M. jannaschii	VMD-GI**W**RTP**L**GD**V****K****C**DEEFVEE

B

C

Figure 3.5: **Identification of a functional nuclear export sequence in Memo homologues.** -
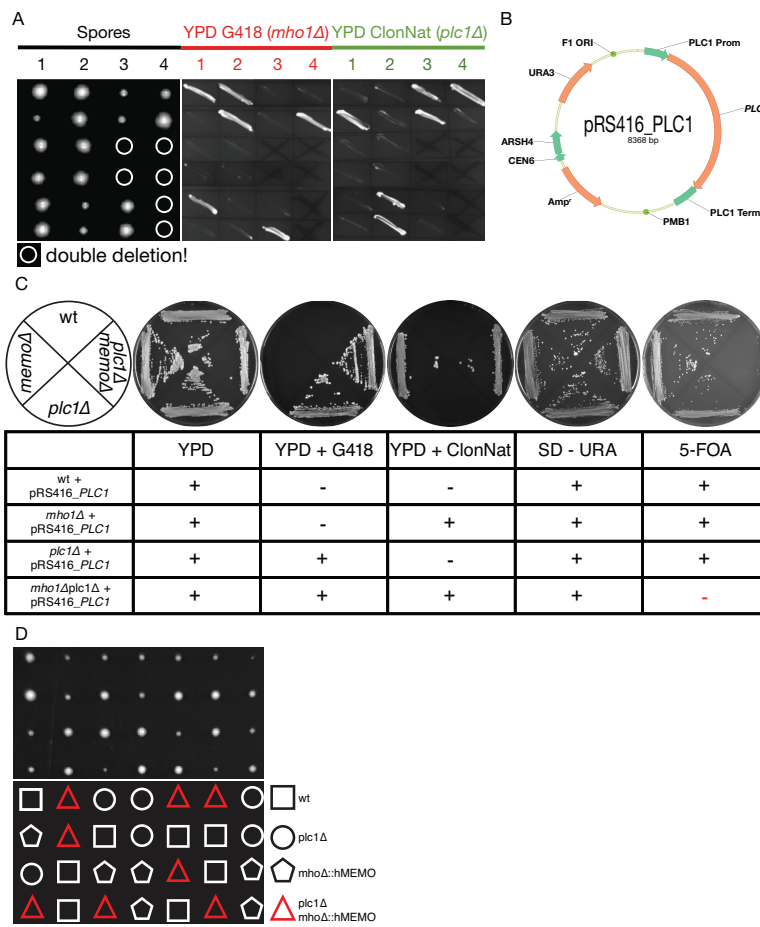
Figure 3.6: *MEMO* is synthetic lethal with *PLC1*. -
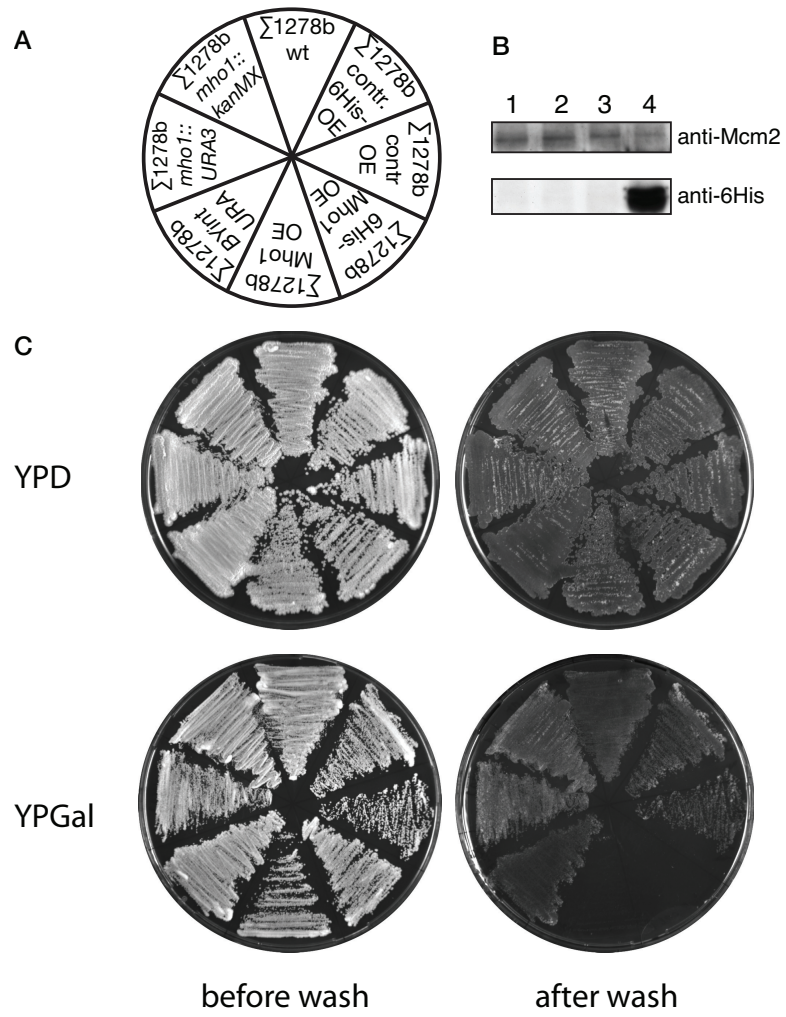
Figure 3.7: Overexpression of Mho1 abolishes invasive growth in the haploid Σ1278B strain. -

3.12   Supplemental material
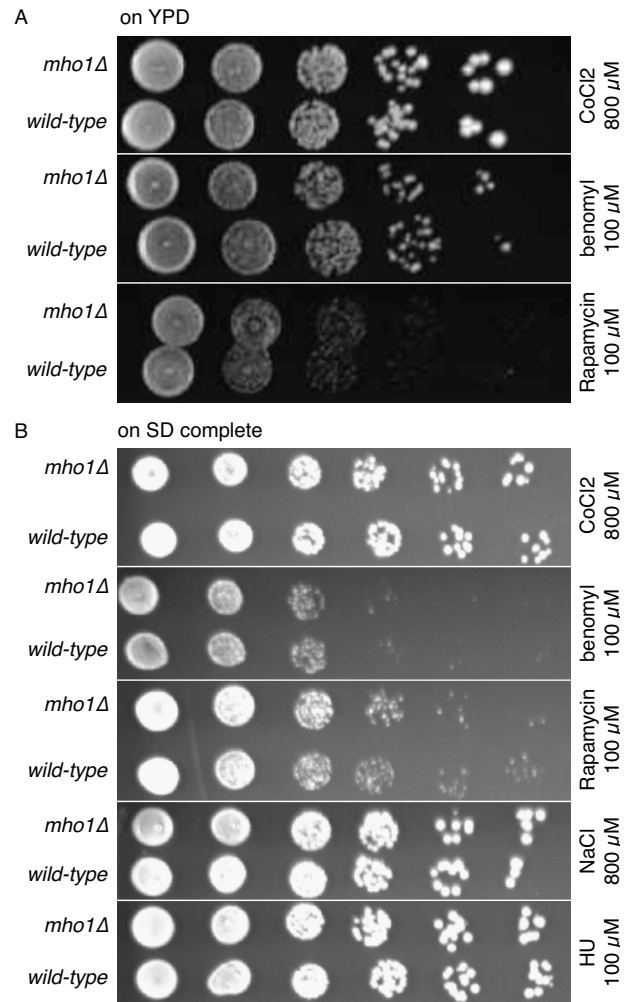
Figure 3.8: Spotting assay of wild-type and *mho1Δ* strains on various compounds -
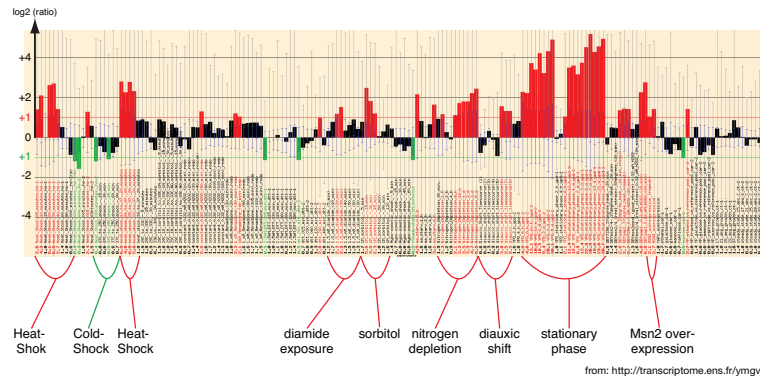
Figure 3.9: *MHO1* expression analysis -

Regulation of *MHO1* and *PLC1* expression levels in response to environmental stress conditions:

experiment	expression	
	MHO1	*PLC1*
Response to stationary phase, 1-13 days (25°C)	Upregulated > 12-fold within 12 hrs and remains elevated	Upregulated slowly; reaches a maximum of ~ 2-fold after 2 days
Response to stationary phase, 5 days (30°C)	Rapidly induced; 16-fold within 10 hrs	Upregulated slowly; reaches a maximum of ~ 2-fold after 2 days
Response to nitrogen deple-tion over 3 days	Rapidly upregulated 5-fold	Slowly upregulated 1.5 fold
Cold shock 37° to 25°C	Downregulation of > 2 fold	Unchanged
Heat shock (17-33°C) to 37°C	Rapidly upregulated > 5-fold	Unchanged

Arraydata from Gasch et al., Mol Biol Cell, 2000

Figure 3.10: Comparison of published *MHO1* and *PLC1* microarray data -

A

B

GENE	Function
Aro80	Zinc finger transcriptional activator of the Zn2Cys6 family; activates transcription of aromatic amino acid catabolic genes in the presence of aromatic amino acids
Gcn4	Basic leucine zipper (bZIP) transcriptional activator of amino acid biosynthetic genes in response to amino acid starvation; expression is tightly regulated at both the transcriptional and translational levels
Gcr2	Transcriptional activator of genes involved in glycolysis; interacts and functions with the DNA-binding protein Gcr1p
Hot1	Transcription factor required for the transient induction of glycerol biosynthetic genes GPD1 and GPP2 in response to high osmolarity; targets Hog1p to osmostress responsive promoters; has similarity to Msn1p and Gcr1p
Hsf1	Trimeric heat shock transcription factor, activates multiple genes in response to stresses that include hyperthermia; recognizes variable heat shock elements (HSEs) consisting of inverted NGAAN repeats; posttranslationally regulated
Ino2	Component of the heteromeric Ino2p/Ino4p basic helix-loop-helix transcription activator that binds inositol/choline-responsive elements (ICREs), required for derepression of phospholipid biosynthetic genes in response to inositol depletion
Ino4	Transcription factor required for derepression of inositol-choline-regulated genes involved in phospholipid synthesis; forms a complex, with Ino2p, that binds the inositol-choline-responsive element through a basic helix-loop-helix domain
Met4	Leucine-zipper transcriptional activator, responsible for the regulation of the sulfur amino acid pathway, requires different combinations of the auxiliary factors Cbf1p, Met28p, Met31p and Met32p
Msn2	Transcriptional activator related to Msn4p; activated in stress conditions, which results in translocation from the cytoplasm to the nucleus; binds DNA at stress response elements of responsive genes, inducing gene expression
Msn4	Transcriptional activator related to Msn2p; activated in stress conditions, which results in translocation from the cytoplasm to the nucleus; binds DNA at stress response elements of responsive genes, inducing gene expression
Opi1	Transcriptional regulator of a variety of genes; phosphorylation by protein kinase A stimulates Opi1p function in negative regulation of phospholipid biosynthetic genes; involved in telomere maintenance
Stp1	Transcription factor, undergoes proteolytic processing by SPS (Ssy1p-Ptr3p-Ssy5p)-sensor component Ssy5p in response to extracellular amino acids; activates transcription of amino acid permease genes and may have a role in tRNA processing
Stp2	Transcription factor, activated by proteolytic processing in response to signals from the SPS sensor system for external amino acids; activates transcription of amino acid permease genes
Yap5	Basic leucine zipper (bZIP) transcription factor
Yap6	Putative basic leucine zipper (bZIP) transcription factor; physically interacts with the Tup1-Cyc8 complex and recruits Tup1p to its targets; overexpression increases sodium and lithium tolerance; computational analysis suggests a role in regulation of expression of genes involved in carbohydrate metabolism

Figure 3.11: *MHO1* promoter analysis -

Figure 3.12: IP3 signaling pathway -

3.13   Supplemental Table S1

Gene	Function (from www.yeastgenome.org
BUB1[1]	Protein kinase involved in the cell cycle checkpoint into anaphase; forms complex with Mad1p and Bub3p crucial to preventing cell cycle progression into anaphase in the presence of spindle damage
BUB3[1]	Kinetochore checkpoint WD40 repeat protein that localizes to kinetochores during prophase and metaphase, delays anaphase in the presence of unattached kinetochores
CBF2[1]	Essential kinetochore protein, component of the CBF3 multisubunit complex that binds to the CDEIII region of the centromere; Cbf2p also binds to the CDEII region possibly forming a different multimeric complex, ubiquitinated in vivo
MAD2[1]	Component of the spindle-assembly checkpoint complex; delays the onset of anaphase in cells with defects in mitotic spindle assembly; regulates APC/C activity during prometaphase and metaphase of meiosis I
ARG82/IPK2[2]	Inositol polyphosphate multikinase (IPMK), sequentially phosphorylates $Ins(1,4,5)P_3$ to form $Ins(1,3,4,5,6)P_5$; also has diphosphoinositol polyphosphate synthase activity; regulates arginine-, phosphate-, and nitrogen-responsive genes
IPK1[2]	Inositol 1,3,4,5,6-pentakisphosphate 2-kinase, nuclear protein required for synthesis of 1,2,3,4,5,6-hexakisphosphate (phytate), which is integral to cell function
KCS1[2]	Inositol hexakisphosphate (IP_6) and inositol heptakisphosphate (IP_7) kinase; generation of high energy inositol pyrophosphates by Kcs1p is required for many processes such as vacuolar biogenesis, stress response and telomere maintenance
VIP1[2]	Inositol hexakisphosphate (IP_6) and inositol heptakisphosphate (IP_7) kinase; IP_7 production is important for phosphate signaling; involved in cortical actin cytoskeleton function, and invasive pseudohyphal growth
RAS1[3]	GTPase involved in G-protein signaling in the adenylate cyclase activating pathway, plays a role in cell proliferation; localized to the plasma membrane; homolog of mammalian RAS proto-oncogenes
RAS2[3]	GTP-binding protein that regulates the nitrogen starvation response, sporulation, and filamentous growth; farnesylation and palmitoylation required for activity and localization to plasma membrane; homolog of mammalian Ras proto-oncogenes
IRA2[3]	GTPase-activating protein that negatively regulates RAS by converting it from the GTP- to the GDP-bound inactive form, required for reducing cAMP levels under nutrient limiting conditions, has similarity to Ira1p and human neurofibromin

GPA2[3]	Nucleotide binding alpha subunit of the heterotrimeric G protein that interacts with the receptor Gpr1p, has signaling role in response to nutrients; green fluorescent protein (GFP)-fusion protein localizes to the cell periphery

Table 3.4: Genes that were tested as SL with memoΔ based on their known roles in the cAMP/PKA/PLC pathways - [1]: Published genes having a SL phenotype with *plc1*Δ. [2]: The four inositol polyphosphate kinases downstream of Plc1 which further process IP$_3$ to IP$_4$, IP$_5$, and IP$_6$. [3]: Genes involved the cAMP/PKA pathway signalling.

4

Results

4.1 TAPtagging Mho1

To answer the question if Mho1 has putative binding partners in yeast we performed a TAP tag experiment. The endogenous protein was tagged at the C-terminus with a TAP (Tandem Affinity Purification) tag (90). The TAP tag consists of two IgG binding domains of *Staphylococcus aureus* protein A (ProtA) and a calmodulin binding peptide (CBP) separated by a TEV (Tobacco Etch Virus) protease cleavage site. Because the endogenous protein is tagged by insertion of a fusion cassette at the 3'-end of the gene on the chromosome, the expression is still controlled under the endogenous promoter and by this kept close to natural level. The C-terminal TAP-tag fusion cassette consists of the CBD sequence, the TEV cleavage site and the ProtA sequence so that the ProtA module is located at the extreme C-terminus of the fusion protein. On the same fusion cassette there is also a *HIS3MX6* marker for selection integration of the cassette (Figure 4.1 (37)).

The significant advantage of this technique is the two separate purification steps of the fusion protein to reduce false positive hits, e.g. non specific protein binding to the tag or to the protein complex to be pulled down. First ProtA binds tightly to an IgG matrix, then the TEV protease cuts the tag at the TEV cleavage site and by this eluting the proteins under native conditions (Figure 4.2). The eluate of this first affinity purification step is then incubated with calmodulin-coated beads in the presence of calcium. After washing, which removes contaminants and remnants TEV protease, the bound material is released under mild conditions with EGTA (Figure
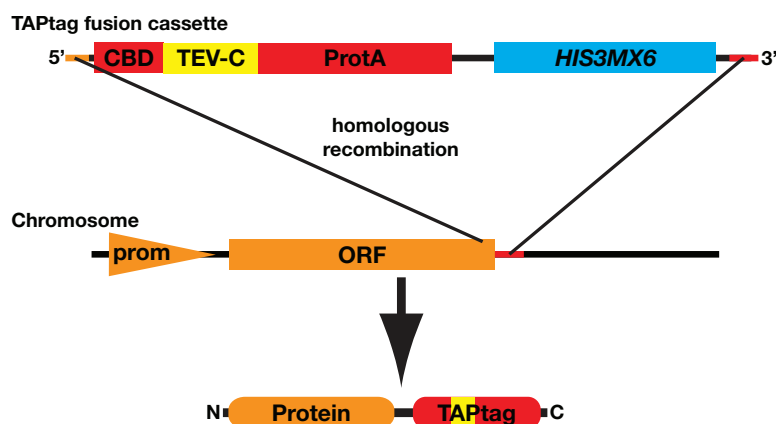
Figure 4.1: Insertion of C-terminal fusion cassette - The TAPtag fusion cassette encodes for the TAPtag (A CBP (calmodulin binding domain. followed by TEV-C (TEV cleavage site) and two IgG binding domains from Protein A) and the *HIS3MX6* selection marker. At the 5' and 3' end the fusion cassette shares homology to the sites of integration on the chromosome. The cassette gets integrated in frame at the 3' end of the gene and by this deleting the STOP codon. The TAPtagged gene encodes for the protein with a TAP tag at its C-terminus. As the gene is still controlled under its endogenous promoter, protein levels are close to natural levels.

4.2). The final elutant can either be used for silver or coomassie gel analysis (Figure 4.2) or can directly be used for Mass spectrometry analysis (Figure 4.2).

For our analysis we used a Mho1-TAP tagged strain and the wild-type BY4741 strain. Both strains were grown to OD_{600} 2 or 12, harvested, lysed and affinity purified as described in the method section. The final elutant was split into two fractions and TCA precipitated. One fraction was used for loading on a SDS-PAGE gradient gel from sigma and subsequent staining with silver ions (see Figure 4.3).

The second fraction was send to the in-house protein analysis facility for mass-spectrometry analysis. The samples were Trypsin digested and analysed using a LTQ Orbitrap Velos (Thermo Scientific) equipped with Agilent 1100/1200 Nanoflow LC System for nano-spray MS (Agilent Technologies). The Data could be analyzed using the Mascot (Matrix Science) software.

Mass spectrometry analysis identified two proteins pulled down only with Mho1 but not in the wild-type control (The control was a wild-type strain not expressing a TAP-tagged protein but grown, lysed and purified in parallel to the MHo1-TAP strain).

- Ubp3: Ubiquitin-specific protease involved in transport and osmotic response
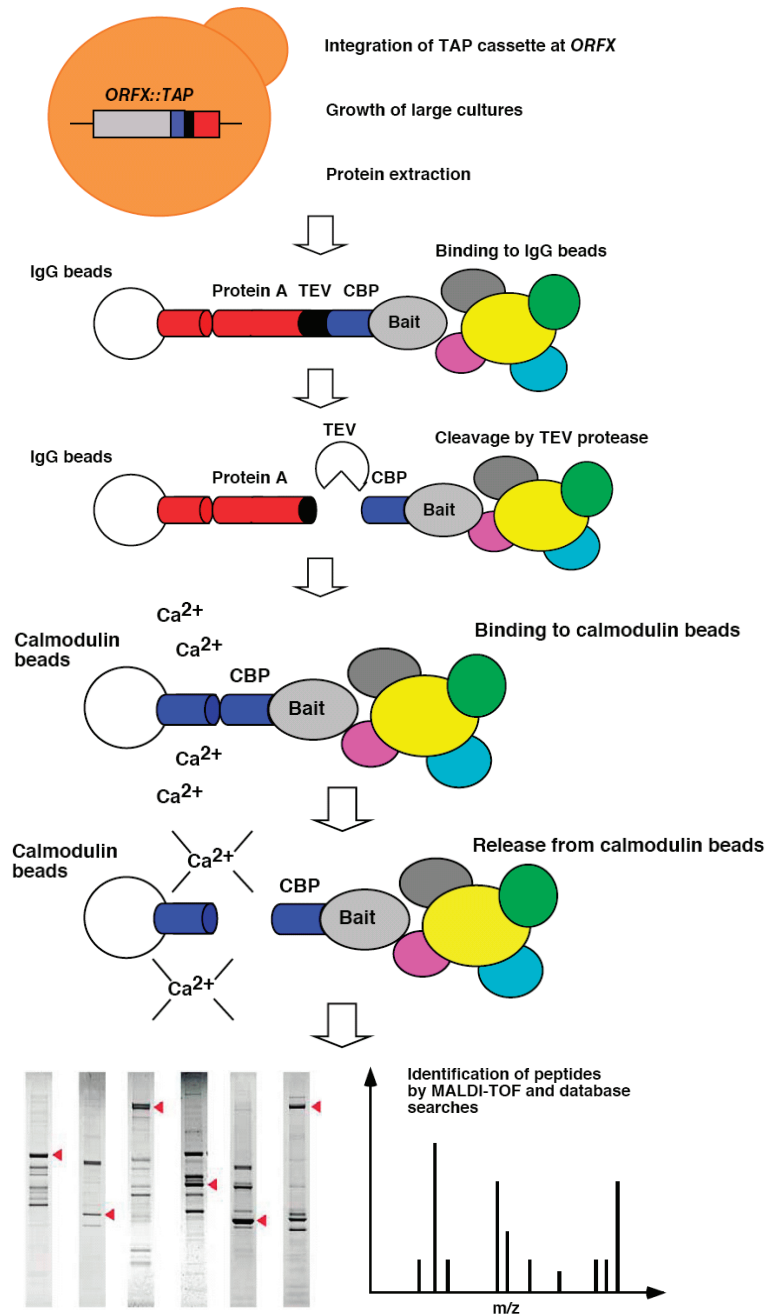
Figure 4.2: TAPtagging of Mho1 - The fusion protein was expressed from yeast cells having TAP tagged the endogenous *MHO1* gene. Whole cell lysate (WCL) was run over a column with IgG-Sepharose beads binding the Protein A tag. After washing the Mho-TAP fusion protein and associated proteins were eluted by cleavage with TEV (Tobacco Etch Virus) protease. The elutant was runover a second column with calmodulin beads. In the presence of Ca^{2+} the calmodulin binding domain from the TAP tag can bind. The second elution is done by chelating Ca2+ with EDTA and so releasing the Mho1 protein complex from the beads. The elutant can be used for SDS-PAGE and silver staining or for mass spectrometry analysis.
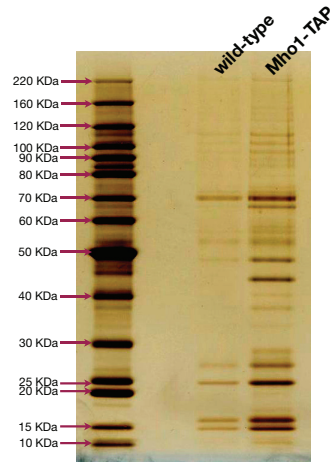
Figure 4.3: Sliver gel Mho1-TAP and BY4741 strains - The figure shows the final elutant of a TAP tag purification using a Mho1-TAP strain and the wild-type strain BY4741

- Hsp60: Tetradecameric mitochondrial chaperonin required for ATP-dependent folding of precursor polypeptides and complex assembly

- Mho1: TAP tagged protein in this experiment, was only found in the Mho1-TAP sample (positive control)

Next we wanted to find out how stringent the interaction between Mho1 and the two found protein is. We ran again a TAP tag experiment, but increased the NaCl concentration during the purification steps from 150 mM to 300 mM and 500 mM. With 300 mM NaCl only Hsp60 could be pulled down with Mho1. A further increase to 500 mM NaCl abolished all interactions between Mho1 binding partners. Only Mho1 (the TAP tagged protein) was identified by mass. spec.

In an other experiments we TAP tagged potential interaction partners of Mho1 and analyzed the final elutant after the two purification steps specifically for Mho1 fragments. We have chosen to TAP tag the following proteins:

- Ubp3: was pulled down with Mho1

- Arp1: Actin-related protein of the dynactin complex; required for spindle orientation and nuclear migration. In the yeast-2-hybrid screen from (49) Mho1 was found to interact with Arp1

- Cof1: Cofilin, promotes actin filament depolarization in a pH-dependent manner; binds both actin monomers and filaments and severs filaments. In A yeast 2 hybrid screen performed by Maria Meira using a blood cDNA library Cof1 was one of the identified binding partners of Memo. Meira et. al, 2009 showed that in mammalian cells Memo interacts with cofilin after HRG stimulation (70)

- Hsp60 could not be TAP tagged. It seams that the essential protein Hsp60 is not functioning or is miss folded after TAP tagging.

Non of the TAP tagged protein could pull down Mho1. The TAP tag experiment itself worked fine. We could identify several already published interactions in our assay. With Cof1 we could pull down:

- Act1: Actin, structural protein involved in cell polarization, endocytosis, and other cytoskeletal functions

- Srv2: CAP (cyclase-associated protein) subunit of adenylyl cyclase complex

As further control to assure ourselves that the TAP-tagging experiment was successful we compared our hit with with already published data sets. With Arp1 we could pull down Jnm1 (Component of the yeast dynactin complex, consisting of Nip100p, Jnm1p, and Arp1p; required for proper nuclear migration and spindle partitioning during mitotic anaphase). But interestingly we could also pull down many members of the T-complex protein 1 subunits. Those are molecular chaperone; which assists the folding of proteins upon ATP hydrolysis. They are known to play a role, in vitro, in the folding of actin and tubulin. In yeast the T-complex protein 1 subunits may play a role in mitotic spindle formation.

With this experiment we showed that Mho1 could only pull down Hsp60. The interaction between Mho1 and Hsp60 is stringent, even the increase of the NaCl concentration to 300 mM could not interrupt this interaction. Whether this interaction is real, meaning the two protein interact in the cell, or if this is just a post lysis interaction we could not answer. However, Hsp60 is a molecular chaperone mainly localizing to the mitochondrial matrix and we never could see Mho1 localize to the mitochondria. We think that this observed interaction is likely to be an experimental artrefact and not a true interaction occurring in living cells.

4.2   dSLAM (SL Screen)

One of the reasons why we choose *S. cerevisiae* as model system to elucidating Mho1 function is the possibility to do large scale genetics. Synthetic lethal interaction is a major tool to get insight into molecular pathway. If a strain harboring two deletion which alone are viable in combination show a slow growing phenotype (synthetic sick) or do not grow at all (synthetic lethal) shows a high possibility that the two encoded genes function in two distinct, but complementary pathways (Figure 1.9). We used the novel dSLAM (heterozygote diploid-based synthetic lethality analysis with microarrays) technique (71, 79, 80) to screen for synthetic interaction partners of *MHO1*. The dSLAM screen has two main advantages compared to the "conventional" described in the chapter "3.5.7 SL Screen". First, we could start with a diploid heterozygous deletion collection instead of a haploid deletion collection. This means also the essential deletions are included in the screen giving the possibility to find synthetic rescue interactions (the deletion of an essential gene is rescued by the deletion of a second gene). And second, al the deletion strains are molecularly bar-coded, they all have two unique 20 base pair tags flanked by universal priming sites. This feature is crucial as it means all the deletion strains can be pooled and handled in liquid. The system is comparable to the one we all know from the stores when we go grocery shopping. The product of interest is tagged with a bar code. At the cash register the bar code gets scanned and provides information about the product, the price, but also how many pieces are left in the shelf (Figure 4.4).

Figure 4.4: BAR code and scanner -

The genetic bar code of the deletion strains consists of 20 bp. Instead of a scanner, the bar code can get amplified by PCR, hybridization on a chip and read by a microarray scanned. This gives us information which mutants are present before and after a "change", e.g. before and after introduction of the query deletion (Figure 4.5).

Figure 4.5: Scanning of molecular BAR codes -

The dSLAM experiment was performed as described in (79) (A flowchart of the dSLAM experiment is shownn in Figure 4.6). We used the *Sal*I *Eco*RI cut plasmid pSO142-4 for exchanging the *kanMX* marker of the *memo*Δ strain with the *pTEF_pURA3-URA3_tTEF* cassette.

We run the whole dSLAM experiment twice using the *URA3* selection marker for deleting Memo in the pool of diploid heterozygous deletion strains. The obtained results after chip analysis and data processing are shown in figure 4.7.

For both experiments we obtained potential genes being SL with *MHO1*. But when we plotted the two experiments against each other we could not see any correlation. Genes which showed up in the first experiment to be SL with Mho1 did not show up in the second or vice versa. The known SL interaction partner of *MHO1*, *PLC1* did not show up in any of the dSLAM experiments. This may be because the signal from the *plc1*Δ strain was not amplified enough and was lower than the set threshold, meaning the single and the double deleted strain grew too slow.

To further analyze the dSLAM method we repeated the experiment again with a different selection marker, using the *kanMX* marker (106) from the plasmid pAG25 (40) to construct the query deletion cassette. We performed the dSLAM experiment six times in parallel. Data analysis and cross comparison of the single experiment showed again no correlation between the six experiments. The signal from the chip analysis was very low for most strains which is an indication for poor growth in the final selection medium.

4.3 Microarray (Does Mho1 control transcription?)

As Memo/Mho1 localizes predominantely to the nucleus in mammalian and yeast cells we wanted to answer the question if Mho1 in yeast affects the transcription of genes and if so if this is a direct or indirect effect. We extracted RNA from wild-type and *mho1*Δ strains. Both strains were harvested either during growth in mid log phase (low
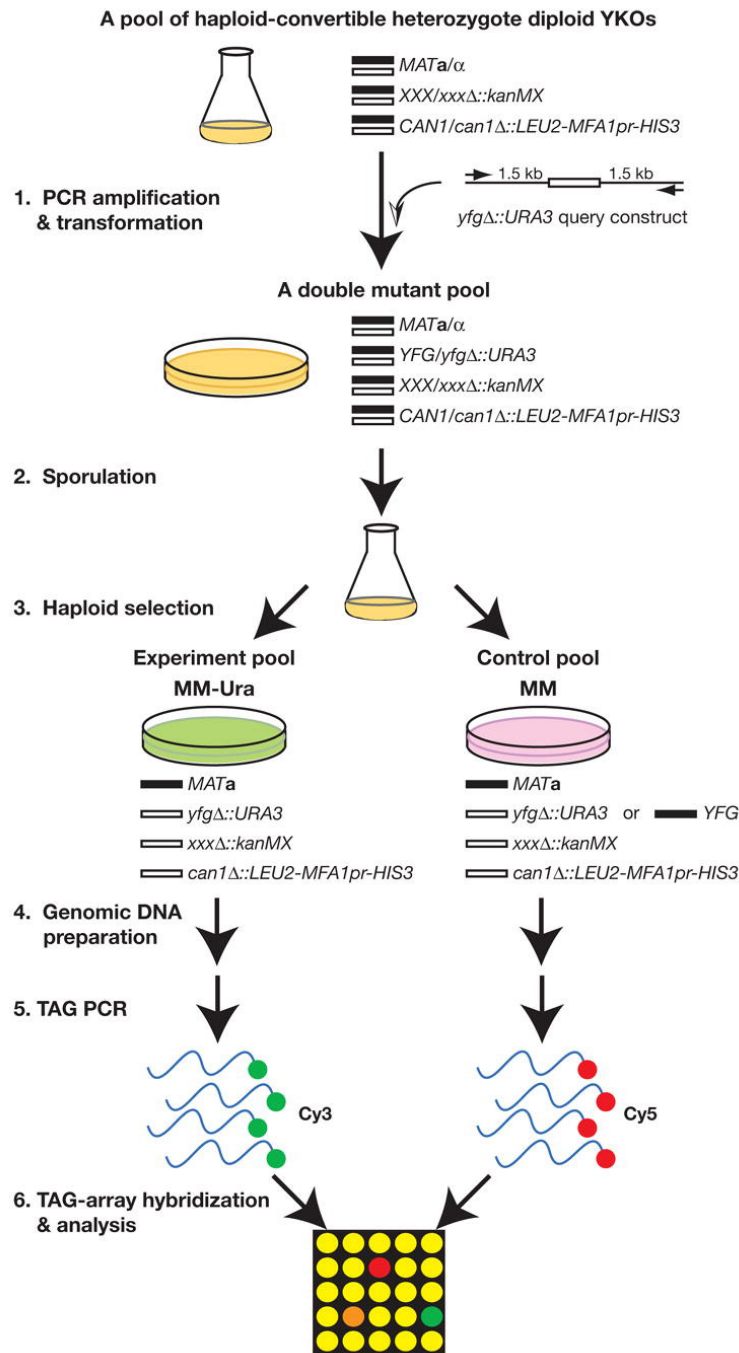
Figure 4.6: Flowchart of a dSLAM screen - Figure from (79)
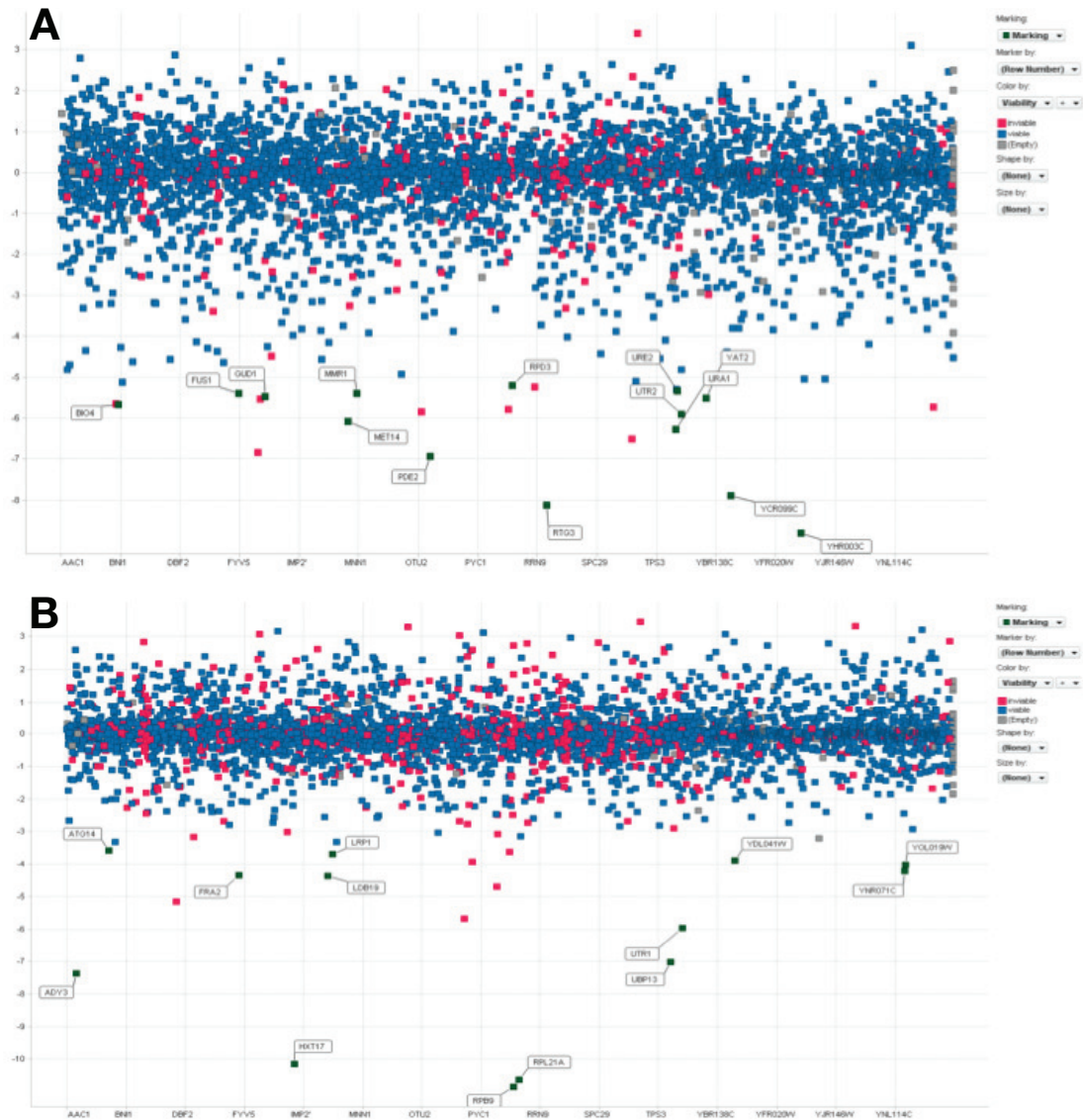
Figure 4.7: dSLAM results - Shown are the figures made with spotfire presenting the results of the two dSLAM experiments. Each deletion strain is represented by a square. All blue squares are non essential gene deletions whereas the red ones represent the essential gene deletion. The grey squares are labeled with "empty" and are mostly dubious ORFs or are not annotated. On the y-axis the genes are aligned according their names starting with A. On the x-axis the "relative survival rate" is shown (if the single deletion strain grows the same as the double deleted strain this value is 0. If the double deleted strain is synthetic lethal the value is highly negative, whereas if the double deleted strains grown much better it is shown by a positive value. So all the blue squares below the -5 mark on the x-axis show a synthetic sick or lethal phenotype with *mho1Δ*.

expression of Mho1) or after 48h in stationary phase (strong upregulation of Mho1).
Evaluation of microarrays was done as described in Materials and Methods. From
duplicate analysis of wild-type or deletion strains grown to mid-log phase or stationary
phase, we selected those probe sets with a Log2 average contrast signal of at least 5,
an adjusted p-value < 0.05 and an absolute Log2 fold change of > 1 (2-fold in linear
space).

In table 4.1 all the genes are shown that show at least a 2 fold change in $mho1\Delta$
strains compared to wild-type strains when cells were harvested during growth in mid-
log phase. Under this growth condition Mho1 is expressed at very low levels.

Systematic name	Common name	Log2 FC	Description
snR49	SNR49	1.21	H/ACA box small nucleolar RNA (snoRNA)
YPR202W		1.21	Putative protein of unknown function with similarity to telomere-encoded helicases
tL(UAA)Q	tL(UAA)Q	-2.31102	Mitochondrial tRNA-Leu, required for mitochondrial translation and indirectly for maintenance of the mitochondrial genome
YDL246C	SOR2	-1.02082	Protein of unknown function; protein sequence is 99% identical to the Sor1p sorbitol dehydrogenase
YER188W		-1.06896	Dubious open reading frame unlikely to encode a protein
YIR040C		-1.44395	Dubious open reading frame unlikely to encode a protein
YLR157W-D		-1.836005	Putative protein of unknown function; identified by gene-trapping, microarray-based expression analysis, and genome-wide homology searching

**Table 4.1: Genes changed in $mho1\Delta$ strain compared to wild-type when grown
to mid-log phase** - In this table all the genes having at least a 2 times fold change in
$mho1\Delta$ cells compared to wild-type cells when the cells are grown to mid-log phase.

In table the table 4.2 all the genes are shown that show at least a 2 fold change in
*mho1*Δ strains compared to wild-type strains when cells were harvested after 48 hours
in stationary phase. Under this growth conditions Mho1 is rapidly upregulated up to
16 times. .

Systematic name	Common name	Log2 FC	Description
tQ(UUG)E2		-1.99	tRNA-Gln; thiolation of uridine at wobble position
YBR174C		-1.14	Dubious open reading frame unlikely to encode a protein
YEL020C-B		-3.24	Dubious open reading frame unlikely to encode a protein
YER146W	LSM5	-1.13	Lsm (Like Sm) protein; part of heteroheptameric complexes (Lsm2p-7p and either Lsm1p or 8p): cytoplasmic Lsm1p complex involved in mRNA decay
YGL069C	SRF3	-1.35	Dubious open reading frame, unlikely to encode a protein

**Table 4.2: Genes changed in *mho1*Δ strain compared to wild-type when grown
to stationary phase** - In this table all the genes having at least a 2 times fold change
in *mho1*Δ cells compared to wild-type cells when the cells are grown for 48 hours into
stationary phase.

Even though Mho1 gets strongly upregulated during stationary phase and localizytion of the protein is mainly nuclear our analysis suggest that Mho1 has little or
no influence on the transcription of other genes. It is highly unlikely that Mho1 is a
regulator of transcription or even a transcription factor.

4.4 Could Memo/Mho1 be an enzyme? - Enzymatic activity assays

4.4.1 Is Memo a Non-heme Dioxygenase?

The structure from Memo was solved by Qiu et. al (89) and was shown to by structurally
homologue to LigB, the catalytic β-subunit of the protocatechuate 4,5-dioxygenase

LigAB from *Sphingomonas paucimobilis* (47)(102). LigAB is a class III nonheme
iron(II)-dependent extradiol-type catechol dioxygenase that catalyzes oxidative cleav-
age of substituted catechols in bacterial aromatic degradation pathways (76). To test
is Memo might have a similar enzymatic activity even though it is missing a Glu in
the vestigial active site (see also section 1.1.2 Memo protein structure is homologous to
non heme iron dioxygenases) we designed an enzymatic cleavage assay with potential
substrates. To 1 mM of substrate 300 nM of purified Memo was added. Enzymatic
activity, aromatic ring opening, was monitored by spectrometric measurement at 280
nm. Interestingly we could detect the cleavage after addition of purified Memo (Figure
4.8)
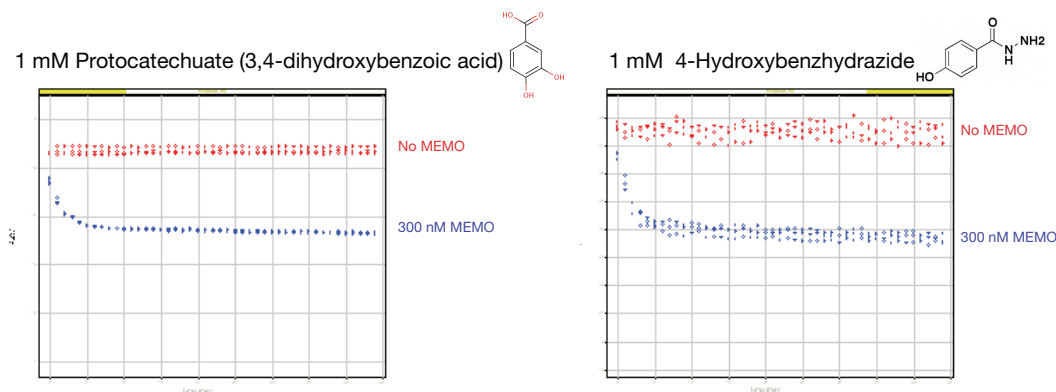
Figure 4.8: Enzymatic activity of Memo in an aromatic ring opening assay -

To include a control we purified the human protein mCMTP2 the same way from
bacteria as we did for memo. Both purified proteins, Memo and mCMTP2 showed the
same enzymatic activity (Figure 4.9).

This results indicates that the seen activity in the assay is due to bacteria contami-
nation from the purification process. Non-heme dioxygenases are abundant in bacteria
and a small contamination could already lead to the measured activity.

4.4.2 Mho1 with point mutation in the vestigial active site can com-
plement for the wild-type protein

Memo sequence is highly conserved from mammals to yeast and bacteria. Protein
sequence analysis showed more then 50% similarity between the human and the yeast
protein. Especially specific amino acids in the vestigial active site are conserved in

1 mM Pyrocatechol (1,2-dihydroxybene)

1 mM Protocatechuate (3,4-dihydroxybenzoic acid)
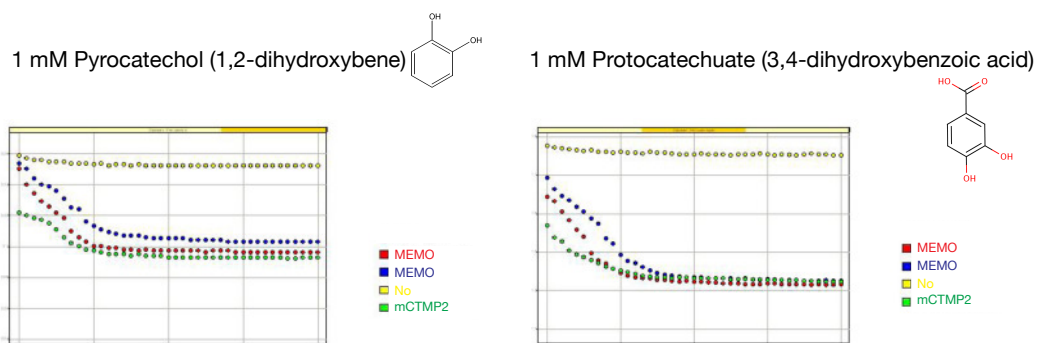
Figure 4.9: Enzymatic activity of Memo including a control -

all kingdoms of live. All organisms expressing a Memo homolog do have three His, one Cys, and one Asp in this conserved site (see figure 3.1). We hypothesized that if Memo is an enzyme this conserved amino acids are most likely to be essential for the enzymatic activity. To test our hypothesis we took advantage of the synthetic lethal phenotype between $mho1\Delta$ and $plc1\Delta$. We made several strain where we replaced the endogenous *MHO1* gene with *mho1* having mutated His47, His80, and Cys284. We crossed the newly made mutation strains with a $plc1\Delta$ strains, let them sporulate and dissected the spores (Figure 4.10).
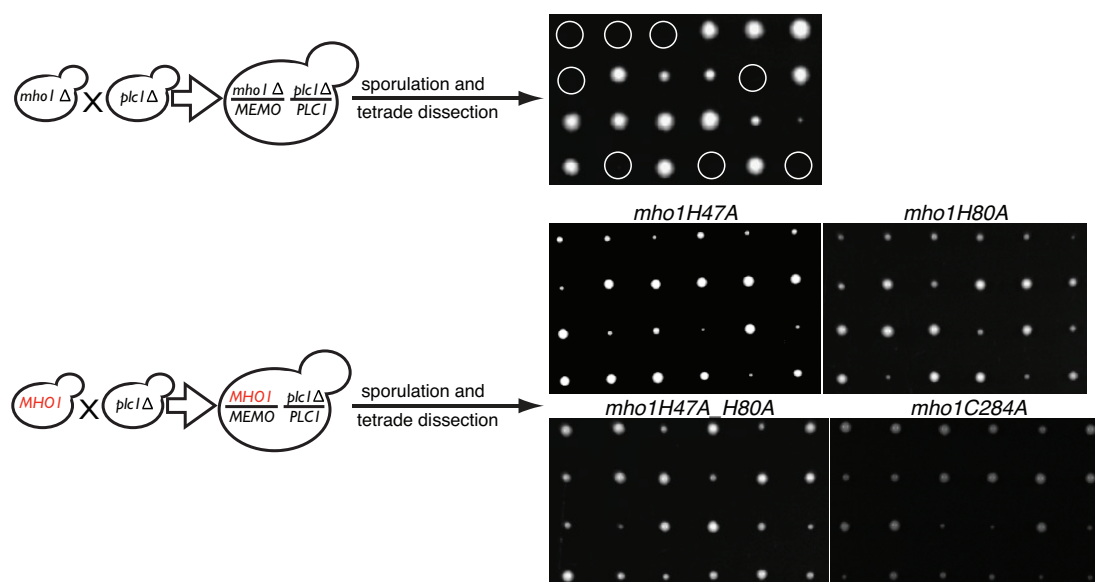
Figure 4.10: Complementation of wild-type Mho1 with mutated Mho1 -
If an $mho1\Delta$ strain is crossed with a $plc1\Delta$ strain and the resulting diploid strain sporulates only spores having a single gene deletion or are wild-type can grow. All spores having the $mho1\Delta plc1\Delta$ genotype can not grow (indicated by a white circle). If in a $mho1\Delta$ strain a mutated *mho1* with amino acid substitutions in the vestigial active site is reintroduced all four spores can grow again showing the complementary potential of the point mutated gene. In the figure the dissection of four strains having reintroduced the mutated genes *mho1H47A, mho1H80A, mho1H47A_H80A, and mho1C284A* are shown.

All of the point mutated strains could complement for the wild-type gene in this specific assay. This could mean that a potential enzymatic activity of Mho1 is not needed to rescue the SL phenotype between $mho1\Delta$ and $plc1\Delta$ or the enzymatic activity is not dependent on those residues. We could also think of a dual role of Memo, being an adaptor protein with enzymatic activity. Also a third scenario is possible. While

our lab was trying to purify human Memo in bacteria we saw that Memo having those point mutation always ended up in the pellet, meaning they were not soluble anymore. It could also indicate a miss folding of the protein. So we could speculate that the enzyme in the vestigial active site are essential for the protein folding and 3D structure and not for enzymatic activity.

4.5 Accumulation of ROS (Reactive Oxygen Species)

Preliminary results in our laboratory showed that MEMO KO or KD cells are more sensitive to ROS-inducing stress conditions. If MEMO KO cells were grown in medium containing the ROS inducer $CoCl_2$ they showed a higher rate of apoptosis compared to wild-type MEFs. To check if the induced apoptosis in is due to higher ROS levels in MEMO depleted cells we performed a flow cytometry based assay for measuring intracellular ROS levels. We used the Image-iT LIVE Green Reactive Oxygen Species Detection Kit from Molecular Probes (Invitrogen) and the wild-type and MEMO KO MEFs. Intracellular ROS levels could be made detectable by the conversion of a dye by ROS to a fluorescent product. This made it possible to measure ROS levels with FACS by using standard fluorescent filter sets. This kit uses *tert*-butyl hydroperoxide (TBHP) to induce ROS. The wild-type and MEMO KO MEFs were grown in DMEM supplemented with 10% FCS to 80-90% confluency in 10 cm dishes. ROS was induced by TBHP for 1 hour. We measured twice 20'000 cells for each condition

FACS measurement of ROS induced wild-type and MEMO KO MEFs are shown in Figure 4.11. Both, MEMO wild-type and KO cells showed the same levels of intracellular ROS and both have same numbers of dead cells 4.11 showing that short time treatment of MEMO KO cells does not make them more apoptotic then wt MEFs.

In figure 4.12 the superimposition of the analyzed wild-type and MEMO KO MEFs. All cells were induced the same way for 1 hour and do not show any difference in ROS levels, indicated by the nice overlay of all FL1-H intensity curves.

It is more likely that the observed increase in apoptotic cells after ROS induction in MEMO KO cells is due to higher sensitivity to ROS and not to higher ROS levels in KO cells. It is comparable to temperature sensitive mutants, they stop growing or die when shifted to the non permissive temperature so it seems that MEMO KO cells enter
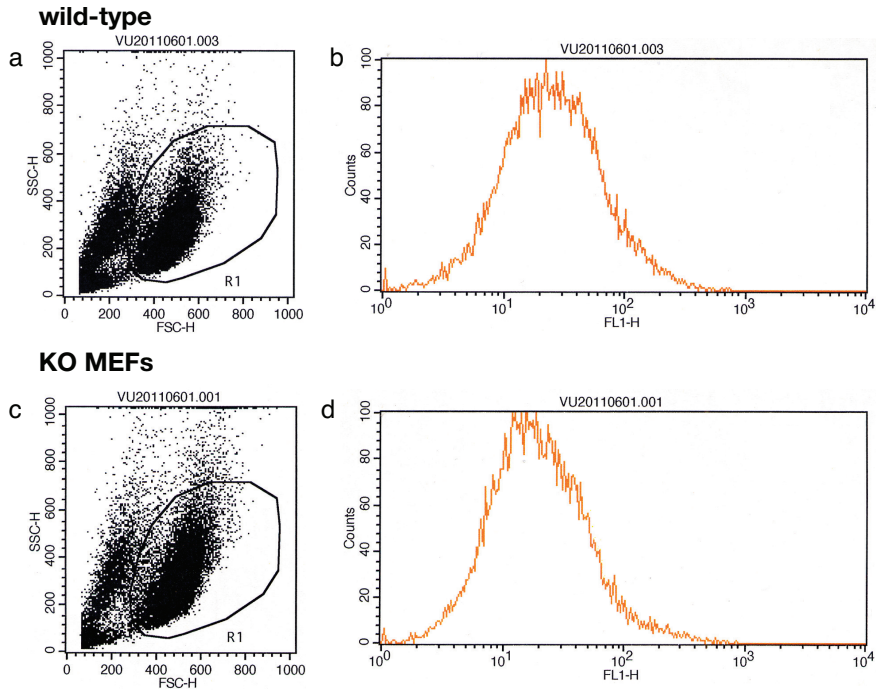
Figure 4.11: FACS measurement of ROS induced wild-type and MEMO KO MEFs - In the panels (a) and (c) we set the gate to select for living cells. The FSC-H axis shows the cell size and the SSC-H axis shows cellular density. In the panels (b) and (d) the actual measurement for intracellular ROS levels is shown. The FL1-H axis shows the intensity of fluorescent light which correlates with the levels of intracellular ROS.
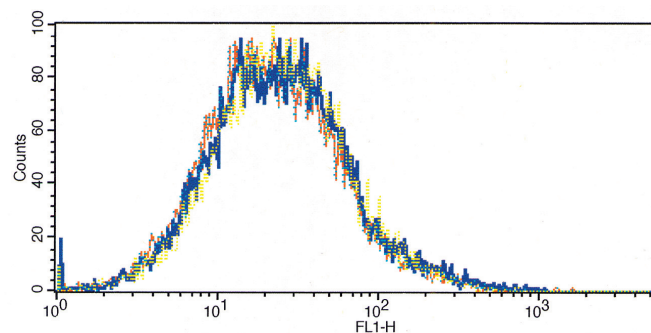
Figure 4.12: Superimposition of ROS levels in wild-type and MEMO KO MEFs - This figure shows the superimposition of the curves showing intracellular ROS levels in wild-type and MEMO KO MEFs. All curves nicely overlay indicating no difference in ROS levels after induction with TBHP.

apoptosis when internal ROS levels are above a given threshold whereas wild-type cells still are fine.

The same ROS sensitive phenotype could not be found in yeast cells. mho1Δ and wild-type cells did not show any difference in growth when grown in medium containing CoCl$_2$ or H$_2$O$_2$. We also tried to use the Image-iT LIVE Green Reactive Oxygen Species Detection Kit for labeling the ROS levels in yeast cells but we were not able to get a good signal for FACS analysis.

4.6 Subcellular fractionation

To illustrate Memo localization in mammalian cells not only by fluorescent and confocal microscopy we did subsellular fractionation of the three cell lines T47D, MDA-MB-231, and SKBR3. All of them showed different endogenous levels of the tyrosine kinase receptor ErbB2. The SKBR3 cells have massive overexpression of ErbB2, T47D show lower level and in MDA-MB-231 ErbB2 is even lower expressed (Figure 4.13 top line). We did the subcellular fractionation of those cell lines with cells growing in full medium (DMEM + 10%FCS) and in full medium and induced for 20 minutes with HRG. We checked Memo subcellular localization in the cytoplasm (C), nucleus (N), and at the membrane (M). As membrane marker we used the ER integral protein calnexin and as marker for the nuclear fraction we choose lamin A/C a protein from the nuclear envelope (Figure 4.13).

Memo localization in T47D cells when grown in full medium is cytoplasmic but also nuclear and at the membrane (comparison for protein amount between the fractions is not possible due to the used protocol, see also material and methods). Upon treatment with 10 nm of HRG for 20 minutes we could observe a slight accumulation of Memo in the nucleus and at the membrane (Figure 4.13 top line). The other two cell lines (MDA-MB-231 and SKBR3) showed similar subcellular Memo distribution (MDA-MD-231 less nuclear and at the membrane then SKBR3) but induction with HRG hat no effect on Memo localization (Figure 4.13). We think the the different expression levels of ErbB2 in the various cell line could be the explanation for this observation. In SKBR3 cells ErbB2 is overexpressed and by this constitutively active, so HRG induction did not largely effect those cells. MDA-MB-231 cell do not express ErbB, so they are independent of HRG induction. T47D cells have moderate ErbB2 levels compared to
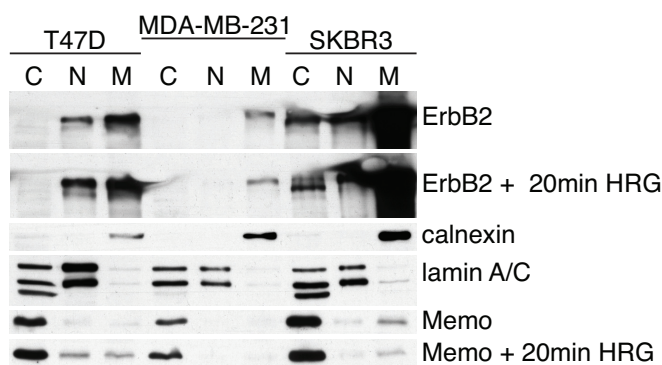
Figure 4.13: Subcellular fractionation of T47D, NDA-MB-231, and SKBr3 cells - T47D, NDA-MB-231, and SKBr3 cells were incubated in full medium containing or full medium and stimulated for 20min with HRG, disrupted by glass-glass homogenization (Dounce) and fractionated into cytoplasmic (C), nuclear (N), and membrane (M) fractions. Equal volumes were subjected to SDS-PAGE and subsequent immunoblotting. Calnexin was used as a marker for the membrane and lamin A/C for the nuclear fraction.

SKBR3 cells and do react to HRG induction. This could be the explanation for our observed shift in Memo localization.

So far we only did confocal microscopy and signal quantification with Memo stained SKBR3 cells (see the Paper section 3.3.5). The microscopical analysis confirmed the findings of the subcellular localization of Memo. It would be interesting to confirm Memo localization in T47D cells by confocal microscopy, because it seems that in those cells Memo localization changes upon HRG treatment.

5

Discussion

5.1 Finding Memo

5.1.1 Localization in mammalian cells

In this study we have shown that Memo localizes predominantly to the nucleus but can also be found in the cytoplasm and on the membrane upon induction with the appropriate growth factor. Analysis performed by confocal microscopy showed that nuclear Memo is evenly distributed throughout the nucleus but is excluded from nucleoli and does not localize to the nuclear membrane. Memo encodes for a nuclear export sequence (NES) and we demonstrated that Memo gets actively exported from the nucleus via exportins. Nuclear export could be blocked with addition of leptomycin B (LMB) to the medium, which lead to an accumulation of Memo and, by this showing that Memo diffuses by a certain rate through the nuclear pore complex. As Memo is approximately 33 kDa in size and proteins up to 50 kDa can diffuse through the nuclear pore complex this seems plausible. Nuclear accumulation of Memo after LMB treatment can be enhanced by inducing the cells with the appropriate growth factor (here we induced SKBR3 cells with HRG), showing evidence that also the nuclear import can be directed by active import. When we analyzed the amino acid (AA) sequence of ErbB2 no classical nuclear localization signal (NLS) was found using bioinformatic prediction tools. Usually NLS consist of bipartite basic AA stretch separated by roughly 10 AAs. Interestingly Memo has a Tyrosine residue at position 210, which was found to be phosphorylated in a screen (91). Interestingly this site shows the highest probability to be phosphorylated when using a prediction software (12) and this specific Tyr 210 in

Memo is conserved throughout evolution (Figure 5.1). Yeast cells, which do not have any dedicated tyrosine kinases at all, have serine or threonine residues close to that side and bioinformatic analysis showed (48) that those residues have a high probability to be phosphorylated (Figure 5.1). We speculate that this phosphorylation is the trigger to the import from the cytoplasm to the nucleus. Figure 5.2 shows a potential working model how Memo localization could be regulated in SKBR3 cells.

```
H. sapienas      -------SQGEIYRSIEHLDKMGMSIIEQLDPV
M. musculus      -------SQGEIYRSIEHLDKMGMSIIEQLDPV
R. norvegicus    -------SQGEIYRSIEHLDKMGMSIIEQLDPV
B. taurus        -------SQGEIYRSIEHLDKMGMSIIEQLDPV
D. rerio         -------SQGEIYRSIEHLDKMGMGIIEQLDPI
C. elegans       -------SSIPIYEQITNMDKQGMSAIETLNPA
D. discoideum    -------KEVPIYKYIEELDRKGMEIIESGDPV
S. pombe         ---RGGPTSPKIYESISNLDHIGMKIIETKSSD
S. cerevisiae    ARSKLSHHQVPIWQSIEIMDRYAMKTLSDTPNG
```

Figure 5.1: Potential phospho Y-, S-, and T-sites in Memo and Mho1 - The figure shows a short stretch of a multiple sequence alignment. In red the potential phospho-Y site is highlighted and how it is conserved throughout evolution. *S. pombe* have such a Y-site even though they do not have any dedicated tyrosine kinases. In green the serine and threonine residues with the highest probability to be phosphorylated are shown (calculated with the phosphorylation prediction software (48).

5.1.2   Localization in yeast cells

In yeast cells regulation of Mho1 localization seems to be different than in mammalian cells. Mho1 is never found at the cellular membrane. This may be due to the lack of dedicated tyrosine-kinases in yeast and the interaction of Memo with ErbB2 (or tyrosine-kinases in general) a mammalian specific interaction leading to the membrane localization of Memo. Similar to mammalian cells Mho1 in yeast is also found more than 60 - 70 % in the nucleus and to a lesser extent in the cytoplasm (see also Figure 3.4D). Mho1 is clearly excluded from the vacuole. This organelle is not present in mammalian cells but is mostly similar to lysosomes or endosomes.

With our Mho1-GFP fusion strain we showed that Mho1 does not shuttle from the cytoplasm to the nucleus or vice versa in all tested conditions. However we found that Mho1 expression levels do respond fast to environmental changes. A change in growth temperature can lead to up- or downregulation of Mho1 within 20 minutes
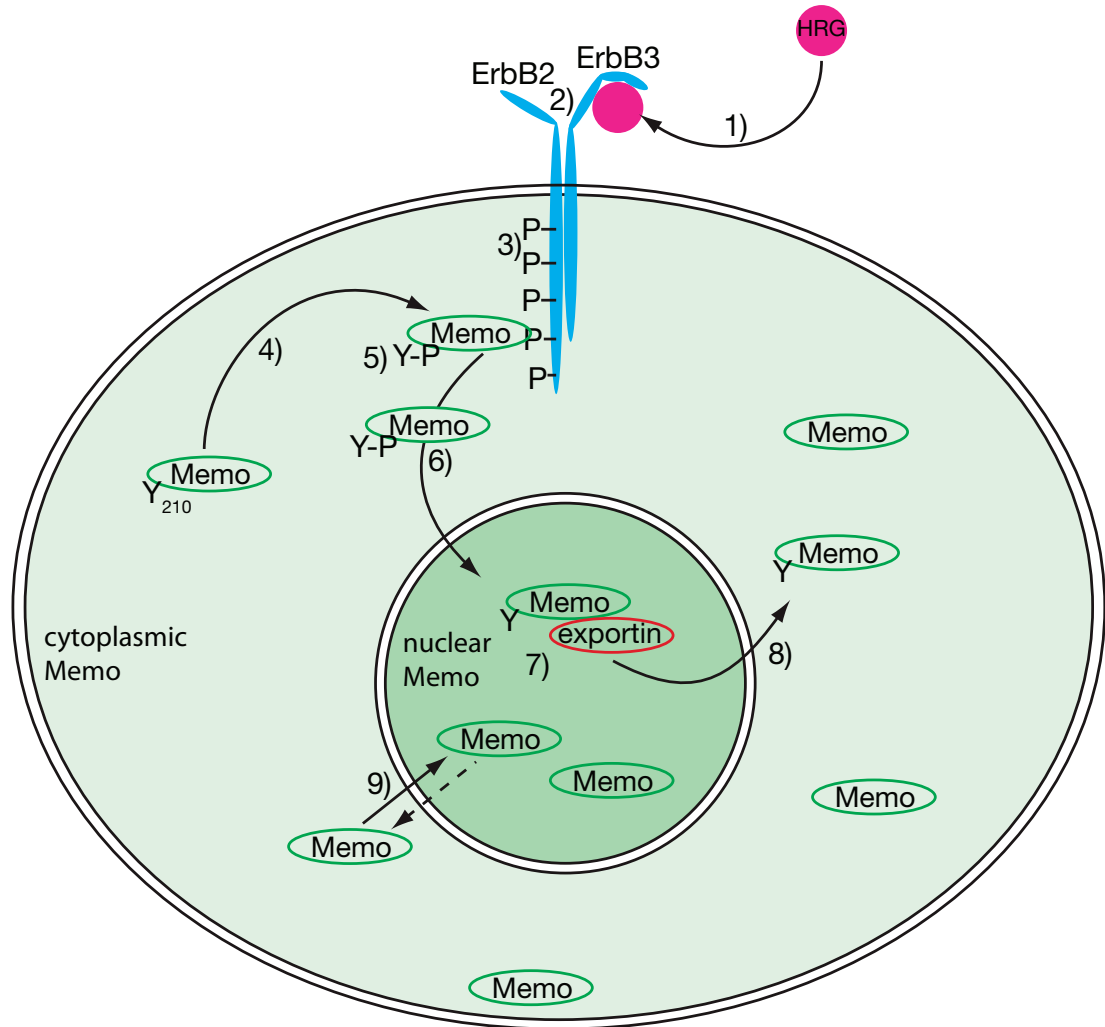
Figure 5.2: Model for Memo-shuttling in SKBR3 cells - 1) HRG binds to ErbB3
2) Hetero-dimerization of ErbB3 with ErbB2 3) Autophosphorylation of Tyrosine residues
in the cytoplasmic tail of ErbB2 4) Memo gets recruited to a specific phospho-Tyrosine
(67) 5) Phosphorylation of the Tyrosine 210 on the surface of Memo 6) Recognition of the
Tyrosine 210 and active import into the nucleus 7) Memo gets dephosphorylated and the
NES of Memo gets recognized by exportins and Memo is actively exported 8) Cytoplasmic
Memo is "ready" for the next round of activation 9) passive diffusion of Memo through the
nuclear pore complex. If cells are in starvation medium containing LMB they accumulate
Memo in the nucleus suggesting that Memo gets only actively exported or diffusion into
the nucleus is more efficient.

(35). Changes in the Growth media like nitrogen depletion or growth stationary phase changes Mho1 expressionlevels within 1 - 2 hours (35). It seems that in yeast cells not the localization of Mho1 is altered after certain stimuli (heat, cold, nitrogen,...) but transcription and translation are tightly regulated and by this changing the concentration of protein in the different organelles.

In mammalian cells experiments showed that Memo levels do not change upon induction of the cells with HRG or if the cells are starved or grown in full media. We speculate that Memo/Mho1 localization in both, mammalian and yeast cells, is essential for proper function but the regulation is different. In mammalian cells Memo can freely diffuse in and out the nucleus but upon stimulation the protein gets actively imported and exported from the nucleus. We proved that by blocking the nuclear export with leptomycin B in unstimulated and stimulated cells and quantified protein concentration with confocal microscopy and measuring fluorescent intensity. In yeast cells where Mho1 is predominantly nuclear the protein level is efficiently up- or downregulated in reaction to various external stimuli. In the figure 5.3 we show a model for Mho transcriptional control and localization in yeast.
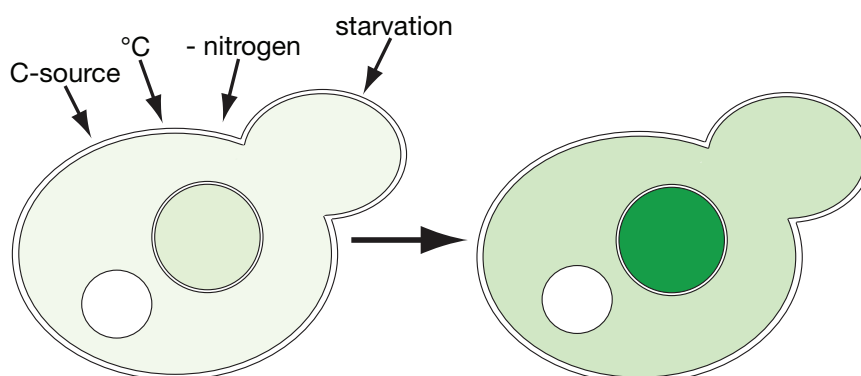
Figure 5.3: Model for transcriptional control and localization of Mho1 in yeast cells - Mho1 protein levels vary according to the intensity of green in the figure. A cell growing in log-phase express about 300 - 350 molecules per cell (37). After the cells sense "stress" induction Mho1 gets upregulated, most likely via Msn2/Msn4. The localization of the Mho1 protein remains the same but at much higher level (indicated by the dark green color). In some "stress" condition Mho1 gets upregulated more than 32-fold (35).

5.2   Is Memo an Enzyme?

We tested if Memo could have an class III non-heme dioxygenase activity like its structural homolog LigAB from *Sphingomonas paucimobilis*. In an enzymatic activity assay developed by us we measure the cleavage of an aromatic ring. We could show that Memo and mCTMP2 (the Akt inhibitor CTMP (carboxyl-terminal modulator protein (72)) we used as negative control) showed the same enzymatic "activity". As both proteins were expressed and purified by the same protocol in bacteria, this is likely the observed dioxygenase activity is "contamination" from the purification process. Dioxygenases are widely expressed in bacteria only tiny amounts of contamination could explain the observed enzymatic activity. Second, Protocatechuate one of the substrates used in our assay is a substrate for protocatechuate 3,4-dioxygenase that belong to the intradiol family of non-heme dioxygenases (17, 33, 34) not to the extradiol family of non-heme dioxygenases like LigAB. This supports our hypotesis that the observed activity is due to cross-contamination and not due to the enzymatic activity of the purified proteins.

It is unlikely that Memo encodes for a dioxygenase of this class. First no specific enzymatic activity for Memo could be observed in our assay and second all known class III dioxygenases have a Glu in the active site and use non-haem Fe(II) or non-haem Fe(III) to cleave the aromatic ring (16). Qiu et. al (89) showed that the iron-coordinating glutamate found in dioxygenases is replaced with a cysteine in Memo and no evidence for iron binding was found by (89).

5.2.1   If not a dioxygenase, could Memo be an other enzyme?

There are some speculations that Memocould be an enzyme in archea. In *Methanocaldococcus jannashii* all but one enzymatic step from the mevalonate pathway are known (Figure 5.4). The only missing enzyme in the archeal mevalonate pathway is the enzyme which decarboxylases mevalonate phosphate to isopentyl phosphate.

Grochowski et. al (42) propose that the protein MJ0304 (the Momo homolog of *M. jannaschii*) could be the missing link. They base their hypothesis on chromosomal alignment of genes. In most archeal species genes encoding for proteins of a pathway colocalize together on the chromosome. Analysis of archea "operons" showed that homologs of MJ0304 often are on the same chromosomal stretch as genes coding for enzymes of the mevalonate pathway (Figure 5.5)
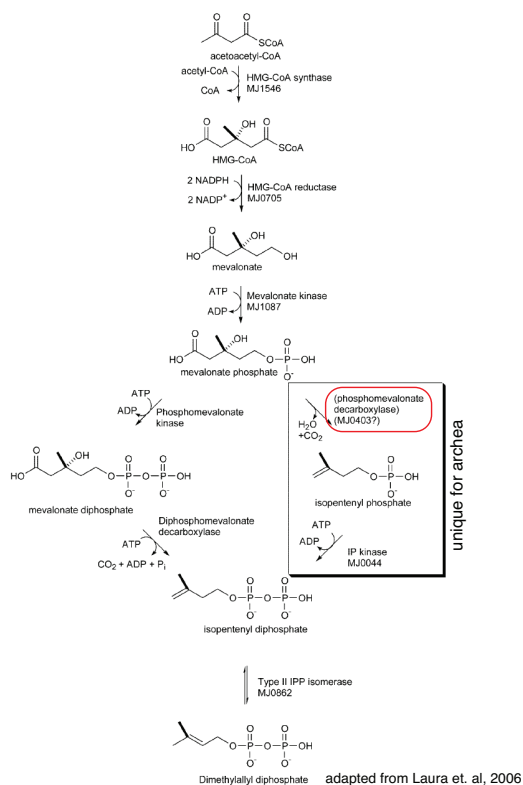
Figure 5.4: Mevalonate pathway in archea and eukaryotes - The figure shows the mevalonate pathway ant the difference in archea and other eukaryotic cells. The only unknown enzyme is the phosphomevalonate decarbocylase. Grochowski et. al (42) speculate that this decarboxylase step could be done by the Protein MJ0304. Interestingly MJ0304 is the archeal homolog of Memo (Figure adapted from (42)).
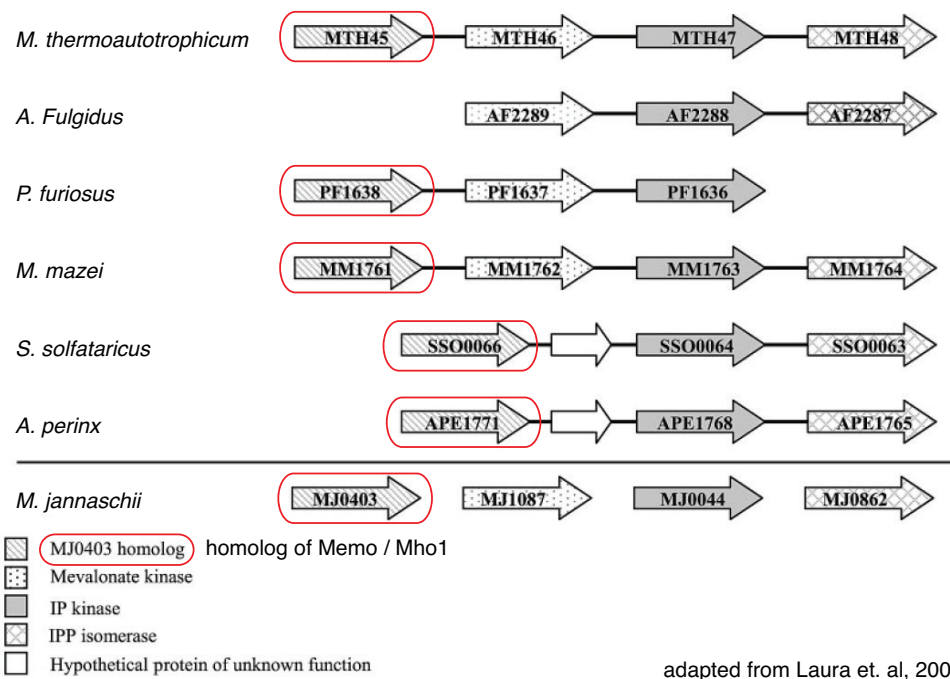
Figure 5.5: Chromosomal organization of genes coding for mevalonate pathway enzymes in representative archaea. - The corresponding genes from *M. jannaschii* are indicated for comparison but are not colocalized on the chromosome (Figure adapted from (42). Highlighted with a red round rectangle is MJ0304, a potential decarboxylase and the archeal homolog of Memo.

It is unlikely that Memo / Mho1 are decabocylases in the mevalonate pathway. In eukaryotes all enzymes of the mevalonate pathway are known and it is highly improbable that Memo / Mho1 are a "backup carbocylase" in case the first fails its job. It is still possible that Memo has decarboxylase or another enzymatic activity.

Could memo then be an other decarboxylase? We do not known. There is no screen for decarbocylases and as we do not know the potential substrate we can not run an enzymatic activity assay.

So far we can not exclude a potential enzymatic activity of Memo. I hope that people from the Hynes lab are going to solve the Memo riddle in the near future!

5.3   *MHO1* and *PLC1* are synthetic lethal in *S. cerevisiae*

In a synthetic lethal screen done by Maria Maira in the lab of Prof. Matthias Peter in Zürich *PLC1* showed up as a potential synthetic lethal interaction partner of *MHO1*. *PLC1* was the only hit in this SL screen. We then made the two single deleted haploid deletion strains and after mating and dissection of the resulting spores we showed that all double deleted spores could germinate but stopped in proliferation after 2 - 10 cell cycles. This let us hypothesize that according to the amount of Plc1 or Mho1 protein the individual spores got from the mother cell defines how many cell cycles the double deleted cells can undergo until the stop dividing as a result of not enough Plc1 or Mho1 in the cell. By reintroducing a CEN/ARS plasmid expressing PLC1 under its endogenous promotor we could rescue the SL phenotype and as soon as the cells lost the plasmid again growth was inhibited. This proved that the observed SL phenotype is a true stop in proliferation and SL is not only observed due to a germination defect of the double deleted spores.

5.3.1   Rescue with *PLC1* expression

We could also rescue the SL phenotype of *plc1*Δ and *mho1*Δ by replacing the endogenous *MHO1* gene with its human homologue *MEMO*. This showed us that even though Memo was found as a phospho-tyrosine binding protein which pulls-down with ErbB2 and yeast do not have any dedicated tyrosine kinases at all, the human gene can complement for its yeast homologue in this assay. We propose that this rescue can be

explained with a conserved "activity" of Memo or an other function other than P-Typ binding of Memo.

5.3.2 Mutation of the vestigial active site

As shown in Figure 1.2 Memo and the class III non-heme dioxygenase show structural homology. Memo has a altered "active" site compared to the dioxygenase and expresses two histidine and one glutamate where the dioxygenase has two histidine and a cysteine. Nevertheless we showed that all the amino acids facing the vestigial active site in Memo are conserved throughout evolution (Figure 3.1B). We mutated those amino acids in the yeast gene by site-directed mutagenesis to create the the mutated genes: *mho1H47A*, *mho1H80A*, *mho1H47A_H80A*, and *mho1C284A*. Our idea was that if Memo is an enzyme the point mutation of these evolutionary highly conserved amino acids might impair the enzymatic activity. Because we do not know the potential substrate of the hypothetical enzyme Mho1/Momo we could not develop an enzymatic activity assay with cell lysates or purified protein. Instead we took advantage of the SL phenotype between *mho1Δ* and *plc1Δ*. We replaced the endogenous *MHO1* gene with the potentially active dead mutations we made (point mutations in the vestigial active site). All tested point mutations could rescue for the wild type gene. However the *mho1C284A* mutations showed a slow growing phenotype when compared to the other tested mutations an the wild type gene. This suggest that the Cys284 has a crucial role in the proper unction of Mho1. We did not the test the triple mutation of all three His in the vestigial active site, but the single and double point mutation of the His to Ala in the vestigial active site did not show a phenotype in our complementation assay. This result could be an other hint that Mho1/Memo is not an enzyme, but one could also argue that Mho1 does not need an enzymatic activity to rescue the SL phenotype. We can only say that the mutations of the two histidine 47 and 80 to alanine did not affect the rescue of the synthetic lethality, so Mho1H47A_H80A did fulfill the same function than the wild-type protein in this assay. The *plc1 Δ mho1A284C* mutated strain was a bit slower growing but the mutated protein could also complement for the wild-type protein (see Figure 4.10).

We showed that Memo is not only conserved from bacteria to human but the human gene can also complement for its yeast homolog. We also made various expression vectors for use in mammalian cells expressing the yeast gene MHO1 combined with

several Tags and GFP. We would like to answer the question if the yeast gene can complement for the human gene in migration and adhesion assays and where the yeast protein localizes to in a mammalian cell.

But the main question remains still unanswered: **"Why are *MHO1* and *PLC1* synthetic lethal?"**

5.4   Can the microarray results explain the SL phenotype of *mho1Δ* and *plc1Δ*

In mammalian cells Memo gets recruited to the membrane after induction with growth factors like HRG or EGF. We also showed that Memo can be imported and exported actively from the nucleus. However Mho1/Memo is predominantly found in the nucleus in yeast and mammalian cells. Due to this localization pattern we wanted to know if Mho1 could be a transcription factor or if Mho1 regulates transcription of other genes. In a microarray experiment we compared gene expression in wild-type, *mho1Δ*, and *plc1Δ* strains. Because Mho1 is highly upregulated in stationary phase we harvested the cells in mid-log phase and after 48 h growth in YPD.

Analysis of the data showed that wild-type and mho1Δ strains show almost the same gene expression patterns. Only mRNA levels of a few genes was altered between wild-type and mho1Δ strain in both conditions. That the array data comparing the mRNA levels of wt and deletion strain grown to mid-log phase showed almost no changes (see table 4.1) could be explained by the fact that there is little Mho expression when yeast cells are grown under these conditions, but also when cells were harvested after 48 h of growth in YPD most genes expression patterns were unchanged (see table 4.2) even though Mho1 is upregulated up to 16 fold or even more under these conditions (35).

The results from our microarray comparing gene expression of wild-type and *mhoΔ* strains grown in mid-log phase and 48 h in stationary phase showed almost no difference between the two strains. This finding together with the fact that the Mho1/Memo protein does not show any known DNA binding domain let us conclude that is highly unlikely that Mho1 is a transcription factor. Also it does not look like Mho1 influences the transcription of other genes in the cells. In our microarray results only in both conditions only 9 genes were up or down regulated in *mhoΔ* strains compared to wild-type. All but one of them are "dubious open reading frames" or "protein of

unknown function". The biggest expression change between the two strains showed the gene *YEL020C-B* which was more then 8-times downregulated in a *mho*Δ strain when grown to stationary phase. *YEL020C-B* encodes for a "dubious open reading frame unlikely to encode for a protein". The only "known" gene showing up in our micro array experiment was *LSM5*. In *mho*Δ *LSM5* is approximately 2-fold downregulated compared to wild-type strains. Lsm5 is part of two heteroheptameric complexes, Lsm2p-7p and either Lsm1p or Lsm8p. The complex containing Lsm1-7p is predominately cytoplasmic and mutations in that complex all cause defects in mRNA degradation (45)(9). It was also shown that depletion of the essential proteins Lsm2-5p or Lsm8p are defective in processing tRNA (59), rRNA (57), and snoRNA (58). However, we do not think that the downregulation of *LSM5* in *mho*Δ strains has an effect on the cell. As Lsm5 is involved in mRNA decay a significant downregulation of the protein would have a big effect on the mRNA levels in our microarray experiment, but almost all mRNA levels are the same as in wild-type. Because we did a tiling array, we were also able to detect other classes of RNA, like tRNA, rRNA, or snoRNA. Again, if LSM5 would be significantly downregulated we would expect a lot of RNAs to show up, but we detected only two tRNAs and one snoRNA to be changed in all experimental setup. Even though Lsm5 is an interesting candidate and give us a lot of possibilities to speculate about its contribution to the synthetic lethal phenotype between *mho1*Δ and *plc1*Δ we showed that the observed 2-fold downregulation in the *mho1*Δ strain is not enough to have an effect on its RNA levels.

6

Materials & methods

6.1 yeast cells

6.1.1 Yeast lysates

6.1.1.1 Yeast lysates for TAPtag assay (MM400)

The appropriate TAP tagged yeast strains were grown in 2 l of YPD to the needed OD_{600}. In our experiment to OD_{600} of 2 and 12. The cells were spun down in 1 l centrifuge bottles at 6000 RPM for 85 minutes min and pellets were resuspended in 100ml H_2O and transferred to 250ml bottle and spun in an SLA-1500 rotor at 4000 rpm for 10 min. The pellet was resuspended in 1/4 Volume of 1x lysis buffer (6mM Na_2HPO_4, 4mM NaH_2PO_4*H_2O, 1% NP-40, 150 mM NaCl, 2 mM EDTA, 1 mM EGTA, 50 mM NaF, 4 μg/ml leupeptin, 0.1 mM Na_3VO_4, and per 50 ml lysis buffer 1 complete tablet, EDTA free (Roche Cat.# 1873580) and 500 $_mu$l 0.1 M PMSF). The cells were then pipetted into a 50 ml Falcon tube containing liquid N_2 and stored at -80C. For the lysis the Retsch (Haan, Germany) MM400 Mixer Mill was used. The two grinding jars (01.462.0216) and the two grinding balls (05.368.0062) were pre-chilled in liquid N_2 and 7.5g of frozen cell beads were added to each of the grinding jars. Jars were again chilled in liquid N_2 and then grinded for 3 minutes at 30Hz. Chilling and grinding cycle was repeated another two times (total 9 minutes grinding). The obtained yeast powder was used for TAP tag purification experiments.

6.1.1.2   Yeast lysates for western blot and reductase assay

Yeast cells were grown in the appropriate medium to the needed OD_{600}. Cells were harvested by centrifugation and resuspended in lysis buffer. Acid washed glass beads were added to the cells in 2 ml eppendorf tubes (Sigma-Aldrich, St. Louis, Missouri). The tubes were vortexed for 3 times 1 minute at full speed at 4C followed by 5 minutes on ice. After centrifugation the supernatant was collected and stored at -20C for further use.

6.1.1.3   Total RNA Isolation from S. cerevisiae

Approximately 50 ml of yeast cultures at OD_{600}=0.5 were harvested by centrifugation and pellet was resuspended in in 2.4 ml AE Buffer (AE = 50mM NaAcetate pH 5.2, 10mM EDTA) and transferred to an RNase-free Nalgene (Thermo Fisher Scientific, NY) Oak Ridge phenol-resistant centrifuge tube (15 ml size). 160 ?l 25% SDS and 2.4 ml acid phenol (pH 4.3, purchased as unbuffered saturated liquefied phenol (Fischer BP1751I-400)) were added and mixed by vortexing. After a 10 min incubation at 65C with vortexing every minute the samples were placed for 5 min on ice. Samples were spun down for 15 min at 12'000 g (10'000 rpm in a SS-34 rotor) and supernatant was transferred into a pre-spun (5 min at 1500 rpm) 15 ml Phase Lock Gel tube (Eppendorf, Hamburg, Germany) and 2.6 ml chloroform (Fischer BP1145-1) was added and mixed by shaking. Samples were spun down for 10 min at 3000 rpm in a tabletop centrifuge (Beckman). The supernatant was poured into a new RNase-free Nalgene Oak Ridge centrifuge tube and 1/10 volume 3M NaAcetate (pH 5.2-5.6) and equal volume of room temperature Isopropanol were added,mixed and spun down for 45 min at 17'500 g (12'000 rpm in a SS-34 rotor). The pellet was washed with 1 ml 70% EtOH and spun again 20 at 17'500 g. EtOH was poured off and pellet was dried in a speed vac on low heat for 15 min. The pellet was resuspended in 100 μl water and transfer to an RNase-free Eppendorf tube. Quantitate of RNA was measured with NanoDrop and 1 μg was run on a 1% agarose gel. Expected yields should be around 0.4 mg of total RNA. The RNA samples were stored at -80C.

6.1.2 Fishing experiments and screens

6.1.2.1 TAP (Tandem Affinity Purification)

All TAP tagged strains are from the Open Biosystems (Huntsville, Alabama) "Yeast TAP-Tagged Collection for profiling the yeast proteome". Picking of the correct strains was checked by verification PCR with the appropriate oligos. All strains have a C-terminal TAP insertion cassette contains the coding region for a modified version of the TAP (Tandem Affinity Purification) tag, which consists of a calmodulin binding peptide, a TEV (Tobacco Etch Virus) cleavage site and two IgG binding domains of *Staphylococcus aureus* protein A, as well as the *HIS3MX6* selectable marker. The background strain is the Mata BY4741.

The strains were inoculated in 10 ml YPD and grown over night at 30C. Next day the pre-culture was diluted in 2 l YPD and grown at 30C in a shaking incubator (180 rpm) to an OD_{600} of 2 or 12. The cells were harvested by centrifugation at 4C and lysed as described above. The yeast powder was used for TAP tag purification. The TAP tag purification protocol was adapted by Marc Bhler from (90) and (88):

The powder was put in a chilled glass beaker to warm up at room temperature until it started thawing at the edges. 2 ml of lysis buffer containing freshly added protease inhibitors was added per g of lysed yeast cells and mixed rapidly with a spatula to obtain a homogenous suspension. NaCl concentration was increased, if needed more than 150 mM, by adding 5 M NaCl and stirring in the cold room. The lysates were transferred to a 50 ml Falcon tube and spun at 12'000 rpm for 25 min at 4C. Supernatant was transferred to a fresh Falcon tube and 400 μl of IgG-Sepharose beads in lysis buffer (1:1) slurry were added and incubated on a rocker at 4 C for 2 hours. The Falcon tube was then spun for 3 min at 500g. Supernatant was poured off and the resins were resuspended in the residual amount of supernatant. Biorad (Hercules, California) polyprep column were equilibrated with 1ml wash buffer (10 mM Tris-HCl, pH 8.0, 150 mM NaCl, 0.1% NP-40). Lysate and beads were pipetted into a Biorad polyprep column with a reservoir and another ml of lysis buffer was added to collect all the beads. The beads were washed 3 times with 10 ml wash buffer followed by a wash with 10 ml TEV-C buffer (10 mM Tris-HCl, pH 8.0, 150 mM KOAc, 0.1% NP-40, 0.5 mM EDTA, 1 mM DTT). The bottom of the column was closed with a stopper and transferred at room temperature and 1 ml of room temp TEV-C buffer containing 5

μl acTEV (50U) was added. The column was sealed and allowed the stand at room temperature for 1-1.5 hours. The eluate was drained into a new coluomn (equilibrated with 1 ml CAM-B buffer (10 mM Tris-HCl, pH 8.0, 150 mM NaCl, 1 mM Mg(OAc)$_2$, 1 mM Imidazole, 2 mM CaCl$_2$, 10 mM βME) and sealed at the bottom). The column was washed twice with 1.5 ml Cam-B containing 0.1% NP-40 and once with 1.5 ml CAM-B buffer containing 0.02% NP-40. The column was eluted with CAM-E buffer (10 mM Tris-HCl, pH 8.0, 150 mM NaCl, 0.02% NP-40, 1 mM Mg(OAc)$_2$, 1 mM Imidazole , 10 mM EGTA, 10 mM βME) containing 0.02% NP-40 into 1.5 ml eppendorf tubes: 100 μl E1 fraction (void), E2 and E3 fraction, 250 μl and 700 μl respectively. The E2 and E3 fraction were pooled and split into two equal fractions. Both were TCA precipitated, one for submission for mass-specometry analysis and one for a gradient SDS gel, followed by silver staining. TCA purification was done as follows: Cold (4C) TCA from a 100% stock was added to a final concentration of 20% and incubated on ice for 20 min followed by full speed centrifugation at 4C. The supernatant was removed and washed with 1 ml of cold (4C) 10% TCA and spun for 20 min full speed at 4C. Supernatant was removed and pellet was washed with 1 ml of cold (-20C) HPLC-grade acetone and spun for 30 min full speed at 4C. Supernatant was removed and the pellet was air-dried at room temperature. Dried pellet was stored at -80C before being submitted to the Protein analysis facility. The samples were then Trypsin digested and analyzed with a LTQ Orbitrap Velos (Thermo Scientific) equipped with Agilent 1100/1200 Nanoflow LC System for nano-spray MS (Agilent Technologies). For processing of the results the software Mascot (Matrix Science) was used.

6.1.2.2   dSLAM

The dSLAM screen was done as described in (79) with some slight modification. In a first step the YKO /yeast knock out) heterozygous diploid strain collection had do be made mating type selectable. To obtain the mating type selectable cassette the plasmid pXP346 (79) was cut with *Spe*I x *Pst*I and run on an 1% agarose gel. The appropriate band was cut out and extracted from the gel. The obtained cassette *can1Δ::LEU2-MFA1pr-HIS3* integrated into the pooled deletion collection by transformation en masse. We obtained approximately 900'000 transformed cells which is about 150 transformants per deletion strain. Next we made a query construct for integrative transformation. For that we toke the *mho1Δ::kanMX* strain and replaced the

selection marker with the *natMX* marker from the plasmid pAG25 (40) or with the *URA3* marker from the plasmid pSO142-2 (79). Genomic DNA from the newly made strains was used as template for a PCR reaction to create the *MHO1* deletion cassette. The two oligos SLS-for (GCCTCACGCACCTTCTATAATACACCAAATAAT-GTCCACTTCTCATTGCA) and SLS-rev (CGACTACTCCGCTTACATGTTCAAG-TACGACTCTACTCACGGTAGATACG) were designed to produce a MHO1 deletion cassette with long flanking homologies (approx. 1.5 kb). This cassette was needed for en mass deletion of *MHO1* in the mating type convertible deletion pool. We obtained 250'000 transformants, approx. 40 transformants per deletion strain. Sporulation, final selection and genomic DNA extraction was done as described in (79). TAP-array PCR, TAG-array-hybridisation on Chip and TAG-array scanning was done at Novartis. Image and Data analysis was done with the help of Sven Schuierer using the software spotfire (Tipco, Palo Alto, California).

6.1.2.3 Microarray

For the microarray analysis, total RNA was prepared from cultures grown at 30C in YPD medium to $OD_{600} = 1.0$ (log phase) and $OD_{600} = 12.0$ (stationary phase). RNA was extracted with hot phenol as described in (93). Biotinylated, fragmented cRNA was hybridized to Affymetrix *S. cerevisiae* Tiling 1.0R Array. Data analysis and gene filtering were done using R/Bioconductor (36). Signal condensation was done using only the RMA from the Bioconductor Affy package. Differentially expressed genes were identified using the empirical Bayes method (F test) implemented in the LIMMA package and adjusted with the false discovery rate method (112). Hierarchical clustering and visualization were done in R. Probe sets with a log 2 average contrast signal of at least 5, an adjusted P value of ¡0.05, and an absolute log 2 fold-change of ¿0.585 (1.5-fold in linear space) were selected. The analyses were performed with RNAs harvested from *mho1Δ*, *plc1Δ*, and wild-type strains.

6.1.3 Enzymatic activity

6.1.3.1 Dioxygenase activity of purified Memo

To check if Memo has a class III extradiol dioxygenase activity we designed an assay using potential substrates and purified Memo. Purification of Memo was described previ-

ously in Qui et. al, 2008) (89). As extradiol dioxygenases in bacteria are manly aromatic ring opening enzymes, we chose the substrates protocatechuate (3,4-dihydroxybenzoic acid) and pyrocatechol (1,2-Dihydroxybenzene). Enzymatic activity of extradiol dioxygenases could be observed by absorption measurement at A_{260}. The opening of the aromatic ring is detected by a change in the absorption. 300nM of purified protein per assay was used. As negative control we used the human protein mCTPM2 that was purified in parallel to Memo.

6.2   mammalian cells

6.2.1   Antibodies and Reagents

Recombinant heregulin β 1 (HRG) was purchased from R&D Systems (Minneapolis, MN, USA) and solubilized in PBS + 0.1% BSA.

The following antibodies were used:

Memo (70) rat anti-α-tubulin antibody (supernatant from hybridoma cells) 6His Mcm2

secondary ab:

Alexa-Fluor 546 conjugated anti-rat antibody (Molecular Probes, Eugene, OR) Alexa-Fluor 488 conjugated anti-mouse antibody (Molecular Probes, Eugene, OR)

6.2.2   Cell Culture

MEFs (Mouse Embryonic Fibroblasts) and SKBr3 breast tumor cells were cultured in Dulbecco's modified Eagle's medium supplemented with 10% fetal bovine serum (FBS) (GIBCO Invitrogen, Basel, Switzerland) and 2 mM glutamine at 37 C, 5% CO_2.

6.2.3   Microscopy

6.2.3.1   Testing of the Memo anti-body for IF

We have chosen the Memo inducible KO MEFs for testing the monoclonal Memo antibody. In those cells we can get rid of all Memo protein and so clearly define the specificity of the anti-body in fluorescent microscopy. Both MEFs, wild-type and KO, were grown in 8-well ibidi μ-slides over night in DMEM containing 10% FCS. Cells were fixed in 4% PFA and permeabilized with 0.1% Triton-X. As econdary anti body for Memo

staining we used the Alexa-Fluor 488 conjugated anti-mouse antibody. Microtubules were stained with a rat anti tubulin anti body and withe a secondary Alexa-Fluor 546 conjugated anti-rat antibody. Nucleus was visualized with Hoechst. In the Figure 6.1 the wild-type and the MEMO KO MEFs are shown. The Memo anti body shows a nice nuclear staining (but excluded from the nucleoli) and a less strong homogeneous cytoplasmic staining. In the MEMO KO MEFs almost all signal in the green (Memo) channel is gone if the same parameters for image accusation were applied for both cells. We concluded that the monoclonal Memo anti body shows a high specificity if used for IF and only shows a weak unspecific signal in the cytoplasm.
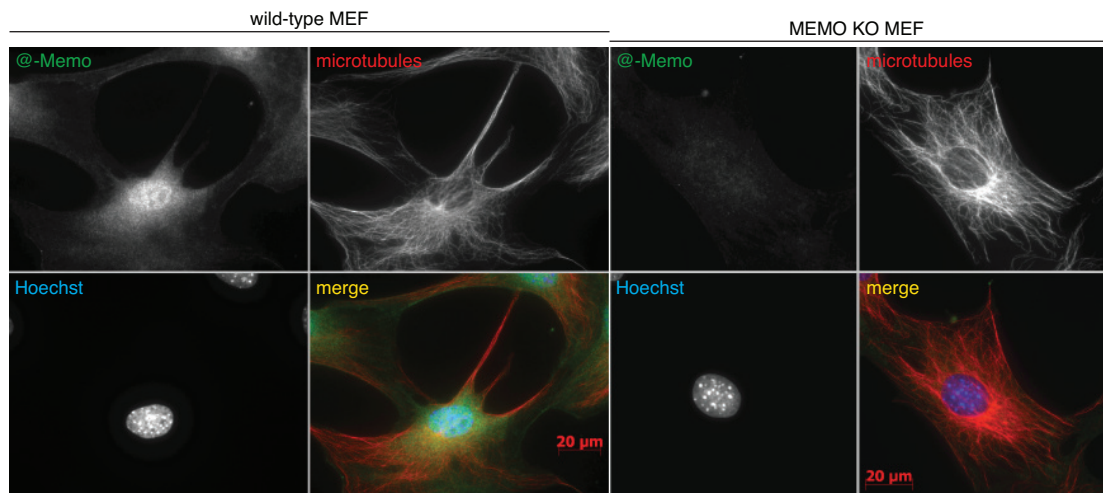
Figure 6.1: Testing of the monoclonal Memo anti body for IF - The figure shows wild-type and MEMO KO MEFs stained for Memo using our lab monoclonal mouse anti Memo anti body. The cells are also stained for microtubules and DNA. Wild-type MEFs show a clear nuclear Memo staining which is excluded from the nucleoli and a less intense homogenous cytoplasmic staining. Using the same staining protocol and the same accusation settings for MEMO KO MEFs almost no single is visible. Only a faint cytoplasmic single is detectable.

6.2.3.2 Immunofluorescence microscopy

SKBR3 cells were grown on glass coverslips (BD Biosciences, San Diego, CA) coated with 25 μg/m rat-tail collagen I (Roche Diagnostics) and MEFs were grown on μ-Slides 8well from ibidi (Martinsried, Germany), in DMEM containing 10% FCS at 37C and stimulated with 10 nM HRG for 20 minutes. Cells were fixed with 4% paraformaldehyde

and 3% sucrose in PBS, permeabilized in 0.2% Triton X-100 in PBS, and blocked with 1% BSA in PBS before incubation with the primary rat anti-α-tubulin antibody and mouse anti-Memo antibody. Alexa-Fluor 546 conjugated anti-rat antibody (Molecular Probes, Eugene, OR) and Alexa-Fluor 488 conjugated anti-mouse antibody (Molecular Probes, Eugene, OR) were used as secondary antibodies. F-actin was stained at room temperature with 2 U/ml FITC-labeled phalloidin (Molecular Probes, Eugene, OR). Cells were washed with PBS-Tween 0.1% and mounted with a mounting solution (ProLong Gold Antifade Reagent, Molecular Probes). Mounted samples were examined using Axioimager Z1 microscope (Carl Zeiss, Feldbach, Switzerland) or using the Laser Scanning Microscope Axio Imager Z2 with the LSM 700 scanning head.

Pictures from MEFs were taken with the following equipment: The Axioimager Z1 microscope (Carl Zeiss, Feldbach, Switzerland) was equipped with a X-Cite 120 EXFO Metal Halide for fluorescence and Halogen for TL, a motorized XYZ stage, and a Plan-APOCHROMAT 100x/1.4 DIC Oil objective. GFP/Alexa488 (Zeiss #10) and DAPI (Zeiss #49) filter sets were used (Carl Zeiss, Feldbach, Switzerland). Fluorescence excitation was controlled by a shutter. We used an AxioCam MRm (1388 x 1040 pixels, Pixel size 6.45 μm) back-illuminated cooled charge-coupled device camera mounted on the primary port. We used the AxioVision software from Zeiss for data acquisition, processing and analysis.

Pictures from SKBR3 cells were taken with the following equipment: Axio Imager Z2 with the LSM 700 scanning head was equipped with the Laser lines: 405 (5mW), 488 (10mW), 555 (10mW), 639 (5mW); and the Lights: Coolled 405, 490, 565 (RL), Halogen (TL), a motorized XYZ stage, and the objectives: Plan-Apochromat 20x/0,8 M27; EC Plan-Neofluar 40x/1,30 Oil M27; Plan-Apochromat 63x/1,40 Oil DIC M27. The Axio Imager Z2 had 2 Epifluorescence PMTs and 1 Transmission PMT. For acquisition we used the ZEN2010 software from Zeiss. Data were further processed and analyzed with Imaris from Bitplane Scientific Software (Zurich, Switzerland).

6.2.4 Subcellular fractionation

The cells were washed and detached by scraping in PBS, then homogenized and fractionated following the Membrane Preparation by Homogenization protocol from Current Protocols in Cell Biology online (Unit 7.10, support protocol 1; Wiley Interscience, John Wiley & Sons Inc, Malden, MA). All buffers were supplemented with either 10

μM CaCl$_2$ or 1 mM EGTA. Equal volumes of each fraction were used for subsequent SDS-PAGE and western blotting with specific antibodies.

6.2.5 Analysis of intracellular ROS levels by FACS

To elucidate if MEMO KO MEFs accumulate more ROS than wild-type MEFs after stress induction we performed a flow cytometrs assay to measure intracellular ROS levels. We used the Image-iT LIVE Green Reactive Oxygen Species Detection Kit from Molecular Probes (Invitrogen) and the wild-type and MEMO KO MEFs. All chemicals and reagents were provided with the mentioned kit.

The wild-type and MEMO KO MEFs were grown in DMEM supplemented with 10% FCS to 80-90% confluency in 10 cm dishes. Medium was changed to PBS/Ca/Mg buffer which was supplemented with carboxyl-H$_2$DCFDA to a working concentration of 25 μM. Cells were protected from light and incubated for 60 minutes at 37C. Medium was changed to DMEM plus 10% FCS supplemented with 100 μM TBHP (*tert*-butyl hydroperoxide) to induce ROS. Negative control cells were put in DMEM plus 10% FCS. ROS was induced for 60 minutes at 37C and 5% CO$_2$. Cells were then washed with PBS/Ca/Mg. Cells were detached with 0.0% Trypsin/EDTA (invitrogen) and kept on ice in PBS/Ca/Mg for FACS analysis. Cells were quickly analyzed by fluorescent microscopy to ensure prober induction of ROS in induced cells and the lack of signal in the control cells. Cells were measured by FACS detecting fluorescence with the FL-1 H channel (505-530 nm). Foreach duplicate we measured 20'000 cells.

7

Appendix

7.1 microarray - alternative analysis

To get more information out of the microarray analysis discussed in the section "4.3 Microarray(Does Mho1 control transcription?)" we used an other approach to to analyze the data.

We used a wild-type, a *mho1Δ*, and a *plc1Δ* strain. Each strain was grown to mid-log phase and to stationary phase. The microarray was performed as described in "materials and methods".

First we determined the fold change of each gene in each strain when stationary phase is compared to mid-log phase. We then knew how each strain regulates its gene sets. Second we compared the changes of each group to the other two, e.g. the genes which are up-regulated in a wild-type strain when stationary phase is compared to mid-log phase are compared to genes up-regulated in a *mho1Δ* strain when stationary phase is compared to mid-log phase. So we compared all three strains agains each other and displayed the results in a Venn diagram (see Figure 7.1). As threshold we choose a fold change of 1.5 . This means a gene has to be up- or down-regulated at least 1.5 fold more in one strain when stationary phase is compared to mid-log phase then in an other.

In Figure 7.2 the Venn diagram of the up-regulated genes are shown. In this figure it is shown that 46 genes are at least 1.5 fold more up-regulated in a *mho1Δ* strain then in a wild-type or *plc1Δ* strain. And 52 genes are up-regulated in *mho1Δ* or *plc1Δ*
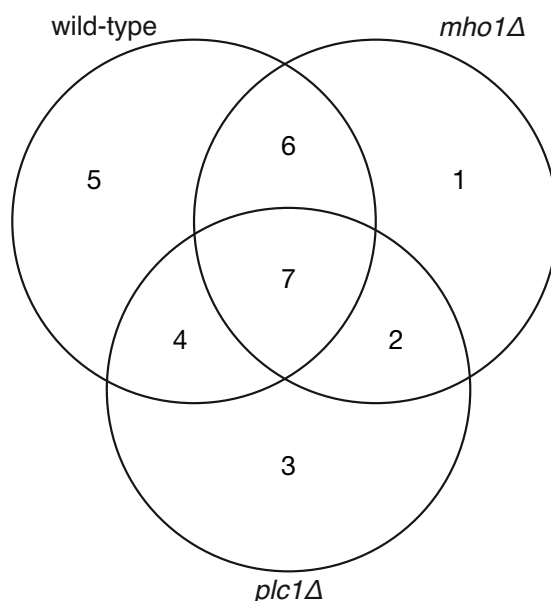
Figure 7.1: How to interpret the Venn diagram - The three circles represent the genes up- or down regulated in stationary phase compared to mid-log phase. In 7 all the genes are represented which are regulated the same for all three strains. In 1 only genes are present which are unique for the *mho1*Δ strain, and so on...

strains but not in a wild-type strain. The gene names and the log2 fold change are shown in Figure 7.3

The same analysis we also did for all the genes being down regulated when stationary phase is compared to mid-log phase. The Venn diagram is shown in Figure 7.4 and the list of genes in Figure 7.5 shows the 104 genes downregulated at lest 1.5 fold more in the *mho1*Δ strain compared to wild-type and *plc1*Δ strains and in Figure 7.6 the genes significantely more gownregulated in *mho1*Δ and *plc1*Δ strains compared to wild-type.

What does this result mean? What is the biological relevance of these results?

As here we are comparing two rations against each other and the maximal difference a fold change of two we think the observed differences between the *mho1*Δ and the wild-type strain is experimental noise. By comparing the absolute values between the two strain in each of the observed conditions no significant difference was observable (see section "4.3 Microarray(Does Mho1 control transcription?)").
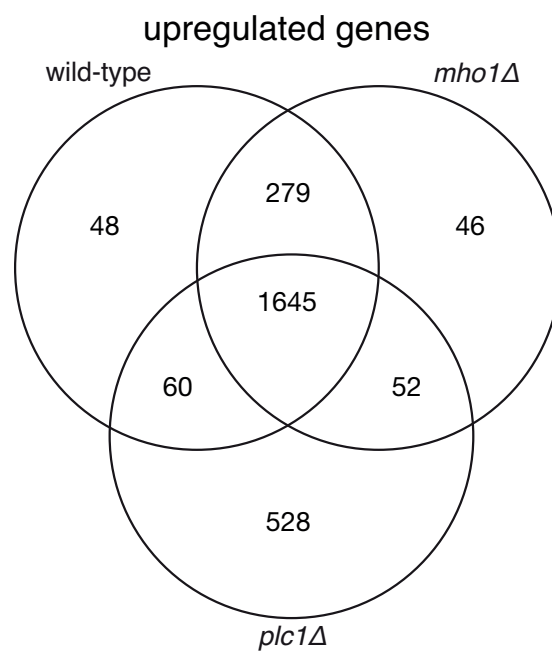
Figure 7.2: **Venn diagram of UP-regulated genes** -

		1			2	
	Sys. Name	Com. Name	logFC	Sys. Name	Com. Name	logFC
1	Q0065	AI4	1.085	HRA1	HRA1	0.96713
2	YBR021W	FUR4	0.613	TLC1	TLC1	0.61264
3	YBR033W	EDS1	0.726	YAR029W		0.82564
4	YCL004W	PGS1	0.588	YBR005W	RCR1	0.70764
5	YCR025C		0.597	YBR126W-A		0.71245
6	YCR063W	BUD31	0.624	YBR180W	DTR1	0.59254
7	YDR126W	SWF1	0.634	YCR037C	PHO87	0.64276
8	YDR319C	YFT2	0.652	YDL175C	AIR2	0.73144
9	YDR402C	DIT2	0.694	YDR098C-B		0.81107
10	YDR476C		0.625	YDR129C	SAC6	0.59328
11	YDR490C	PKH1	0.705	YDR132C		0.73448
12	YEL028W		0.852	YDR246W	TRS23	0.64038
13	YEL062W	NPR2	0.644	YDR261W-B		0.60605
14	YEL071W	DLD3	0.602	YDR517W	GRH1	0.65123
15	YER038C	KRE29	0.686	YEL065W	SIT1	0.69361
16	YGL263W	COS12	0.836	YFL029C	CAK1	0.79436
17	YGR010W	NMA2	0.622	YFR030W	MET10	0.67683
18	YGR011W		0.785	YFR034W-A		0.962
19	YGR212W	SLI1	0.589	YGL002W	ERP6	0.5988
20	YHR022C		0.613	YGL034C		0.77978
21	YIL134C-A		0.647	YGL114W		0.59408
22	YJL052C-A		0.93	YGL158W	RCK1	0.62315
23	YJL136W-A		0.75	YHL009C	YAP3	0.60074
24	YKL055C	OAR1	0.621	YHL030W-A		1.98581
25	YLR235C		0.592	YIL102C		0.77732
26	YLR237W	THI7	0.725	YJL027C		0.73831
27	YLR315W	NKP2	0.64	YJL094C	KHA1	0.63647
28	YLR316C	TAD3	0.625	YJR137C	ECM17	0.73292
29	YLR446W		0.884	YLR097C	HRT3	0.63179
30	YML066C	SMA2	0.586	YLR151C	PCD1	0.71077
31	YMR007W		0.674	YLR157W-D	YLR157W-A	2.20561
32	YMR182C	RGM1	0.658	YLR412C-A		0.67273
33	YMR316C-A		0.933	YMR004W	MVP1	0.60053
34	YNL008C	ASI3	0.654	YMR077C	VPS20	0.66662
35	YNL095C		0.587	YMR135W-A		0.63058
36	YNL114C		1.233	YMR154C	RIM13	0.62434
37	YNL204C	SPS18	0.594	YNL033W		0.80253
38	YNL329C	PEX6	0.598	YNL046W		0.71747
39	YOR382W	FIT2	0.685	YNL279W	PRM1	0.61379
40	YPL006W	NCR1	0.589	YOL013C	HRD1	0.59775
41	YPL133C	RDS2	0.621	YOL073C		0.73685
42	YPL251W		1.39	YOL147C	PEX11	0.66601
43	YPR066W	UBA3	0.599	YOR010C	TIR2	0.75158
44	YPR085C	ASA1	0.587	YOR072W-A		0.91181
45	snR51	SNR51	0.716	YOR075W	UFE1	0.59066
46	snR70	SNR70	0.825	YOR107W	RGS2	0.62225
47				YPL151C	PRP46	0.64315
48				YPL162C		0.65595
49				YPR040W	TIP41	0.62062
50				YPR158C-D		0.67626
51				snR86	SNR86	0.61665
52				tG(CCC)D	SUF3	1.03013

Figure 7.3: List of upregulated genes - 1) Genes only upregulated in *mho1*Δ strains
and 2) genes upregulated in *mho1*Δ and *plc1*Δ strains
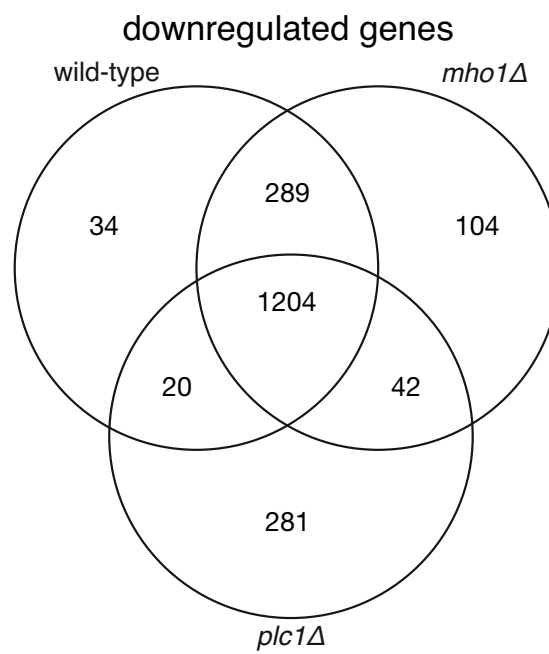
Figure 7.4: **Venn diagram of DOWN-regulated genes** -

	Sys. Name	Com. Name	logFC		Sys. Name	Com. Name	logFC
1	YAR008W	SEN34	-0.65075	53	YIL068C	SEC6	-0.64354
2	YAR015W	ADE1	-0.63537	54	YJL072C	PSF2	-0.666585
3	YBL036C		-0.60839	55	YJL081C	ARP4	-0.599185
4	YBL057C	PTH2	-0.876105	56	YJL125C	GCD14	-0.63153
5	YBR009C	HHF1	-0.61297	57	YJR002W	MPP10	-0.61983
6	YBR022W	POA1	-0.629705	58	YJR112W	NNF1	-0.675005
7	YBR073W	RDH54	-0.618515	59	YJR141W		-0.660955
8	YBR112C	CYC8	-0.65732	60	YKL042W	SPC42	-0.587665
9	YBR161W	CSH1	-0.60706	61	YKL082C	RRP14	-0.70801
10	YBR202W	MCM7	-0.642525	62	YKL108W	SLD2	-0.60682
11	YBR254C	TRS20	-0.810015	63	YKR008W	RSC4	-0.723105
12	YCR052W	RSC6	-0.664525	64	YLR095C	IOC2	-0.65395
13	YCR077C	PAT1	-0.65394	65	YLR319C	BUD6	-0.721715
14	YDL043C	PRP11	-0.68753	66	YLR330W	CHS5	-0.619145
15	YDL092W	SRP14	-0.860395	67	YML009W-B	YML010W-A	-0.66249
16	YDL099W	BUG1	-0.752245	68	YML061C	PIF1	-0.708765
17	YDL118W		-0.999255	69	YMR005W	TAF4	-0.68563
18	YDL119C		-0.59716	70	YMR016C	SOK2	-0.58978
19	YDL179W	PCL9	-0.66168	71	YMR158W	MRPS8	-0.719785
20	YDL187C		-0.95519	72	YMR178W		-0.646295
21	YDL235C	YPD1	-0.670935	73	YMR233W	TRI1	-0.74824
22	YDR052C	DBF4	-0.636175	74	YMR321C		-0.986925
23	YDR167W	TAF10	-0.600795	75	YNL122C		-0.590945
24	YDR240C	SNU56	-0.629665	76	YNL140C		-1.74378
25	YDR396W		-0.635885	77	YNL212W	VID27	-0.6648
26	YDR397C	NCB2	-0.69565	78	YNL213C		-0.6651
27	YDR469W	SDC1	-0.787855	79	YNL252C	MRPL17	-0.65393
28	YDR510C-A		-0.82388	80	YNL272C	SEC2	-0.616955
29	YDR510W	SMT3	-0.715765	81	YOL006C	TOP1	-0.661415
30	YDR514C		-0.675735	82	YOL028C	YAP7	-0.61975
31	YEL017W	GTT3	-0.75083	83	YOL038C-A		-0.7617
32	YEL020C-B		-2.979025	84	YOL070C	NBA1	-0.691065
33	YEL037C	RAD23	-0.70773	85	YOL144W	NOP8	-0.633865
34	YER001W	MNN1	-0.788755	86	YOR076C	SKI7	-0.723415
35	YER059W	PCL6	-0.5986	87	YOR252W	TMA16	-0.641355
36	YER063W	THO1	-0.73968	88	YOR306C	MCH5	-0.66177
37	YER064C		-0.631755	89	YPL007C	TFC8	-0.650765
38	YER112W	LSM4	-0.695575	90	YPL038W	MET31	-0.75321
39	YER151C	UBP3	-0.694905	91	YPL051W	ARL3	-0.664535
40	YER165C-A		-0.605695	92	YPL127C	HHO1	-0.68846
41	YGL061C	DUO1	-0.74662	93	YPL199C		-0.763925
42	YGL122C	NAB2	-0.608475	94	YPL204W	HRR25	-0.58734
43	YGL188C-A		-0.914595	95	YPL225W		-0.726885
44	YGL244W	RTF1	-0.64098	96	YPR046W	MCM16	-0.806755
45	YGL246C	RAI1	-0.64859	97	YPR055W	SEC8	-0.632595
46	YGR047C	TFC4	-0.64804	98	YPR104C	FHL1	-0.64242
47	YGR092W	DBF2	-0.602395	99	YPR105C	COG4	-0.651305
48	YGR140W	CBF2	-0.6546	100	YPR107C	YTH1	-0.61865
49	YGR271C-A	EFG1	-0.79754	101	YPR120C	CLB5	-0.603105
50	YGR276C	RNH70	-0.63751	102	YPR173C	VPS4	-0.68484
51	YHR167W	THP2	-0.657265	103	YPR175W	DPB2	-0.61632
52	YIL008W	URM1	-0.63462	104	snR72	SNR72	-0.686595

Figure 7.5: List of down upregulated genes for *mho1*Δ - 1) Genes only downreg-
ulated in *mho1*Δ strains

	Sys. Name	Com. Name	logFC
		2	
1	YAL024C	LTE1	-0.60884
2	YBR094W	PBY1	-0.656315
3	YCL014W	BUD3	-0.67685
4	YCR013C		-1.253455
5	YDL096C	OPI6	-0.734
6	YDR228C	PCF11	-0.745425
7	YDR310C	SUM1	-0.70708
8	YDR424C	DYN2	-0.6589
9	YDR468C	TLG1	-0.6752
10	YEL007W	TOS9	-0.79289
11	YEL053W-A		-0.830495
12	YGL068W	MNP1	-0.77291
13	YGR082W	TOM20	-0.657985
14	YGR084C	MRP13	-0.781145
15	YGR091W	PRP31	-0.615135
16	YGR233C	PHO81	-0.60495
17	YHR012W	VPS29	-0.655205
18	YIL041W	GVP36	-0.67645
19	YIL138C	TPM2	-0.7563
20	YJL115W	ASF1	-0.677875
21	YJL173C	RFA3	-0.77405
22	YKL119C	VPH2	-0.736675
23	YLR021W	IRC25	-0.64222
24	YLR096W	KIN2	-0.73345
25	YLR337C	VRP1	-0.647425
26	YLR354C	TAL1	-0.616095
27	YNL070W	TOM7	-0.924595
28	YNL121C	TOM70	-0.70357
29	YNL185C	MRPL19	-0.81541
30	YNL259C	ATX1	-0.66965
31	YNR017W	TIM23	-0.622385
32	YOL005C	RPB11	-0.924305
33	YOL102C	TPT1	-0.73365
34	YOR073W	SGO1	-0.74521
35	YOR094W	ARF3	-0.72123
36	YOR144C	ELG1	-0.63969
37	YOR166C	SWT1	-0.608125
38	YOR197W	MCA1	-0.653435
39	YOR286W	AIM42	-0.641065
40	YOR320C	GNT1	-0.682665
41	YPL041C		-0.63179
42	YPR169W	JIP5	-0.636765

Figure 7.6: List of down upregulated genes for *mho1*Δ **and** *plc1*Δ - 2) genes
downregulated in *mho1*Δ and *plc1*Δ strains

References

[1] A E ADAMS, D I JOHNSON, R M LONGNECKER, B F SLOAT, AND J R PRINGLE. **CDC42 and CDC43, two additional genes involved in budding and the establishment of cell polarity in the yeast Saccharomyces cerevisiae**. *J Cell Biol*, **111**(1):131–42, Jul 1990. 14

[2] A E ADAMS AND J R PRINGLE. **Relationship of actin and tubulin distribution to bud growth in wild-type and morphogenetic-mutant Saccharomyces cerevisiae**. *J Cell Biol*, **98**(3):934–45, Mar 1984. 13

[3] B ALBERTS, D BRAY, AND J LEWIS. *Molecular Biology of the Cell*. Taylor and Francis, 4 edition, 2002. 34

[4] D C AMBERG. **Three-dimensional imaging of the yeast actin cytoskeleton through the budding cell cycle**. *Mol Biol Cell*, **9**(12):3259–62, Dec 1998. 13

[5] B. ANTONSSON, S. MONTESSUIT, L. FRIEDLI, M. A. PAYTON, AND G. PARAVICINI. **Protein kinase C in yeast. Characteristics of the Saccharomyces cerevisiae PKC1 gene product**. *J Biol Chem*, **269**(24):16821–8, 1994. Antonsson, B Montessuit, S Friedli, L Payton, M A Paravicini, G Comparative Study United states The Journal of biological chemistry J Biol Chem. 1994 Jun 17;269(24):16821-8. 32

[6] S. F. ASHBY AND W. NOWELL. **The Fungi of Stigmatomycosis**. *Annals of Botany*, **40**(1):69–84, 1926. 16

[7] Y AYAD-DURIEUX, P KNECHTLE, S GOFF, F DIETRICH, AND P PHILIPPSEN. **A PAK-like protein kinase is required for maturation of young hyphae and septation in the filamentous ascomycete Ashbya gossypii**. *J Cell Sci*, **113 Pt 24**:4563–75, Dec 2000. 19

[8] Y Y BAHK, Y H LEE, T G LEE, J SEO, S H RYU, AND P G SUH. **Two forms of phospholipase C-beta 1 generated by alternative splicing**. *J Biol Chem*, **269**(11):8240–5, Mar 1994. 34

[9] J D BEGGS. **Lsm proteins and RNA processing**. *Biochem Soc Trans*, **33**(Pt 3):433–8, Jun 2005. 111

[10] A BENDER AND J R PRINGLE. **Use of a screen for synthetic lethal and multicopy suppressee mutants to identify two new genes involved in morphogenesis in Saccharomyces cerevisiae**. *Mol Cell Biol*, **11**(3):1295–305, Mar 1991. 20

[11] G W BIRRELL, G GIAEVER, A M CHU, R W DAVIS, AND J M BROWN. **A genome-wide screen in Saccharomyces cerevisiae for genes affecting UV radiation sensitivity**. *Proc Natl Acad Sci U S A*, **98**(22):12608–13, Oct 2001. 26

[12] N BLOM, S GAMMELTOFT, AND S BRUNAK. **Sequence and structure-based prediction of eukaryotic protein phosphorylation sites**. *J Mol Biol*, **294**(5):1351–62, Dec 1999. 101

[13] D BOTSTEIN, S A CHERVITZ, AND J M CHERRY. **Yeast as a model organism**. *Science*, **277**(5330):1259–60, Aug 1997. 7

[14] T BOULIKAS. **Putative nuclear localization signals (NLS) in protein transcription factors**. *J Cell Biochem*, **55**(1):32–58, May 1994. 39

[15] A BRETSCHER, B DREES, E HARSAY, D SCHOTT, AND T WANG. **What are the basic functions of microfilaments? Insights from studies in budding yeast**. *J Cell Biol*, **126**(4):821–5, Aug 1994. 13

[16] J B BRODERICK. **Catechol dioxygenases**. *Essays Biochem*, **34**:173–89, 1999. 105

[17] C BULL AND D P BALLOU. **Purification and properties of protocatechuate 3,4-dioxygenase from Pseudomonas putida. A new iron to subunit stoichiometry**. *J Biol Chem*, **256**(24):12673–80, Dec 1981. 105

[18] LOUIS FRIEDMAN CARL SAGAN, BRUCE MURRAY. **www.planetary.org**. 8

[19] CHARLES N COLE AND JOHN J SCARCELLI. **Transport of messenger RNA from the nucleus to the cytoplasm**. *Curr Opin Cell Biol*, **18**(3):299–306, Jun 2006. 41

[20] MICHAEL COSTANZO, ANASTASIA BARYSHNIKOVA, JEREMY BELLAY, YUNGIL KIM, ERIC D SPEAR, CAROLYN S SEVIER, HUIMING DING, JUDICE L Y KOH, KIANA TOUFIGHI, SARA MOSTAFAVI, JEANY PRINZ, ROBERT P ST ONGE, BENJAMIN VANDERSLUIS, TARAS MAKHNEVYCH, FRANCO J VIZEACOUMAR, SOLMAZ ALIZADEH, SONDRA BAHR, RENEE L BROST, YIQUN CHEN, MURAT COKOL, RAAMESH DESHPANDE, ZHIJIAN LI, ZHEN-YUAN LIN, WENDY LIANG, MICHAELA MARBACK, JADINE PAW, BRYAN-JOSEPH SAN LUIS, ERMIRA SHUTERIQI, AMY HIN YAN TONG, NYDIA VAN DYK, IAIN M WALLACE, JOSEPH A WHITNEY, MATTHEW T WEIRAUCH, GUOQING ZHONG, HONGWEI ZHU, WALID A HOURY, MICHAEL BRUDNO, SASAN RAGIBIZADEH, BALÁZS PAPP, CSABA PÁL, FREDERICK P ROTH, GURI GIAEVER, COREY NISLOW, OLGA G TROYANSKAYA, HOWARD BUSSEY, GARY D BADER, ANNE-CLAUDE GINGRAS, QUAID D MORRIS, PHILIP M KIM, CHRIS A KAISER, CHAD L MYERS, BRENDA J ANDREWS, AND CHARLES BOONE. **The genetic landscape of a cell**. *Science*, **327**(5964):425–31, Jan 2010. 23

[21] D L DANKORT, Z WANG, V BLACKMORE, M F MORAN, AND W J MULLER. **Distinct tyrosine autophosphorylation sites negatively and positively modulate neu-mediated transformation**. *Mol Cell Biol*, **17**(9):5410–25, Sep 1997. 3

[22] B A DAVLETOV AND T C SÜDHOF. **A single C2 domain from synaptotagmin I is sufficient for high affinity Ca2+/phospholipid binding**. *J Biol Chem*, **268**(35):26386–90, Dec 1993. 32

[23] N DIVECHA, A J LETCHER, H H BANFIC, S G RHEE, AND R F IRVINE. **Changes in the components of a nuclear inositide cycle during differentiation in murine erythroleukaemia cells**. *Biochem J*, **312 (Pt 1)**:63–7, Nov 1995. 34

131

[24] T Dobzhansky. **Genetics of Natural Populations. Xiii. Recombination and Variability in Populations of Drosophila Pseudoobscura**. *Genetics*, **31**(3):269–290, May 1946. 20

[25] C G dos Remedios, D Chhabra, M Kekic, I V Dedova, M Tsubakihara, D A Berry, and N J Nosworthy. **Actin binding proteins: regulation of cytoskeletal microfilaments**. *Physiol Rev*, **83**(2):433–73, Apr 2003. 2

[26] D G Drubin and W J Nelson. **Origins of cell polarity**. *Cell*, **84**(3):335–44, Feb 1996. 12

[27] Stacia R Engel, Rama Balakrishnan, Gail Binkley, Karen R Christie, Maria C Costanzo, Selina S Dwight, Dianna G Fisk, Jodi E Hirschman, Benjamin C Hitz, Eurie L Hong, Cynthia J Krieger, Michael S Livstone, Stuart R Miyasato, Robert Nash, Rose Oughtred, Julie Park, Marek S Skrzypek, Shuai Weng, Edith D Wong, Kara Dolinski, David Botstein, and J Michael Cherry. **Saccharomyces Genome Database provides mutant phenotype data**. *Nucleic Acids Res*, **38**(Database issue):D433–6, Jan 2010. 7

[28] C M Field and D Kellogg. **Septins: cytoskeletal polymers or signalling GTPases?** *Trends Cell Biol*, **9**(10):387–94, Oct 1999. 14

[29] F P Finger and P Novick. **Spatial regulation of exocytosis: lessons from yeast**. *J Cell Biol*, **142**(3):609–12, Aug 1998. 13

[30] J S Flick and J Thorner. **Genetic and biochemical characterization of a phosphatidylinositol-specific phospholipase C in Saccharomyces cerevisiae**. *Mol Cell Biol*, **13**(9):5861–76, Sep 1993. 28

[31] H Fried and U Kutay. **Nucleocytoplasmic transport: taking an inventory**. *Cell Mol Life Sci*, **60**(8):1659–1688, Aug 2003. 37

[32] H Fujisawa and O Hayaishi. **Protocatechuate 3,4-dioxygenase. I. Crystallization and characterization**. *J Biol Chem*, **243**(10):2673–81, May 1968. 105

[33] H Fujisawa, K Hiromi, M Uyeda, M Nozaki, and O Hayaishi. **Oxygenated form of protocatechuate 3,4-dioxygenase, a non-heme iron-containing dioxygenase, as reaction intermediate**. *J Biol Chem*, **246**(7):2320–1, Apr 1971. 105

[34] A. P. Gasch, P. T. Spellman, C. M. Kao, O. Carmel-Harel, M. B. Eisen, G. Storz, D. Botstein, and P. O. Brown. **Genomic expression programs in the response of yeast cells to environmental changes**. *Mol Biol Cell*, **11**(12):4241–57, 2000. Gasch, A P Spellman, P T Kao, C M Carmel-Harel, O Eisen, M B Storz, G Botstein, D Brown, P O HG-00450/HG/NHGRI NIH HHS/United States HG-00983/HG/NHGRI NIH HHS/United States Research Support, Non-U.S. Gov't Research Support, U.S. Gov't, P.H.S. United states Molecular biology of the cell Mol Biol Cell. 2000 Dec;11(12):4241-57. 104, 110

[35] Robert C Gentleman, Vincent J Carey, Douglas M Bates, Ben Bolstad, Marcel Dettling, Sandrine Dudoit, Byron Ellis, Laurent Gautier, Yongchao Ge, Jeff Gentry, Kurt Hornik, Torsten Hothorn, Wolfgang Huber, Stefano Iacus, Rafael Irizarry, Friedrich Leisch, Cheng Li, Martin Maechler, Anthony J Rossini, Gunther Sawitzki, Colin Smith, Gordon Smyth, Luke Tierney, Jean Y H Yang, and Jianhua Zhang. **Bioconductor: open software development for computational biology and bioinformatics**. *Genome Biol*, **5**(10):R80, 2004. 117

[36] Sina Ghaemmaghami, Won-Ki Huh, Kiowa Bower, Russell W Howson, Archana Belle, Noah Dephoure, Erin K O'Shea, and Jonathan S Weissman. **Global analysis of protein expression in yeast**. *Nature*, **425**(6959):737–41, Oct 2003. 83, 104

[37] Guri Giaever, Angela M Chu, Li Ni, Carla Connelly, Linda Riles, Steeve Véronneau, Sally Dow, Ankuta Lucau-Danila, Keith Anderson, Bruno André, Adam P Arkin, Anna Astromoff, Mohamed El-Bakkoury, Rhonda Bangham, Rocio Benito, Sophie Brachat, Stefano Campanaro, Matt Curtiss, Karen Davis, Adam Deutschbauer, Karl-Dieter Entian, Patrick Flaherty, Francoise Foury, David J Garfinkel, Mark Gerstein, Deanna Gotte, Ulrich Güldener, Johannes H Hegemann, Svenja Hempel, Zelek Herman, Daniel F Jaramillo, Diane E Kelly, Steven L Kelly, Peter Kötter, Darlene LaBonte, David C Lamb, Ning Lan, Hong Liang, Hong Liao, Lucy Liu, Chuanyun Luo, Marc Lussier, Rong Mao, Patrice Menard, Siew Loon Ooi, Jose L Revuelta, Christopher J Roberts, Matthias Rose, Petra Ross-Macdonald, Bart Scherens, Greg Schimmack, Brenda Shafer, Daniel D Shoemaker, Sharon Sookhai-Mahadeo, Reginald K Storms, Jeffrey N Strathern, Giorgio Valle, Marleen Voet, Guido Volckaert, Ching-yun Wang, Teresa R Ward, Julie Wilhelmy, Elizabeth A Winzeler, Yonghong Yang, Grace Yen, Elaine Youngman, Kexin Yu, Howard Bussey, Jef D Boeke, Michael Snyder, Peter Philippsen, Ronald W Davis, and Mark Johnston. **Functional profiling of the Saccharomyces cerevisiae genome**. *Nature*, **418**(6896):387–91, Jul 2002. 26

[38] A Goffeau, B G Barrell, H Bussey, R W Davis, B Dujon, H Feldmann, F Galibert, J D Hoheisel, C Jacq, M Johnston, E J Louis, H W Mewes, Y Murakami, P Philippsen, H Tettelin, and S G Oliver. **Life with 6000 genes**. *Science*, **274**(5287):546, 563–7, Oct 1996. 6

[39] A. L. Goldstein and J. H. McCusker. **Three new dominant drug resistance cassettes for gene disruption in Saccharomyces cerevisiae**. *Yeast*, **15**(14):53, 1999. 89, 117

[40] D Görlich and U Kutay. **Transport between the cell nucleus and the cytoplasm**. *Annu Rev Cell Dev Biol*, **15**:607–60, 1999. 39

[41] Laura L Grochowski, Huimin Xu, and Robert H White. **Methanocaldococcus jannaschii uses a modified mevalonate pathway for biosynthesis of isopentenyl diphosphate**. *J Bacteriol*, **188**(9):3192–8, May 2006. 105, 106, 107

[42] J L Hartman, 4th, B Garvik, and L Hartwell. **Principles for the buffering of genetic variation**. *Science*, **291**(5506):1001–4, Feb 2001. 20

[43] L H Hartwell, J Culotti, J R Pringle, and B J Reid. **Genetic control of the cell division cycle in yeast**. *Science*, **183**(4120):46–51, Jan 1974. 14

[44] W He and R Parker. **Functions of Lsm proteins in mRNA degradation and splicing**. *Curr Opin Cell Biol*, **12**(3):346–50, Jun 2000. 111

[45] C Heinrich, C Keller, A Boulay, M Vecchi, M Bianchi, R Sack, S Lienhard, S Duss, J Hofsteenge, and N E Hynes. **Copine-III interacts with ErbB2 and promotes tumor cell migration**. *Oncogene*, **29**(11):1598–610, Mar 2010. 3

[46] L Holm and C Sander. **Mapping the protein universe**. *Science*, **273**(5275):595–603, Aug 1996. 4, 94

[47] Christian R Ingrell, Martin L Miller, Ole N Jensen, and Nikolaj Blom. **NetPhosYeast: prediction of protein phosphorylation sites in yeast**. *Bioinformatics*, **23**(7):895–7, Apr 2007. 102

[48] T Ito, T Chiba, R Ozawa, M Yoshida, M Hattori, and Y Sakaki. **A comprehensive two-hybrid analysis to explore the yeast protein interactome**. *Proc Natl Acad Sci U S A*, **98**(8):4569–74, Apr 2001. 86

[49] J J Jacoby, H P Schmitz, and J J Heinisch. **Mutants affected in the putative diacylglycerol binding site of yeast protein kinase C**. *FEBS Lett*, **417**(2):219–22, Nov 1997. 30

[50] Matilda Katan. **New insights into the families of PLC enzymes: looking back and going forward**. *Biochem J*, **391**(Pt 3):e7–9, Nov 2005. 33

[51] I Kaverina, O Krylyshkina, and J V Small. **Microtubule targeting of substrate contacts promotes their relaxation and dissociation**. *J Cell Biol*, **146**(5):1033–44, Sep 1999. 1

[52] C G Kim, D Park, and S G Rhee. **The role of carboxyl-terminal basic amino acids in Gqalpha-dependent activation, particulate association, and nuclear localization of phospholipase C-beta1**. *J Biol Chem*, **271**(35):21187–92, Aug 1996. 34

[53] Michael Köhli, Virginie Galati, Kamila Boudier, Robert W Roberson, and Peter Philippsen. **Growth-speed-correlated localization of exocyst and polarisome components in growth zones of Ashbya gossypii hyphal tips**. *J Cell Sci*, **121**(Pt 23):3878–89, Dec 2008. 20

[54] Zen Kouchi, Tomohide Shikano, Yoshikazu Nakamura, Hideki Shirakawa, Kiyoko Fukami, and Shunichi Miyazaki. **The role of EF-hand domains and C2 domain in regulation of enzymatic activity of phospholipase Czeta**. *J Biol Chem*, **280**(22):21015–21, Jun 2005. 32

[55] S J Kron and N A Gow. **Budding yeast morphogenesis: signalling, cytoskeleton and cell cycle**. *Curr Opin Cell Biol*, **7**(6):845–55, Dec 1995. 14

[56] Joanna Kufel, Christine Allmang, Elisabeth Petfalski, Jean Beggs, and David Tollervey. **Lsm Proteins are required for normal processing and stability of ribosomal RNAs**. *J Biol Chem*, **278**(4):2147–56, Jan 2003. 111

[57] Joanna Kufel, Christine Allmang, Loredana Verdone, Jean Beggs, and David Tollervey. **A complex pathway for 3' processing of the yeast U3 snoRNA**. *Nucleic Acids Res*, **31**(23):6788–97, Dec 2003. 111

[58] Joanna Kufel, Christine Allmang, Loredana Verdone, Jean D Beggs, and David Tollervey. **Lsm proteins are required for normal processing of pre-tRNAs and their efficient association with La-homologous protein Lhp1p**. *Mol Cell Biol*, **22**(14):5248–56, Jul 2002. 111

[59] Tanja la Cour, Lars Kiemer, Anne Mølgaard, Ramneek Gupta, Karen Skriver, and Søren Brunak. **Analysis and prediction of leucine-rich nuclear export signals**. *Protein Eng Des Sel*, **17**(6):527–36, Jun 2004. 41

[60] D A Lauffenburger and A F Horwitz. **Cell migration: a physically integrated molecular process**. *Cell*, **84**(3):359–69, Feb 1996. 1

[61] W S Lo, E I Raitses, and A M Dranginis. **Development of pseudohyphae by embedded haploid and diploid yeast**. *Curr Genet*, **32**(3):197–202, Sep 1997. 14

[62] M. C. Lorenz, N. S. Cutler, and J. Heitman. **Characterization of alcohol-induced filamentous growth in Saccharomyces cerevisiae**. *Mol Biol Cell*, **11**(1):183–99, 2000. Lorenz, M C Cutler, N S Heitman, J Research Support, Non-U.S. Gov't United states Molecular biology of the cell Mol Biol Cell. 2000 Jan;11(1):183-99. 16

[63] Pek Yee Lum, Christopher D Armour, Sergey B Stepaniants, Guy Cavet, Maria K Wolf, J Scott Butler, Jerald C Hinshaw, Philippe Garnier, Glenn D Prestwich, Amy Leonardson, Philip Garrett-Engele, Christopher M Rush, Martin Bard, Greg Schimmack, John W Phillips, Christopher J Roberts, and Daniel D Shoemaker. **Discovering modes of action for therapeutic compounds using a genome-wide screen of yeast heterozygotes**. *Cell*, **116**(1):121–37, Jan 2004. 26

[64] H D Madhani and G R Fink. **The riddle of MAP kinase signaling specificity**. *Trends Genet*, **14**(4):151–5, Apr 1998. 14

[65] Romina Marone, Daniel Hess, David Dankort, William J. Muller, Nancy E. Hynes, and Ali Badache. **Memo mediates ErbB2-driven cell motility**. *Nat Cell Biol*, **6**(6):22, 2004. 1, 3, 103

[66] A M Martelli, R S Gilmour, V Bertagnolo, L M Neri, L Manzoli, and L Cocco. **Nuclear localization and signalling activity of phosphoinositidase C beta in Swiss 3T3 cells**. *Nature*, **358**(6383):242–5, Jul 1992. 34

[67] M. Meira, R. Masson, I. Stagljar, S. Lienhard, F. Maurer, A. Boulay, and N. E. Hynes. **Memo is a cofilin-interacting protein that influences PLCgamma1 and cofilin activities, and is essential for maintaining directionality during ErbB2-induced tumor-cell migration**. *J Cell Sci*, **122**(Pt 6):787–97, 2009. Meira, Maria Masson, Regis Stagljar, Igor Lienhard, Susanne Maurer, Francisca Boulay, Anne Hynes, Nancy E Research Support, Non-U.S. Gov't England Journal of cell science J Cell Sci. 2009 Mar 15;122(Pt 6):787-97. Epub 2009 Feb 17. 2, 26, 34, 87, 118

[68] Pamela B Meluh, Xuewen Pan, Daniel S Yuan, Carol Tiffany, Ou Chen, Sharon Sookhai-Mahadeo, Xiaoling Wang, Brian D Peyser, Rafael Irizarry, Forrest A

Spencer, and Jef D Boeke. **Analysis of genetic interactions on a genome-wide scale in budding yeast: diploid-based synthetic lethality analysis by microarray.** *Methods Mol Biol*, **416**:221–47, 2008. 88

[69] Takahiro Miyawaki, Dimitry Ofengeim, Kyung-Min Noh, Adrianna Latuszek-Barrantes, Brian A Hemmings, Antonia Follenzi, and R Suzanne Zukin. **The endogenous inhibitor of Akt, CTMP, is critical to ischemia-induced neuronal death.** *Nat Neurosci*, **12**(5):618–26, May 2009. 105

[70] R B Moreland, H G Nam, L M Hereford, and H M Fried. **Identification of a nuclear localization signal of a yeast ribosomal protein.** *Proc Natl Acad Sci U S A*, **82**(19):6561–5, Oct 1985. 39

[71] N Mosammaparast and L F Pemberton. **Karyopherins: from nuclear-transport mediators to nuclear-function regulators.** *Trends Cell Biol*, **14**(10):547–556, Oct 2004. 39

[72] Robert Nash, Shuai Weng, Ben Hitz, Rama Balakrishnan, Karen R Christie, Maria C Costanzo, Selina S Dwight, Stacia R Engel, Dianna G Fisk, Jodi E Hirschman, Eurie L Hong, Michael S Livstone, Rose Oughtred, Julie Park, Marek Skrzypek, Chandra L Theesfeld, Gail Binkley, Qing Dong, Christopher Lane, Stuart Miyasato, Anand Sethuraman, Mark Schroeder, Kara Dolinski, David Botstein, and J Michael Cherry. **Expanded protein information at SGD: new pages and proteome browser.** *Nucleic Acids Res*, **35**(Database issue):D468–71, Jan 2007. 28

[73] Y Noda, S Nishikawa, K Shiozuka, H Kadokura, H Nakajima, K Yoda, Y Katayama, N Morohoshi, T Haraguchi, and M Yamasaki. **Molecular cloning of the protocatechuate 4,5-dioxygenase genes of Pseudomonas paucimobilis.** *J Bacteriol*, **172**(5):2704–9, May 1990. 4, 94

[74] K Nomoto, N Tomita, M Miyake, D B Xhu, P R LoGerfo, and I B Weinstein. **Expression of phospholipases gamma 1, beta 1, and delta 1 in primary human colon carcinomas and colon carcinoma cell lines.** *Mol Carcinog*, **12**(3):146–52, Mar 1995. 36

[75] Eric N Olson and Alfred Nordheim. **Linking actin dynamics and gene transcription to drive cellular motile functions.** *Nat Rev Mol Cell Biol*, **11**(5):353–65, May 2010. 38

[76] Xuewen Pan, Daniel S Yuan, Siew-Loon Ooi, Xiaoling Wang, Sharon Sookhai-Mahadeo, Pamela Meluh, and Jef D Boeke. **dSLAM analysis of genome-wide genetic interactions in Saccharomyces cerevisiae.** *Methods*, **41**(2):206–21, Feb 2007. 25, 88, 89, 90, 116, 117

[77] Xuewen Pan, Daniel S Yuan, Dong Xiang, Xiaoling Wang, Sharon Sookhai-Mahadeo, Joel S Bader, Philip Hieter, Forrest Spencer, and Jef D Boeke. **A robust toolkit for functional profiling of the yeast genome.** *Mol Cell*, **16**(3):487–96, Nov 2004. 88

[78] A Pandiella, H Lehvaslaiho, M Magni, K Alitalo, and J Meldolesi. **Activation of an EGFR/neu chimeric receptor: early intracellular signals and cell proliferation responses.** *Oncogene*, **4**(11):1299–305, Nov 1989. 3

[79] Z D Pei and J R Williamson. **Mutations at residues Tyr771 and Tyr783 of phospholipase C-gamma1 have different effects on cell actin-cytoskeleton organization and cell proliferation in CCL-39 cells.** *FEBS Lett*, **423**(1):53–6, Feb 1998. 37

[80] E Peles, R B Levy, E Or, A Ullrich, and Y Yarden. **Oncogenic forms of the neu/HER2 tyrosine kinase are permanently coupled to phospholipase C gamma.** *EMBO J*, **10**(8):2077–86, Aug 1991. 3

[81] Lucy F Pemberton and Bryce M Paschal. **Mechanisms of receptor-mediated nuclear import and nuclear export.** *Traffic*, **6**(3):187–98, Mar 2005. 41

[82] Guido Posern and Richard Treisman. **Actin' together: serum response factor, its cofactors and the link to signal transduction.** *Trends Cell Biol*, **16**(11):588–96, Nov 2006. 38

[83] Stewart GG Priest FG. *Handbook of Brewing.* CRC Press., 2006.

[84] H Prillinger, W Schweigkofler, M Breitenbach, P Briza, E Staudacher, K Lopandic, O Molnár, F Weigang, M Ibl, and A Ellinger. **Phytopathogenic filamentous (Ashbya, Eremothecium) and dimorphic fungi (Holleya, Nematospora) with needle-shaped ascospores as new members within the Saccharomycetaceae.** *Yeast*, **13**(10):945–960, Aug 1997. 16

[85] D Pruyne and A Bretscher. **Polarization of cell growth in yeast.** *J Cell Sci*, **113 (Pt 4)**:571–85, Feb 2000. 13

[86] O Puig, F Caspary, G Rigaut, B Rutz, E Bouveret, E Bragado-Nilsson, M Wilm, and B Séraphin. **The tandem affinity purification (TAP) method: a general procedure of protein complex purification.** *Methods*, **24**(3):218–29, Jul 2001. 115

[87] Chen Qiu, Susanne Lienhard, Nancy E. Hynes, Ali Badache, and Daniel J. Leahy. **Memo is homologous to nonheme iron dioxygenases and binds an ErbB2-derived phosphopeptide in its vestigial active site.** *J Biol Chem*, **283**(5):40, 2008. 2, 5, 44, 93, 105, 118

[88] G Rigaut, A Shevchenko, B Rutz, M Wilm, M Mann, and B Séraphin. **A generic protein purification method for protein complex characterization and proteome exploration.** *Nat Biotechnol*, **17**(10):1030–2, Oct 1999. 83, 115

[89] Klarisa Rikova, Ailan Guo, Qingfu Zeng, Anthony Possemato, Jian Yu, Herbert Haack, Julie Nardone, Kimberly Lee, Cynthia Reeves, Yu Li, Yerong Hu, Zhiping Tan, Matthew Stokes, Laura Sullivan, Jeffrey Mitchell, Randy Wetzel, Joan Macneill, Jian Min Ren, Jin Yuan, Corey E Bakalarski, Judit Villen, Jon M Kornhauser, Bradley Smith, Daiqiang Li, Xinmin Zhou, Steven P Gygi, Ting-Lei Gu, Roberto D Polakiewicz, John Rush, and Michael J Comb. **Global survey of phosphotyrosine signaling identifies oncogenic kinases in lung cancer.** *Cell*, **131**(6):1190–203, Dec 2007. 101

[90] M E Schmitt, T A Brown, and B L Trumpower. **A rapid and simple method for preparation of RNA from Saccharomyces cerevisiae.** *Nucleic Acids Res*, **18**(10):3091–3092, May 1990. 117

[91] D D Shoemaker, D A Lashkari, D Morris, M Mittmann, and R W Davis. **Quantitative phenotypic analysis of yeast deletion mutants using a highly parallel molecular bar-coding strategy.** *Nat Genet*, **14**(4):450–6, Dec 1996. 26

[92] M R Smith, Y L Liu, S R Kim, Y S Bae, C G Kim, K S Kwon, S G Rhee, and H F Kung. **PLC gamma 1 Src homology domain induces mitogenesis in quiescent NIH 3T3 fibroblasts.** *Biochem Biophys Res Commun*, **222**(1):186–93, May 1996. 36

[93] K. S. Spencer, D. Graus-Porta, J. Leng, N. E. Hynes, and R. L. Klemke. **ErbB2 is necessary for induction of carcinoma cell invasion by ErbB family receptor tyrosine kinases.** *J Cell Biol*, **148**(2):385–97, 2000. Spencer, K S Graus-Porta, D Leng, J Hynes, N E Klemke, R L CA 78493-01/CA/NCI NIH HHS/United States Research Support, Non-U.S. Gov't Research Support, U.S. Gov't, Non-P.H.S. Research Support, U.S. Gov't, P.H.S. United states The Journal of cell biology J Cell Biol. 2000 Jan 24;148(2):385-97. 1

[94] K P Stahmann, J L Revuelta, and H Seulberger. **Three biotechnical processes using Ashbya gossypii, Candida famata, or Bacillus subtilis compete with chemical riboflavin production.** *Appl Microbiol Biotechnol*, **53**(5):509–16, May 2000. 20

[95] W T Starmer, P F Ganter, V Aberdeen, M A Lachance, and H J Phaff. **The ecological role of killer yeasts in natural communities of yeasts.** *Can J Microbiol*, **33**(9):783–96, Sep 1987. 16

[96] S Steiner, J Wendland, M C Wright, and P Philippsen. **Homologous recombination as the main mechanism for DNA integration and cause of rearrangements in the filamentous ascomycete Ashbya gossypii.** *Genetics*, **140**(3):973–87, Jul 1995. 20

[97] Lars M Steinmetz, Curt Scharfe, Adam M Deutschbauer, Dejana Mokranjac, Zelek S Herman, Ted Jones, Angela M Chu, Guri Giaever, Holger Prokisch, Peter J Oefner, and Ronald W Davis. **Systematic screen for human disease genes in yeast.** *Nat Genet*, **31**(4):400–4, Aug 2002. 26

[98] C Strambio-De-Castillia, M Niepel, and M P Rout. **The nuclear pore complex: bridging nuclear transport and gene regulation.** *Nat Rev Mol Cell Biol*, **11**(7):490–501, Jul 2010. 39

[99] K Sugimoto, T Senda, H Aoshima, E Masai, M Fukuda, and Y Mitsui. **Crystal structure of an aromatic ring opening dioxygenase LigAB, a protocatechuate 4,5-dioxygenase, under aerobic conditions.** *Structure*, **7**(8):953–65, Aug 1999. 4, 94

[100] V. Robert T. Boekhout. *Yeasts in Food: Beneficial and Detrimental aspects.* Behr's Verlag, 2003. 6

[101] C L Theesfeld, J E Irazoqui, K Bloom, and D J Lew. **The role of actin in spindle orientation changes during the Saccharomyces cerevisiae cell cycle.** *J Cell Biol*, **146**(5):1019–32, Sep 1999. 13

[102] A. Wach, A. Brachat, R. Phlmann, and P. Philippsen. **New heterologous modules for classical or PCR-based gene disruptions in Saccharomyces cerevisiae.** *Yeast*, **10**(13):808, 1994. 20, 89

[103] D S Wang and G Shaw. **The association of the C-terminal region of beta I sigma II spectrin to brain membranes is mediated by a PH domain, does not require membrane proteins, and coincides with a inositol-1,4,5 triphosphate binding site.** *Biochem Biophys Res Commun*, **217**(2):608–15, Dec 1995. 32

[104] D S Wang, R Shaw, J C Winkelmann, and G Shaw. **Binding of PH domains of beta-adrenergic receptor kinase and beta-spectrin to WD40/beta-transducin repeat containing regions of the beta-subunit of trimeric G-proteins.** *Biochem Biophys Res Commun*, **203**(1):29–35, Aug 1994. 32

[105] J. Wendland, Y. Ayad-Durieux, P. Knechtle, C. Rebischung, and P. Philippsen. **PCR-based gene targeting in the filamentous fungus Ashbya gossypii.** *Gene*, **242**(1-2):381–91, 2000. Wendland, J Ayad-Durieux, Y Knechtle, P Rebischung, C Philippsen, P Research Support, Non-U.S. Gov't Netherlands Gene Gene. 2000 Jan 25;242(1-2):381-91. 19, 20

[106] J. Wendland and A. Walther. **Ashbya gossypii: a model for fungal developmental biology.** *Nat Rev Microbiol*, **3**(5):421–9, 2005. Wendland, Jurgen Walther, Andrea Research Support, Non-U.S. Gov't Review England Nature reviews. Microbiology Nat Rev Microbiol. 2005 May;3(5):421-9. 19

[107] Jürgen Wendland, Alexander Dünkler, and Andrea Walther. **Characterization of -factor pheromone and pheromone receptor genes of Ashbya gossypii.** *FEMS Yeast Res*, **11**(5):418–29, Aug 2011. 20

[108] J M Wettenhall and G K Smyth. **limmaGUI: a graphical user interface for linear modeling of microarray data.** *Bioinformatics*, **20**(18):3705–3706, Dec 2004. 117

[109] L J Wickerham, M H Flickinger, and R M Johnston. **The production of riboflavin by Ashbya gossypii.** *Arch Biochem*, **9**:95–8, Jan 1946. 20

[110] E A Winzeler, D D Shoemaker, A Astromoff, H Liang, K Anderson, B Andre, R Bangham, R Benito, J D Boeke, H Bussey, A M Chu, C Connelly, K Davis, F Dietrich, S W Dow, M El Bakkoury, F Foury, S H Friend, E Gentalen, G Giaever, J H Hegemann, T Jones, M Laub, H Liao, N Liebundguth, D J Lockhart, A Lucau-Danila, M Lussier, N M'Rabet, P Menard, M Mittmann, C Pai, C Rebischung, J L Revuelta, L Riles, C J Roberts, P Ross-MacDonald, B Scherens, M Snyder, S Sookhai-Mahadeo, R K Storms, S Véronneau, M Voet, G Volckaert, T R Ward, R Wysocki, G S Yen, K Yu, K Zimmermann, P Philippsen, M Johnston, and R W Davis. **Functional characterization of the S. cerevisiae genome by gene deletion and parallel analysis.** *Science*, **285**(5429):901–6, Aug 1999. 23, 26

[111] T Yoko-o, Y Matsui, H Yagisawa, H Nojima, I Uno, and A Toh-e. **The putative phosphoinositide-specific phospholipase C gene, PLC1, of the yeast Saccharomyces cerevisiae is important for cell growth.** *Proc Natl Acad Sci U S A*, **90**(5):1804–8, Mar 1993. 28

[112] S. J. YORK, B. N. ARMBRUSTER, P. GREENWELL, T. D. PETES, AND J. D. YORK. **Inositol diphosphate signaling regulates telomere length**. *J Biol Chem*, **280**(6):4264–9, 2005. York, Sally J Armbruster, Blaine N Greenwell, Patricia Petes, Thomas D York, John D GM-531576/GM/NIGMS NIH HHS/United States HL-55672/HL/NHLBI NIH HHS/United States Research Support, Non-U.S. Gov't Research Support, U.S. Gov't, P.H.S. United States The Journal of biological chemistry J Biol Chem. 2005 Feb 11;280(6):4264-9. Epub 2004 Nov 23. xi, 31

[113] H YU, K FUKAMI, T ITOH, AND T TAKENAWA. **Phosphorylation of phospholipase Cgamma1 on tyrosine residue 783 by platelet-derived growth factor** regulates reorganization of the cytoskeleton. *Exp Cell Res*, **243**(1):113–22, Aug 1998. 37

[114] KOSSAY ZAOUI, STÉPHANE HONORÉ, DANIEL ISNARDON, DIANE BRAGUER, AND ALI BADACHE. **Memo-RhoA-mDia1 signaling controls microtubules, the actin network, and adhesion site formation in migrating cells**. *J Cell Biol*, **183**(3):401–8, Nov 2008. 1, 2

[115] M ZIMAN, D PREUSS, J MULHOLLAND, J M O'BRIEN, D BOTSTEIN, AND D I JOHNSON. **Subcellular localization of Cdc42p, a Saccharomyces cerevisiae GTP-binding protein involved in the control of cell polarity**. *Mol Biol Cell*, **4**(12):1307–16, Dec 1993. 14

Curriculum vitae Ivan Schlatter

Kontaktadresse	Fliederstrasse 1 CH-4800 Zofingen
Geburtsdatum	11. August 1980
E-Mail-Adresse	Ivan.Schlatter@gmail.com
Telefonnummer	+41 76 535 62 19
Nationalität	Schweiz

Kernkompetenzen

- **Analysieren und Problemlösung:** Das gleichzeitige Arbeiten an zwei Forschungsinstituten, einem akademischen (Friedrich Miescher Institute for Biomedical Research) und einem industriellen (Novartis AG), lehrte mich unabhängig und zielorientiert zu arbeiten, Probleme schnell zu erfassen und erforderte ein hohes Mass an Planung und Koordination, um ein grosses Forschungsprojekt erfolgreich abzuschliessen. Die Resultate werden publiziert und wurden in vielen Seminaren an Kollegen präsentiert.

- **People & Project:** Ich betreute eine Masterstudentin in der täglichen Laborarbeit als auch in der langfristigen Planung des Projektes welches nützliche Daten produzierte.

- **Sprachen:** Deutsch (Muttersprache), Englisch (sehr gut), Italienisch (sehr gut), Französisch (gut)

- **IT:** Macintosh und Windows Betriebssysteme. Microsoft Office Pakete (Word, Excel etc.). Gute Kenntnisse in Adobe Photoshop und Illustrator. Gute Kenntnisse LaTeX.

Arbeitserfahrungen

09.2012-jetzt   **Roche AG, Basel**
                           GMP-Manager MSAT
                           Implementierung des neuen globalen Qualitätssystems (PQS) In
                           der Solida Produktion Basel)
                           (Prozessmonitoring („Track and Trending"), Prozessvalidierung,
                           GMP-Data Management)

03.2007-12.2011   **Mikro- und Zellbiologie bei Novartis AG und am Friedrich
                           Miescher Institute for Biomedical Research, Basel**
                           Laborarbeit in einem akademisch und einem wirtschaftlich
                           ausgerichteten Labor. Betreuung einer Masterstudentin.

02.2006-12.2007   **Novartis Institute for Biomedical Research, Basel**
                           Im "Department für Molecular Pathways" konnte ich an
                           verschiedenen krankheitsrelevanten Zellmodellen arbeiten. Ich
                           konnte an large-scale screens für neue Medikamente
                           mitarbeiten und verwendete dafür Backman Coulter Industrial
                           Robotic Solutions.
                           Praktikum betreut durch Dr. Dominic Hoepfner

11.2006-01.2007   **Biozentrum, Departement Angewandte Mikrobiologie, Basel**
                           Praktikum

Ausbildung

03.2007-12.2011   **PhD "Functional analysis of Memo in yeast and cancer cells"**
                       Friedrich Miescher Institute for Biomedical Research, Basel und
                       Novartis Institute for Biomedical Research, DMP/CMB, Basel
                       Betreut durch Prof. Dr. Nancy E Hynes und Dr. Rao Movva
                       (Ich lernte die meisten Standard Labortechniken für Hefe und
                       Säuger Zellbiologie: DNS Klonierungen und Modifikationen,
                       Proteinanalysetechniken, Fluoreszenz- und Konfokal
                       Mikroskopie, verschiedene Large-Scale-Screens, uvm.)

                       Die Resultate wurden in PLoS One publiziert (I. Schlatter et.al
                       2012).

10.2004-10.2005   **MSc "Function of Dynamins in the filamentous fungus
                       Ashbya gossypii", Universität Basel, Biozentrum**
                       Betreut durch Prof. Dr. Peter Philippsen und Dr. Dominic
                       Hoepfner

10.2000-09.2004   **BSc in Zellbiologie, Universität Basel, Biozentrum**

08.1996-07.2000	**Kantonsschule Zofingen,** Matura Typus C (Naturwissenschaften, Mathematik, Physik)
Konferenzen	Talk an der XXIInd International Conference on Yeast Genetics and Molecular Biology in Bratislava (SK), 2006
	Poster presentationen an der International Summer School in Spetses "From Pluripotency to Senescence Molecular Mechanisms of Development, Diseases and Ageing" 2010; und an den FMI Annual Meetings 2007-2011.

Unterrichten

10.2004-10.2005	Vorbereitung und Durchführung der Laborpraktika und Vorlesungen Videomikroskopie und Transformation von Hefezellen für die ESBS (Ecole supérieure de biotechnologie Strasbourg) gehalten am Biozentrum, Basel
03.2007-12.2011	Vorlesungen und Fragesessions für Studenten an den jährlich gehaltenen "Tage der Genforschung" am FMI, Basel

Interessen und Hobbies

Fussball	Aktiv und passiv
Skifahren	Alg. alle Schneesportarten (Snowboard, Wandern,…)
Lesen	Alle mögliche Literatur
Familie	Alessia (2009), Ennio (2012)

Referenzen

Auf Anfrage